1990

Cytoskeletal Development In The Epidermal Cells Of An Insect, Calpodes Ethlius Stoll (lepidoptera:hesperiidae)

Patric John Delhanty

NOTICE

The quality of this microform is heavily dependent upon the quality of the original thesis submitted for microfilming. Every effort has been made to ensure the highest quality of reproduction possible.

If pages are missing, contact the university which granted the degree.

Some pages may have indistinct print especially if the original pages were typed with a poor typewriter ribbon or if the university sent us an inferior photocopy.

Reproduction in full or in part of this microform is governed by the Canadian Copyright Act, R.S.C. 1970, c. C-30, and subsequent amendments.

AVIS

La qualité de cette microforme dépend grandement de la qualité de la thèse soumise au microfilmage. Nous avons tout fait pour assurer une qualité supérieure de reproduction.

S'il manque des pages, veuillez communiquer avec l'université qui a conféré le grade.

La qualité d'impression de certaines pages peut laisser à désirer, surtout si les pages originales ont été dactylographiées à l'aide d'un ruban usé ou si l'université nous a fait parvenir une photocopie de qualité inférieure.

La reproduction, même partielle, de cette microforme est soumise à la Loi canadienne sur le droit d'auteur, SRC 1970, c. C-30, et ses amendements subséquents.

CYTOSKELETAL DEVELOPMENT IN THE EPIDERMAL CELLS OF AN INSECT, *CALPODES ETHLIUS* STÖLL (LEPIDOPTERA, HESPERIIDAE)

by

Patric J. D. *Delhanty*

Department of Zoology

Submitted in partial fulfilment
of the requirements for the degree of
Doctor of Philosophy

Faculty of Graduate studies
The University of Western Ontario
London, Ontario
November, 1989

ISBN 0-315-55300-6

ABSTRACT

A basic problem in insect metamorphosis is the means by which insects change shape. This can be studied by examining the shape changes of individual epidermal cells. I have found that removal of the basal lamina from the epidermis allows the shape and basal surfaces of these cells to be seen by scanning electron microscopy. In the 5th larval stage of *Calpodes ethlius* the cells extend basal processes or feet. Feet develop in three phases. Just after ecdysis they are short and randomly oriented. The cells are closely packed and their bases have punctate hemidesmosomes. The hemidesmosomes become elongated and axially oriented before commitment to pupation. The feet then also extend, and orient axially. The feet contract late in the stadium, disappearing as the cells move to their pupal positions. This cell rearrangement is facilitated by the formation of wide intercellular lymph spaces. Filopodia span and presumably aid closure of the spaces between the cells at pupation. The changes in the feet suggest that they are prime movers in epidermal morphogenesis.

The disposition of the cytoskeleton is related to the control of cell shape. For example, orientation of the feet may be controlled by selective stabilization of dynamically unstable microtubules. My work on epidermal cells suggests that cytoskeletal shape may also be influenced by somatic inheritance. The cells contain apical bundles of F-actin (shown using rhodaminyl phalloin labelling) which survive for about 36 hours after the 4th-5th larval ecdysis and associate with a transverse cuticle component. The number of bundles is paired in adjacent cells which are presumed to be siblings. The maintenance of cytoplasmic continuity through midbodies connecting siblings may preserve the paired patterns. These patterns are a result of sibling similarity, either in ploidy or by the inheritance of transient determinants for bundle pattern and position.

I have found that the secretory cell of the dermal gland is another epidermal cell whose shape is partly determined by the arrangement of its microfilament skeleton. The cell is distended during the intermoult by accumulation of secretion in vacuoles encapsulated by F-actin. At ecdysis the microfilament capsules collapse while the secretion is discharged and the cell shrivels. The microfilaments form into storage bundles which are then redistributed into capsules. This cycle repeats in each stadium until the cell atrophies in the pupa.

Key words: scanning electron microscopy (SEM), cell processes, hemidesmosomes, lymph spaces, filopodia, metamorphosis, insect epidermal feet, actin bundles, cytoskeleton, cell doublets, insect epidermis, midbody, mitosis, pattern pairing, polyploidy, pore canals, somatic inheritance, dermal gland, insect moulting, F-actin, cuticle secretion.

ACKNOWLEDGMENTS

I am pleased to thank Michael Locke for his support and inspiration during this work, especially while writing this thesis and the accompanying papers.

I am grateful to the following at the University of Western Ontario and others for their help, both mental and material; Drs R. Bailey (statistics), E. Ball (anti-vimentin antibodies), D. R. Bellhouse (statistics), S. Caveney (microinjection), J. C. R. Jones (bullous pemphigoid autoimmune sera, Northwestern University, Chicago), V. I. Kalnins (anti-centrosome antibodies and work in his lab, University of Toronto), D. Kellogg (anti-midbody antibodies, University of California, San Francisco), K. Rogers (anti-centrosome antibodies), C. Sellitto (anti-midbody antibodies, University of Minnesota), Th. Wieland (rhodaminyl phalloin, Max-Planck Insitüt fur Medizinische Forschung, Heidelberg, W. Germany) and Mr Ian Craig. Thanks also to Dr R. R. Shivers for criticizing this manuscript and helping me freeze fracture the epidermis.

I also thank H. Fife, S. Henderson, A. Jackson, H. Kirk, H. Leung, Dr S.R. Palli, J.T. Reddy and other members of the Zoology Department for many useful discussions, help and encouragement.

Finally I thank the Science and Engineering Research Council (UK) for financial support.

DEDICATION

To Mum, Dad and Cathy
who patiently put up with me
while I finished this thesis.

TABLE OF CONTENTS

LIST OF TABLES

LIST OF PLATES

LIST OF APPENDICES

ABBREVIATIONS

bl	basal lamina
br	branch
°C	degrees Celsius
cb	cell body
cr	contractile ring
cu	cuticle
ecd	ecdysial droplets
ecm	ecdysial membrane
EDTA	ethylenediaminetetraacetic acid
ef	epidermal feet
EGTA	ethylene glycol-bis-[2-aminoethyl ether] N,N,N',N' tetraacetic acid
ep	epidermis
ER	endoplasmic reticulum
Fb	F-actin bundle
fc	fine basal connections
Fc	F-actin capsule
FITC	fluorescein isothiocyanate
fp	filopodia
Fr	F-actin ring
GC	Golgi complex
h	hours
Hd	hemidesmosome
HEPES	N-[2-hydroxyethyl] piperazine-N'-[2-ethanesulphonic acid]
HMM	heavy meromyosin
5-HT	5-hydroxytryptamine
kV	kilovolts
L	opening to lymph space
ls	lymph space
mg	milligram
mL	millilitre
mm	millimetre
mM	millimolar

MB	microfilament bundle
MF	microfilament
MT	microtubule
MTOC	microtubule organizing centre
mz	microfilament zonule
µg	microgram
µL	microlitre
µm	micrometre
n	nucleus
P	pupal stadium
PBS	phosphate buffered saline
pc	pore canal-like structure
Phn	phalloidin
PIPES	piperazine-N,N'-bis [2-ethanesulphonic acid]
PMRS	plasma membrane reticular system
RhPhn	rhodaminyl phalloin
rpm	revolutions per minute
RT	room temperature
SB	solubilizing buffer
SEM	scanning electron microscope
sp	sub-apical particle
Sv	secretory vacuole
TEM	transmission electron microscope
tu	tubercle
v	vacuole
Ze	zone of exclusion

CHAPTER 1

INTRODUCTION

Multa auter insecta et aliter nascuutur, atque in primis e rore. insidet hic raphani folio primo vere et spissatus sole in magnitudinem milii cigitur. inde porrigitur vermiculus parvus et triduo mox ciruca, quae adieclis diebus adrescit; fit immobilis, duro cortice, ad tactum tantum movetur, araneo accreta, quam chrysallidem appellant. rupto deinde eo cortice evolat papilio.

(Plin. N.H. XI. xxxvii).

Many insects however are born in other ways as well, and in the first place from dew. At the beginning of spring this lodges on the leaf of a radish and is condensed by the sun and shrinks to the size of a millet seed. Out of this a small maggot develops, and three days later it becomes a caterpillar, which as days are added grows larger; it becomes motionless, with a hard skin, and only moves when touched, being covered with a cobweb growth – at this stage it is called a chrysalis. Then it bursts its covering and flies out as a butterfly.

The cytoskeleton is a characteristic of eukaryotic cells. It lets these cells function in a typically eukaryotic way by helping to drive, for example, intracellular transport, cell movement and cell shape change.

Insect cells have at least two cytoskeletal elements, microtubules and microfilaments. Intermediate filament-like proteins have so far only been found in *Drosophila* Kc cells and salivary glands (Walter & Biessmann, 1984). This study is concerned with changes in the cytoskeletons and shapes of epidermal cells in relation to the development and metamorphosis of larval *Calpodes ethlius* Stöll (Lepidoptera, Hesperiidae). Figure 1 shows the filamentous nature of the epidermal cytoskeletons. Two epidermal cell types are examined, the cells of the epidermis and the secretory cell of the dermal gland.

1.1 The development of epidermal feet in preparation for metamorphosis

The outward form of an insect is dependent on the shape of its cuticle which is secreted by the epidermal cells. At metamorphosis the old cuticle is shed allowing the shape of the insect to change markedly. It follows, then, that the change in shape of the insect must be caused by a change in shape of the epidermis. The epidermal cells are therefore prime movers in the

Fig. 1. The filamentous cytoskeletons and nuclei of epidermal cells. The basal lamina was loosened with 0.25% trypsin in microtubule stabilizing buffer-1 (MSB-1=0.1 M HEPES, 3mM EGTA) for 5 min. The epidermis was then incubated for 5 min in 1% Triton X100 in MSB-2 (50 mM imidazole, 50mM KCl, 0.5 mM $MgCl_2$, 1 mM EGTA, 0.1 mM EDTA, 1 mM 2-mercaptoethanol, 2 M glycerol) to dissolve the membranes. After fixation (2.5% glutaraldehyde in 0.1 M phosphate buffer, pH 7.4) the tissue was processed for SEM as described in materials and methods.

MSB-1 and -2 from (Simmonds *et al.*, 1983).

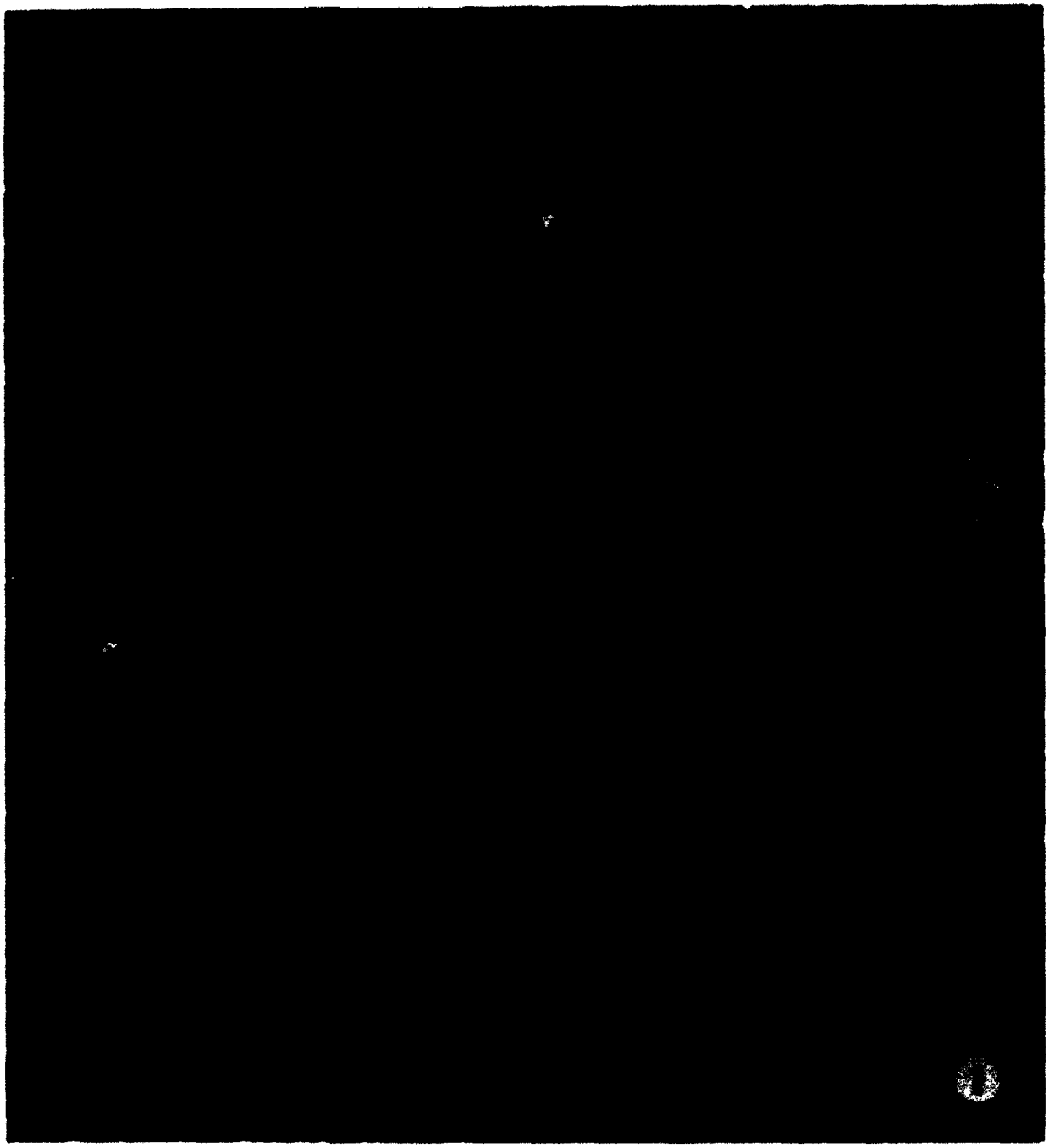

morphogenesis of insects. Scanning electron microscopy (SEM) has been used to examine the basal surfaces of epidermal cells during larvaldevelopment and metamorphosis to gain an insight into how the epidermis changes shape.

The epidermis probably changes shape by rearrangement of its component cells. Work on the development of legs in *Drosophila* confirms that cell rearrangement occurs in morphogenesis (Fristrom, 1988). In flies, adult structures like legs and wings originate from relatively undifferentiated sheets of cells called imaginal discs. The legs begin to take form as short, wide tubes of cells which elongate and become narrow. This change in shape was found to be accomplished by rearrangement of the cells rather than by selective death, division or elongation of the cells in the axis of the leg. Cell rearrangement has also been found to be involved in morphogenesis in other organisms (e.g. *Xenopus* gastrulation and neurulation, Keller & Tibbetts, 1989; *Fundulus* epiboly, Keller & Trinkaus, 1987; avian neurulation, Schoenwolf & Alvarez, 1989) but little has been discovered about the way in which cells move relative to one another.

The structures which may cause the cells to move past each other in *Calpodes* epidermis are the epidermal feet (Locke & Huie, 1981a; Locke & Huie, 1981b). Nardi & Magee-Adams (1986) have found similar structures which correlate with patterning of scale primordial cells in the developing wings of *Manduca sexta*. The feet are cellular basal projections which begin to develop early in the final larval stadium and extend axially until two to three days before pupation. The feet then shorten before the epidermis assumes a pupal shape. The axial orientation of the feet is important in this developmental sequence because at metamorphosis the epidermis shortens in its long axis giving it pupal shape. Presumably the feet pull on neighbouring cells and the underlying basal lamina causing the cells to move axially and intussuscept one another. The problem is how the feet first become axially oriented. This study suggests that axial orientation might be caused by selective survival of axially rather than laterally oriented feet (see chapter 3). The feet may be like the filopodia on neuronal growth cones which only become stabilized when they are able to adhere strongly to neighbouring cells (Goodman *et al.*, 1984). One way in which the feet may become stabilized is by their attachment to the basal lamina through the hemidesmosomes (appendix 3). Although hemidesmosomes can be seen in thin sections their topography on the basal surfaces of the cells is not easily determined using transmission electron

microscopy (TEM) (e.g. Locke, 1985). Scanning electron microscopy, on the other hand, can be used to show the basal cell surfaces and to map the distribution of the hemidesmosomes during development leading up to metamorphosis.

One of the problems with cell rearrangement is that the cells have to be able to move past one another and even change neighbours. However, the junctions which hold the cells together were considered to prevent them from moving easily past each other (Fristrom, 1976; 1988). For this reason, cell rearrangement was neglected as a possible mode of morphogenesis until it was shown to occur in *Drosophila* imaginal disc development. Later, Fristrom (1982) showed that the cell junctions can move to accommodate cell rearrangement. How does the epidermis in *Calpodes* modify its intercellular junctions to allow cell rearrangement? Just before pupation the cells lose most of their junctions and become separated by large intercellular spaces. It is suggested that these spaces are not completely artifactual but may also facilitate movement of the cells past each other. However, cell separation also causes lack of continuity between the cells, except at the apices and bases where cell-cell contact is maintained. Epidermal cells in the pupa are again closely apposed. This poses the problem of how the cells pull themselves together at the larval/pupal transformation. SEM shows that filopodia form and span the spaces. Filopodia have been found between naturally separate cells in the developing fat body in *Calpodes* (Locke, 1987). Some of these filopodia had shortened into knots or coils as if they had contracted. Filopodia were also shown to be contractile in the ascidian *Botryllus schlosseri* (Izzard, 1974). These examples show that it is possible that the filopodia may help to pull the separated cells back together in prepupal *Calpodes* epidermis.

1.2 Paired F-actin patterns in epidermal cell doublets

The shape of a cell may be controlled by either or both of two different sets of cues (Solomon, 1981). The first set originates outside the cell and includes cell-cell contacts and diffusible signals which affect cell motility. A second set comes from information inside the cell, perhaps in the cytoskeleton. Both these models are possible but, as Solomon (1981) comments:

> "...a rigorous test of either model in vivo would require the difficult if not impossible task of isolating a cell in an animal either from its history or from its environment."

Cells in culture can be kept in relatively uniform environments and have consequently been used to obtain most of the data so far on the inheritance of the intracellular information which specifies cell shape. The insect epidermis is similar to a cell culture in that the cells are in a monolayer, their environment is relatively uniform and they are presumably closely genetically related. The epidermis is therefore a suitable *in vivo* system to study the inheritance of determinants of cell shape.

The pattern of certain nuclear components (nucleoli and female heterochromatin) were found to be paired in adjacent epidermal cells in *Calpodes* (Locke, 1988; Locke & Leung, 1985b). After mitosis the cells remain connected by cytoplasmic bridges forming a minimal syncytium of siamese twin cells. These direct links would allow cytoplasmic information specifying cell shape to be shared by both cells in a doublet and thus stabilize the paired pattern. For this reason paired adjacent cells are presumed to be siblings. Cytoskeletal elements have also been shown to be paired in sibling cells in culture (e.g. Albrecht-Buehler, 1977; Solomon, 1979). These results suggested that *Calpodes* epidermis would be a good place to look for paired cytoskeletal patterns. I have found the first evidence for cytoskeletal similarities between natural, non tissue culture, sibling cells.

During the first 36 hours of the fifth larval stadium epidermal cells contain apical bundles of microfilaments. The number of bundles can vary from one to five. One main aim of this part of the investigation was to find evidence for pairing in the number of microfilament bundles in adjacent cells. Another main aim was to determine the function of the bundles and the sequence of their development in the fourth, fifth and pupal stadia.

1.3 Cycles of F-actin redistribution in the dermal glands relate to secretion

Actin bundles also form in the secretory cells of the dermal glands just after every ecdysis (fig. 75) except during the pupal/adult transformation. Dermal glands in Lepidoptera consist of three cells. The duct cell and the

saccule cell form a conduit leading from the very large secretory cell to the cuticle surface. In late fourth stage larvae the secretory cell may be up to 1.6 mm long (Lai-Fook, 1973) and as long as 6 mm by the end of the fifth stadium. The glands reform and grow, becoming larger and more polyploid at every moult (Lai-Fook, 1973) until they are lost after the larval/pupal transformation. The abdominal segments in *Calpodes* each have two glands which hang from the epidermis into the haemolymph just anterior and dorsal to the spiracles. The glands discharge acidic mucopolysaccharides containing sulphate groups (Lai-Fook, 1972) and proteins (Lane *et al.*, 1986) at each ecdysis.

A characteristic of these cells is that they accumulate secretions during the intermoult which they discharge rapidly onto the surface of the cuticle at ecdysis. In mammalian cells this type of rapid secretion is probably controlled by an apical web of actin filaments (Aunis *et al.*, 1987; Burgess & Kelly, 1987; Hoffstein, 1981). It has been suggested that this apical web acts as a barrier to secretion and that its removal or solation allows secretion (Aunis & Bader, 1988; Aunis *et al.*, 1987; Burgoyne & Cheek, 1987; Lelkes *et al.*, 1986). The dermal gland is suitable for studying the mechanism by which it discharges secretion because it is relatively large and easily manipulated. Its development and the timing of its discharge are known. If, as in mammalian cells, secretion is related to microfilament redistribution then dermal gland secretory cells would be expected to have special arrangements of F-actin related to their rapid synchronous discharge. Gland cells labelled with rhodaminyl phalloin at different stages of development showed that changes in F-actin distribution correlated with the cycles of accumulation and discharge of secretion. The mechanism of discharge is probably different from that found in mammalian cells.

The nucleus forms an alveolar network throughout the cell in the fourth (Lai-Fook, 1972) and fifth stadia (chapter 5). This suggested that the structure of the cell may be organized to allow the nucleus to maintain the shortest route for mRNA to travel from the nucleoplasm to the the rough endoplasmic reticulum (RER), and a short cisternal route from the RER to the secretory vacuoles. Cells labelled with rhodaminyl phalloin and observed using epifluorescent confocal microscopy showed remarkable order in the three dimensional spatial relationship between the nucleus and the F-actin associated with the secretory vacuoles.

CHAPTER 2

MATERIALS AND METHODS

2.1 Experimental animal

Observations were made on the dorsal epidermis of *Calpodes ethlius* (Lepidoptera, Hesperiidae). The rearing of larvae and the timing of events in the epidermis have already been described (Dean *et al.*, 1980; Locke, 1970; Locke & Huie, 1981b). To avoid variation due to sexual dimorphism only female larvae were used in time series.

2.2 Chemicals

All chemicals used were purchased from either Fisher Scientific (Toronto, Ont.), J.T. Baker Chemical Co. (Phillipsburg, NJ) or Sigma Chemical Co. (St. Louis, MO) unless otherwise stated.

2.3 The epidermal feet

The problem with observing the epidermis by SEM is that it is covered with a basal lamina that must be removed to show the cell surface (Locke, 1986). This has been accomplished by mechanical removal after critical point drying, with and without pretreatment of live preparations with trypsin. The timing of exposure to trypsin is critical. A short exposure of 1-2 minutes loosens or breaks the hemidesmosomal attachments between the plasma membrane and the basal lamina. Longer exposure also attacks desmosomes and other intercellular connections causing cell separation with the induction of filopodia (Locke, 1987). In this study the aim has been to observe the natural appearance of cells that are abnormal only in the loss of the basal lamina. Although trypsin has usually been used to loosen the basal lamina, similar observations have been made on cells subjected only to fixation, critical point drying and physical removal of the basal lamina. The following procedure was used most commonly. The thorax and the last 3-4 abdominal segments were cut from the larva and the gut pulled out. The resulting tube of integument was washed with phosphate buffered saline, pH 6.9 (PBS= 130 mM NaCl, 5 mM Na_2HPO_4, 1 mM KH_2PO_4), opened ventrally and pinned out in PBS. Regions of the first three

abdominal segments were pinned out separately with flattened but otherwise natural shape and incubated in freshly prepared 0.2% trypsin (Sigma type II, pancreatic) in PBS for 1 to 2 minutes at room temperature (RT) with agitation. Solutions of trypsin must be freshly prepared, since they lose 75% of their activity within 3 hours at room temperature (Stecher, 1968). Orientation was facilitated by leaving the intersegmental muscles at one end of the segment. The flattened segments were then fixed in fresh 5% glutaraldehyde (pH 7.4, 0.1M phosphate buffer with 4% sucrose) for 2–12 hours, washed, dehydrated in ethanol and critical point dried. An additional fixation was used to achieve better preservation of the cells and especially their hemidesmosomes (see figs. 15-16). The fixation above was followed by post-fixation in aqueous 1% OsO_4 for 30 minutes at room temperature, rinsing thoroughly in water and immersion in a 5% glutaraldehyde / 5% tannic acid mixture (pH 7.4, 0.1M phosphate buffer with 4% sucrose) for 1 hour at room temperature. After rinsing in water the tissue was transferred to a half-saturated aqueous uranyl acetate solution for one hour at room temperature, washed, dehydrated and critical point dried. When fixed in glutaraldehyde alone, murine peritoneal macrophages shrink by 45% of their live diameter after critical point drying. Additional tannic acid, OsO_4 and uranyl acetate treatments limit the shrinkage to only 5% (Wollweber *et al.*, 1981).

The hemidesmosomes seen by SEM (e.g. 15B & 16) correspond closely in size and position to those seen in thin section (Locke, 1985; fig. 15A). However attempts to label these structures with antibodies to mammalian desmosomal (desmoplakins I & II, ICN Immunobiologicals, IL; Mueller & Franke, 1983) and hemidesmosomal proteins (Jones *et al.*, 1986; Takahashi *et al.*, 1985) have failed. This was probably because firstly, in mammals at least, hemidesmosomal proteins are not related to desmosomal proteins using immunological criteria (Jones *et al.*, 1986). Secondly, hemidesmosomes in mammals may be immunologically distinct from those in insects. In contrast to TEM (Locke, 1985) and freeze fracture (Shienvold & Kelly, 1976; Shivers & Brightman, 1977) the SEM is a relatively easy way to examine hemidesmosomes in *Calpodes* epidermis.

After mounting on aluminium stubs the basal lamina was stripped off with sticky tape points before sputter coating with gold for 3 minutes. Observations were made with an Hitachi S-570 SEM operating at 20 kV and using the upper

detector. Photographs were taken on Kodak 120 roll film. Nearly a thousand photographs were recorded from about three hundred preparations.

Epidermis was also fixed for normal transmission electron microscopy (see section 2.4) and embedded in araldite. Semi-thin sections were cut so that the development of the lymph spaces during the fifth stadium could be seen. The lateral surfaces apposing the lymph spaces were also viewed directly by SEM of broken pieces of critical point dried epidermis mounted on their edge.

2.4 The epidermal cell doublets

Rhodaminyl phalloin labelling for F-actin

Larvae were injected with 2-4% formaldehyde in PBS, pH 6.9-7.0 at room temperature. They were kept inflated for about 5 minutes and then dissected under PBS or *Calpodes* ringer (17 mM NaCl, 40 mM KCl, 6 mM $CaCl_2$, 70 mM $MgCl_2$, pH 7.0) on a black wax dish. The dorsal integument of the first and second abdominal segments was used in the following procedure but other segments gave similar results. Excised segments of integument were immersed in acetone at 4°C for 1-10 minutes, rinsed in PBS for 1 minute and mounted with the epidermal side up on a glass slide. Excess PBS was drained with filter paper and the tissue quickly covered with 20 µL of PBS containing 1.0 µg/mL rhodaminyl phalloin (from Prof. Th. Wieland, Max-Planck Institüt fur Medizinische Forschung, W. Germany). The slides were incubated in the dark for 30-60 minutes at room temperature. The rhodaminyl phalloin was then replaced by PBS for 1-2 minutes before mounting in a mixture of 90% glycerol in PBS at pH 9.0 containing 1% n-propyl gallate to reduce photobleaching (Giloh & Sedat, 1982). The preparations were sealed under #0 coverslips using wax or nail varnish and observed immediately (although preparations survive for months at 4°C in the dark). Epifluorescence was observed with a Zeiss Photomicroscope II using a rhodamine filter. Fig. 64 is an optical section made using a Biorad / MRC Lasersharp confocal microscope with a rhodamine filter and photographed on Kodak Plus X Pan 35 mm film from a TV monitor. The natural autofluorescence in the integument is in the yellow range and easily removed by the rhodamine filter (fig. 40). The labelling was specific for F-actin since it was blocked by preincubation in an excess of phalloidin (10 µg/mL, Sigma) (fig. 41). Preparations were photographed on Kodak Tri X Pan 35 mm film.

Hoechst 33258 and rhodaminyl phalloin double labelling

To be able to observe nuclei in relation to the actin pattern in each cell, Hoechst 33258 was used to stain the DNA. Exactly the same procedure was used for labelling actin except that the rhodaminyl phalloin was supplemented with 10 µg/mL of the nuclear stain.

Mercury mordanted, haematoxylin stained integument to show the pore canals

Integument was fixed in glutaraldehyde (cacodylate buffer pH 7.2-7.4 with 4% sucrose) for 4 hours, washed in water and two changes of 0.5% tartaric acid pH 5.5 before mordanting in a mixture of 0.5% $HgCl_2$ in 0.5% tartaric acid for 1 hour at 60°C. The tissue was washed in water, stained in haematoxylin for 15 minutes, washed, dehydrated in ethanol, cleared in xylene and mounted. The preparations were observed and photographed as above (from lab files of M. Locke).

Transmission electron microscopy

Larvae were injected at room temperature with 5% glutaraldehyde in 0.1 M phosphate or sodium cacodylate buffer at pH 7.4 containing 2% sucrose. They were kept inflated for 5 minutes at room temperature before the abdomen was cut transversely into short sections. The integument was separated from the fat body and midgut and fixation continued for 1-2 hours. After washing in buffer they were postfixed in 1% OsO_4 for 5-60 minutes at room temperature. All traces of buffer were removed in several changes of distilled water before tissue staining in half-saturated aqueous uranyl acetate overnight at room temperature, followed by dehydration in ethanol and embedding in araldite. Sections were viewed with a Philips EM 300.

Quantitation

Cells were measured from photographs using a Hipad™ digitizer and a video camera connected to an Apple IIe computer. Bioquant (R&M Biometrics, Inc., TN) image analysis software was used to calculate the areas. Nuclear projectional area (πr^2) was calculated from the average of the greatest and least diameters (2r) of each nucleus.

2.5 The dermal gland

Observations were made on the two dermal glands from the second abdominal segment of *Calpodes ethlius* during the pupal and last three larval stadia.

The dermal glands lie anterior and dorsal to the spiracles. They were detached by gently tugging at their saccule cells with forceps. The fluorescence in these isolated dermal glands was then not obscured by rhodaminyl phalloin labelling of the surrounding epidermis, fat body and especially muscle. Isolated glands, although requiring more careful handling, were also easier to find after embedding for TEM.

Rhodaminyl phalloin staining

Larvae were injected through a proleg with 2-4% formaldehyde in PBS at room temperature (RT) and maintained inflated for 1-5 minutes. Larvae were then dissected ventrally under PBS and the dermal glands transferred to a microscope slide in a drop of PBS. Excess saline was removed with filter paper and replaced with 20 µL of 100% acetone at 4°C for 1-2 minutes. Before the acetone evaporated another drop of PBS was added and left for 5 minutes to rehydrate the cells. Excess saline was again removed and replaced with 20 µL of 0.1 µg/mL rhodaminyl phalloin dissolved in PBS. These preparations were incubated at RT for 15-60 minutes in the dark. Excess rhodaminyl phalloin was removed by washing for 1-2 minutes in PBS before mounting in 90% glycerol containing PBS at pH 9.0 with 1% n-propyl gallate. The preparations were sealed under #0 coverslips using wax or nail varnish and observed immediately. Preparations stored at 4°C in the dark kept their activity for months without change in the distribution of the rhodaminyl phalloin label. Actin bundles, often in the nucleus, can be induced in live cells by chemicals such as dimethyl sulphoxide (Fukui & Katsumara, 1979; Sanger *et al.*, 1980). Such artefacts would not have occurred here, because the cells were fixed before labelling. The controls are the same as those that were used for labelling the apical actin bundles in the epidermis. They included: (i) no labelling (fig. 87) and (ii) blocking with 10 µg/mL phalloidin (fig. 88) before rhodaminyl phalloin labelling.

Nuclear and actin double labelling

Dermal glands were fixed and permeabilized in the same way as for rhodaminyl phalloin labelling before incubation for an hour at RT in antibodies to soluble nuclear antigens (autoantibody control ANA positive, speckled; Sigma diagnostics, Sigma Chemical Co., St. Louis MO). They were then rinsed several times in PBS and stained for an hour with FITC tagged secondary antibodies, an Evan's blue counterstain and 2 µg/mL rhodaminyl phalloin. After rinsing in PBS the glands were mounted as before. The anti-nuclear antibodies gave a speckled distribution of labelling throughout the nuclei. Cells labelled with Hoechst 33258 DNA stain had a similar appearance.

Light microscopy

Epifluorescence was observed using a Zeiss Photomicroscope II with a rhodamine filter and photographed on Kodak Tri X Pan 35 mm film at 800 ASA. Preparations were also viewed with a Biorad / MRC Lasersharp confocal microscope using both rhodamine and fluorescein filters and photographed from a TV monitor using Kodak Plus X Pan 35 mm film. Biorad software was used for image analysis.

Scanning electron microscopy

Larvae were injected with 5% glutaraldehyde in 0.1 M phosphate buffer, pH 7.4 with 2% sucrose, and left inflated at RT for at least 5 minutes. The larvae were dissected ventrally, pinned out under PBS, and the muscle and fat body surrounding the dermal glands removed with forceps. The glands from each of the first two abdominal segments were excised with a 5 mm^2 piece of integument and fixed for another hour before being washed in PBS, dehydrated in ethanol, critical point dried and sputter coated for 3 minutes with gold. Observations were made with an Hitachi S-570 SEM operated at 20 kV using the upper detector. Photographs were taken on Kodak 120 roll film.

Transmission electron microscopy

Larvae were fixed as for SEM using either 0.1 M phosphate or 0.1 M sodium cacodylate buffer, dissected in PBS and glands were collected into 0.5 - 1 mL of fixative in 1.5 mL microfuge tubes. They were then centrifuged for 5-10 seconds in a Beckman microfuge at about 15,000 rpm to stop them floating and left at RT for 2.5 hours. The fixative was decanted and replaced three times by

buffer every 10 minutes before postfixation for 1-2 hours in buffered 1% OsO_4. After washing in buffer and water for 15-20 minutes each, the tissue was stained in half-saturated aqueous uranyl acetate overnight at RT. The glands were washed in water, dehydrated in ethanol and embedded in araldite.

Heavy meromyosin (HMM) labelling

Larvae were dissected alive under solubilizing buffer (SB =10 mM PIPES, 1 mM MgSO4, 10 mM EGTA, pH 6.9; (Nishikawa & Kitamura, 1987)), and the dermal glands kept for 10 minutes in 0.05% Triton X100 in SB in 1.5 mL microfuge tubes before being incubated at RT for 60-90 minutes in 4 mg/mL rabbit muscle HMM (Sigma, in 50% glycerol) in SB (giving a final glycerol concentration of about 16%). The HMM was replaced with 5% glutaraldehyde (0.1 M phosphate buffer, 2% sucrose) at RT for 5 minutes, 2.5% glutaraldehyde / 1% tannic acid at RT for 60 minutes, 1% OsO4 for 15 minutes and then rinsed with water. The glands were stained overnight in half saturated uranyl acetate at RT, rinsed, dehydrated and embedded. Under these conditions incubation with 2 mg/mL HMM was too weak to cause labelling, but the microfilaments had separated sufficiently for them to be seen individually (fig. 109).

CHAPTER 3

THE DEVELOPMENT OF EPIDERMAL FEET IN PREPARATION FOR METAMORPHOSIS

"...in the ultimate analysis it is the functional activity of the epidermal cell which is responsible for the growth and form of an insect...it is a cell with great potentialities, for which I have come to entertain a profound respect."

Wigglesworth, 1959

3.1 Introduction

The outward form of an insect depends upon the kind of cuticle and the shape maintained by the epidermis that has secreted it. Both change markedly at metamorphosis. This paper is concerned with epidermal shape changes that precede the larval/pupal transformation of *Calpodes ethlius*.

When the 5th stage larva becomes a pupa, the epidermal cells rearrange themselves to make the axially shorter pupal segment. The changes take place in sequences that correspond in their timing to the other main events of the 5th stadium (fig. 2). The activities of the epidermis divide the stadium into three phases (Locke, 1970). During the first three days the cells deposit little cuticle but prepare for later activity by unravelling their nucleoli (Tuck & Locke, 1985) and synthesizing RNA. Mitosis and cuticle deposition both begin after the commitment peak in the second phase, when the ecdysteroid level is elevated. The deposition of cuticle then increases from one lamella every 6 hours to one every 10 minutes while the cells also divide. In the third phase, the prepupal ecdysteroid peak causes the cells to separate from the larval cuticle and form that of the pupa (Locke & Huie, 1979). Complicated changes in cell shape coincide with the activities in all three phases, documenting Wigglesworth's respect for their potential.

The cells first form basal processes or feet that change from a random to an axial orientation as they elongate (Locke & Huie, 1981a; Locke & Huie, 1981b). The feet then contract as the segment shortens, so changing the relations of the cells to one another in the same way that scale primordial cells are rearranged in *Manduca* wings (Nardi & Magee-Adams, 1986). The

Fig. 2. The main events in the epidermis during the fifth larval stadium of *Calpodes* (data from Dean *et al.*, 1980; Locke, 1985; Locke & Huie, 1981). The activities of the epidermis divide the stadium into three phases which correlate with commitment and premetamorphic peaks in the titre of haemolymph ecdysteroid. Five activities which are related to the morphogenesis of the larva are shown.

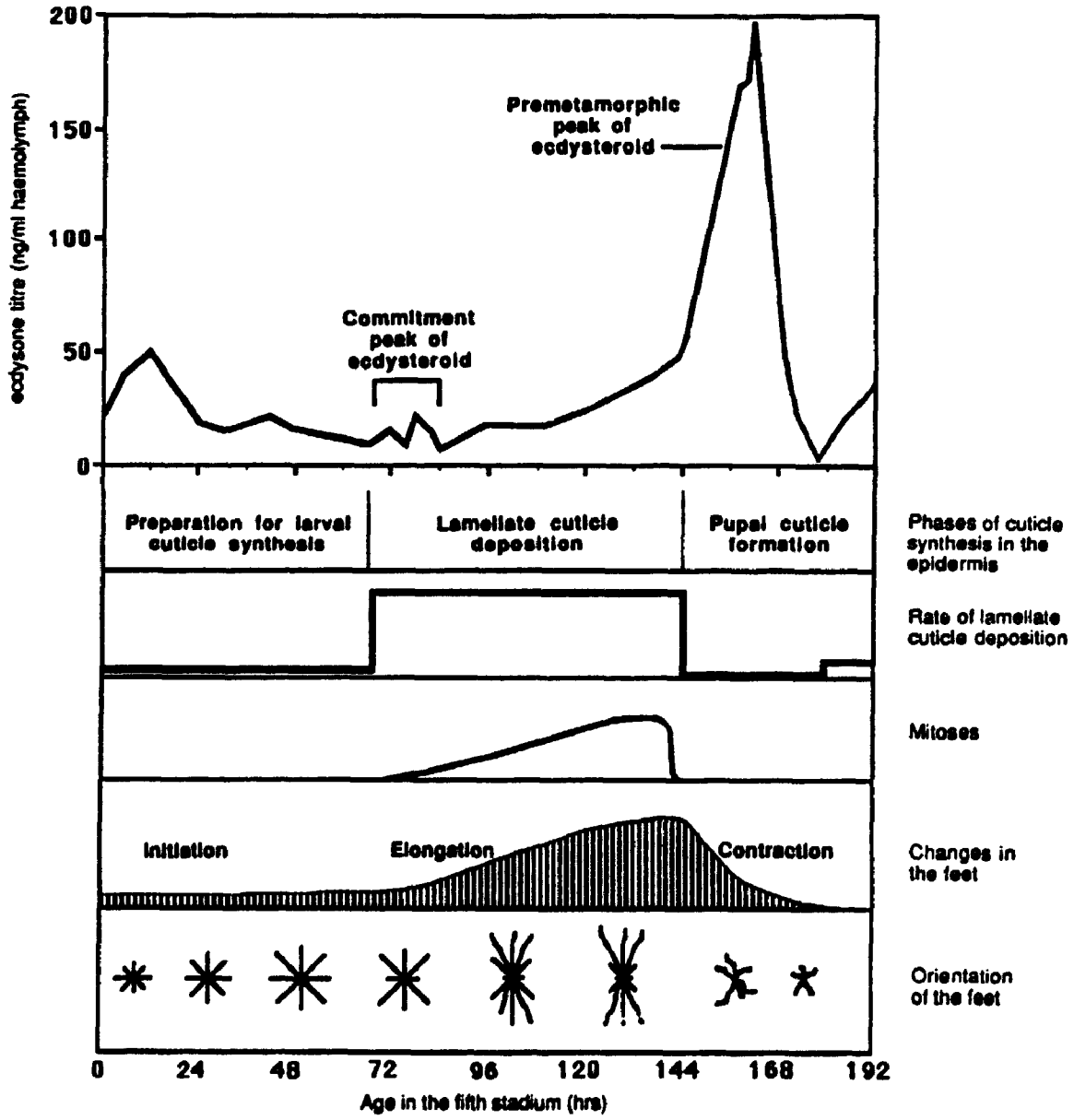
ecdysone titre (ng/ml haemolymph)
200
150
100
50
0
Prometamorphic peak of ecdysteroid
Commitment peak of ecdysteroid
Preparation for larval cuticle synthesis
Lamellate cuticle deposition
Pupal cuticle formation
Phases of cuticle synthesis in the epidermis
Rate of lamellate cuticle deposition
Mitoses
Initiation
Elongation
Contraction
Changes in the feet
Orientation of the feet
0
24
48
72
96
120
144
168
192
Age in the fifth stadium (hrs)

changing shapes of the feet are reproduced in, and probably caused by, the cytoskeleton (figs. 3-5). The feet connect to those of other cells through desmosomes and with the basal lamina through hemidesmosomes (Locke, 1985). Scanning electron microscopy of the exposed basal surface was used to gain insight into the changes in epidermal cell shape that accompany development in the larva and its metamorphosis to the pupa.

3.2 Results

3.2.1 The development of the feet in preparation for metamorphosis

Initial development of the feet

The main changes taking place in the epidermis in relation to other events in the stadium are summarized in fig 6. Immediately after moulting, the basolateral regions of the cells had short, interdigitating processes which had not been resolved in earlier light microscopic observations (Locke & Huie, 1981b). These processes extended without orientation over neighbouring cells for not more than a few micrometers (fig. 7). By a day after ecdysis, most of the processes, now large enough to be called feet, had extended into furrows in the bases of neighbouring cells (fig. 8). This is probably more than the mechanical result of the feet pressing their way into the undersurfaces of cells as they cross them. Even the tips of feet lay flush with the surface as though the neighbouring cells had made way for them during their passage. Thus, the lateral interfaces between cells are far more complex than they appear to be by light microscopy.

The elongation and orientation of the feet in the middle of the stadium

By 66 hours after ecdysis when the larva had just passed the time for commitment to pupation, the feet had grown to form complex knots at junctions between 3 or 4 cells (fig. 9), overlapping one another like the processes on interlocking mammalian kidney podocytes. Although new feet had formed, they had still not extended far over neighbouring cells, being restricted to peripheral zones not more than 10 μm wide around the base of each cell, far short of touching the cells on the other side of their neighbours. By a day after commitment, the feet had extended far across the bases of neighbouring cells (fig. 10). They had become wider and straighter and many were axially

Figs. 3-5. Elongation and then contraction of F-actin bundles in the epidermal feet before larval metamorphosis to the pupa. Controls using competitive binding of phalloidin (see Materials and Methods) show no fluorescence.

Fig. 3. About 70 hours after ecdysis the actin extends in short bundles radiating from the basal edges of the cells (see fig. 9).

Fig. 4. About 150 hours after ecdysis the actin strands are very long and extend over neighbouring cells (see fig. 12).

Fig. 5. Just before pupation the actin strands have contracted. They are replaced by the irregular profiles of cells whose surface areas are reduced to accommodate shortening of the larva (see fig. 14).


0h
3
150h
4
170h
μm
3

Fig. 6. The timing of epidermal changes seen by scanning electron microscopy in the fifth stadium (timing of apolysis from Locke & Huie, 1979). Changes in the feet correlate with changes in the Hd, loss of cell contact with the old cuticle, and loss of cell-cell contact as the lymph space between the cells increases in size and complexity.

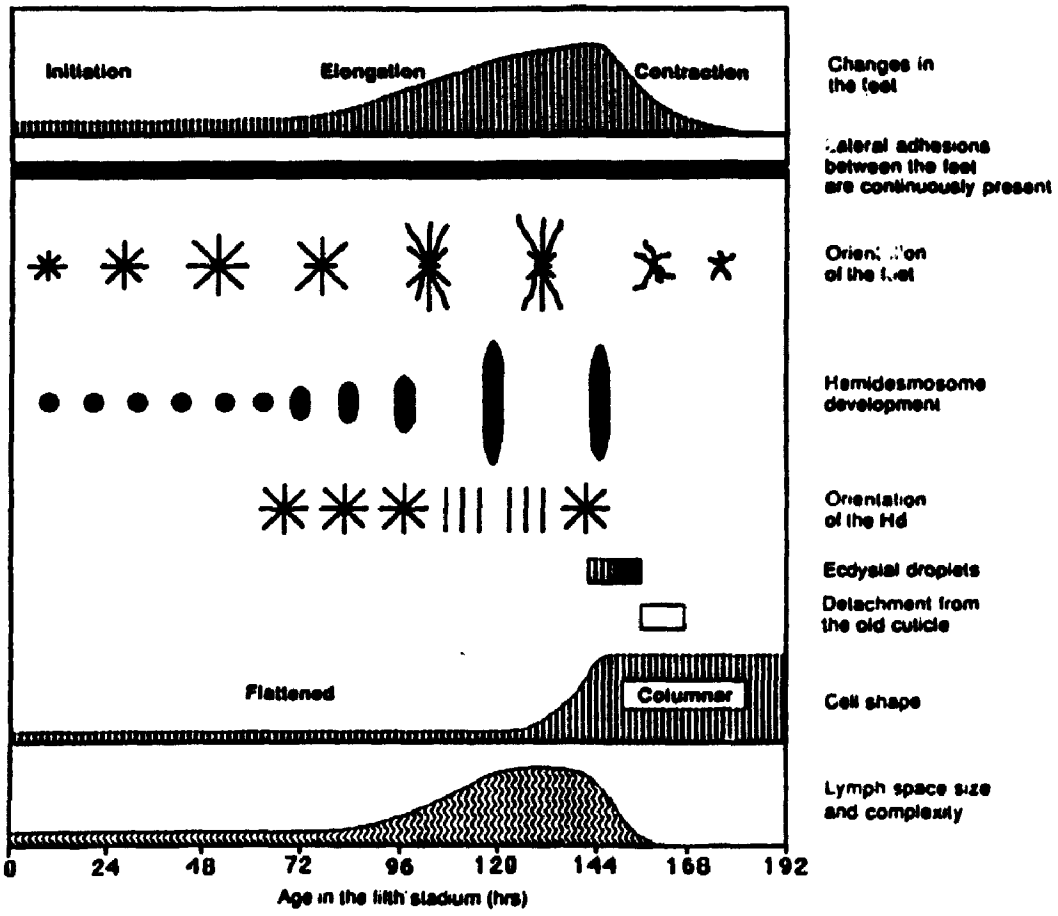
Initiation
Elongation
Contraction
Changes in the feet
Lateral adhesions between the feet are continuously present
Orientation of the feet
Hemidesmosome development
Orientation of the Hd
Ecdysial droplets
Detachment from the old cuticle
Flattened
Columnar
Cell shape
Lymph space size and complexity
0
24
48
72
96
120
144
168
192
Age in the fifth stadium (hrs)

Figs. 7-21. Anterior of larva towards the left.

Figs. 7 & 8. Basal interactions between epidermal cells early in the 5th stadium.

Fig. 7. At ecdysis to the 5th stadium, the bases of the cells (cb) have an irregular outline with short, often interlocking processes, the beginnings of the epidermal feet (ef). A few are flattened and completely underlap neighbouring cells. Cell shrinkage overemphasizes the intercellular lymph spaces. Spot shaped hemidesmosomes (Hd, see 3.2.2) are dispersed across the basal surface of the cell body but are missing from the peripheral processes (fixed in glutaraldehyde with 1% tannic acid).

Fig. 8. By a day after ecdysis, most of the basolateral cell edges have formed processes which often extend without orientation into grooves under nearby cells. The cells keep this form with little change for the next 36 hrs. The extension of the processes presumably increases the volume and complexity of the lymph space (L) between the cells. The Hd are still mostly circular or slightly elongate and absent from the tips of the processes.

Bars = 1 μm.


1
0

Figs. 9-11. The elongation and orientation of the epidermal feet after commitment to pupation.

Fig. 9. After commitment to pupation at 66 hrs the feet lengthen without any particular orientation. They also become more branched, further increasing the complexity of the intercellular lymph spaces which spread under the basal surfaces of the cells (fixed with glutaraldehyde and 1% tannic acid).

Fig. 10. A day after commitment the feet nearly cover the cell bodies. Many have widened and are axially oriented. The feet are joined by fine basal connections (fc) (fixed with glutaraldehyde and 1% tannic acid).

Bars = 1 μm.

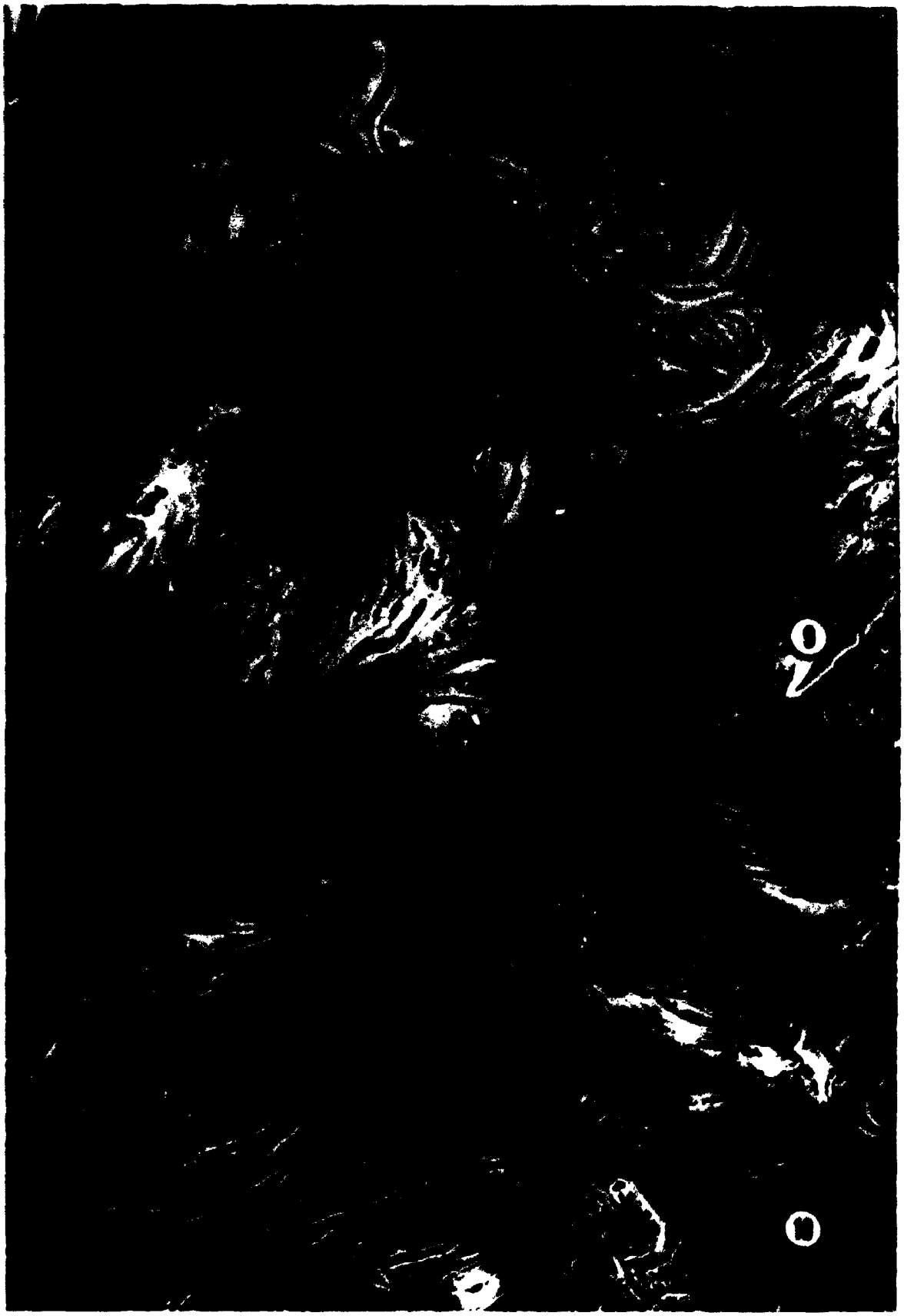

oriented. In the change to axial orientation the feet did not become entangled with one another. That is, laterally projecting feet did not change direction to grow forward and backward, suggesting that orientation is caused by the selection for growth of feet that are already axially oriented, with a loss or failure of growth of those that are not. This contrasts with the idea that the feet first grow and then respond to some orienting influence after becoming mature. Cells were often seen with long axially extended feet but lacking or with only short feet perpendicular to this. By 140 hours almost all of the feet were axially oriented and piled below one another so that they obscured the cell bodies above them (fig. 11). Thus, the intermoult time of elevated ecdysteroid titre (fig. 6) is characterized by the increasing length of axially oriented feet.

The contraction of the feet at the beginning of metamorphosis

The end of the intermoult and the beginning of metamorphosis is signalled by a steeply rising titre of ecdysteroid (the premetamorphic peak, fig. 2). From 156 hours after ecdysis, enough ecdysteroid has been released for pupation to proceed in the absence of the prothoracic glands.

The feet started to shorten and lose their axial orientation at 150 hours and became narrower and curved, exposing the cell bodies. The pattern made by the shortening feet became more complicated, as would be expected if the cells, now free from the apical cuticle, were moving laterally relative to one another to accommodate the axial shortening of the tissue. The shortening of axially oriented feet would be expected to result in a simpler pattern of shorter parallel feet, not the more complex pattern observed (fig. 12). At this time the basal surface decreased in area as the epidermis thickened with a redistribution of the volume to make columnar cells. By 160 hours the cells were almost devoid of feet, the few remaining being short and wide. The surviving basal cell surfaces interlocked in continuously curved outlines as though they had been shaped by the flow of cells moving relative to one another (fig. 13). Eight hours later the feet had completely disappeared and the cells had a simpler basal outline to go with their new columnar shape (fig. 14). The columnar cells were now presumed to be in their pupal positions, since at this time they had begun to deposit the pupal epicuticle.

Fig. 11. When the larva has reached its maximum size 72 hrs after commitment the feet are elongate and so abundant that they obscure the cell bodies. The feet also begin to have an axial orientation. Short side branches (br) extend from the sides of some feet to touch their immediate neighbours. The lymph spaces between the feet now extend over almost the entire basal surface. Adhesions between the feet are easily seen at this stage (see fig. 24).

Figs. 12-14. The loss of axial orientation with shortening of the feet at metamorphosis.

Fig. 12. By 156 hours after ecdysis the feet lose their axial orientation and shorten at the same time as the larva itself shortens. The feet are no longer predominantly straight, presumably because of the rearrangement of the cells to which they are attached.

Bars = 1μm.


11
12

Fig. 13. By 160 hours after ecdysis the feet are fully contracted, all that remain are their smoothed outlines. The shortening of the feet uncovered the cells under which they lay. This simplifies the shape of the reticulate lymph space (L) formed between the feet and the cells.

Fig. 14. By 24 hours prior to ecdysis the cells are almost in their pupal positions and have simplified more uniform basal outlines (fp, filopodia).

Bars = 1μm.

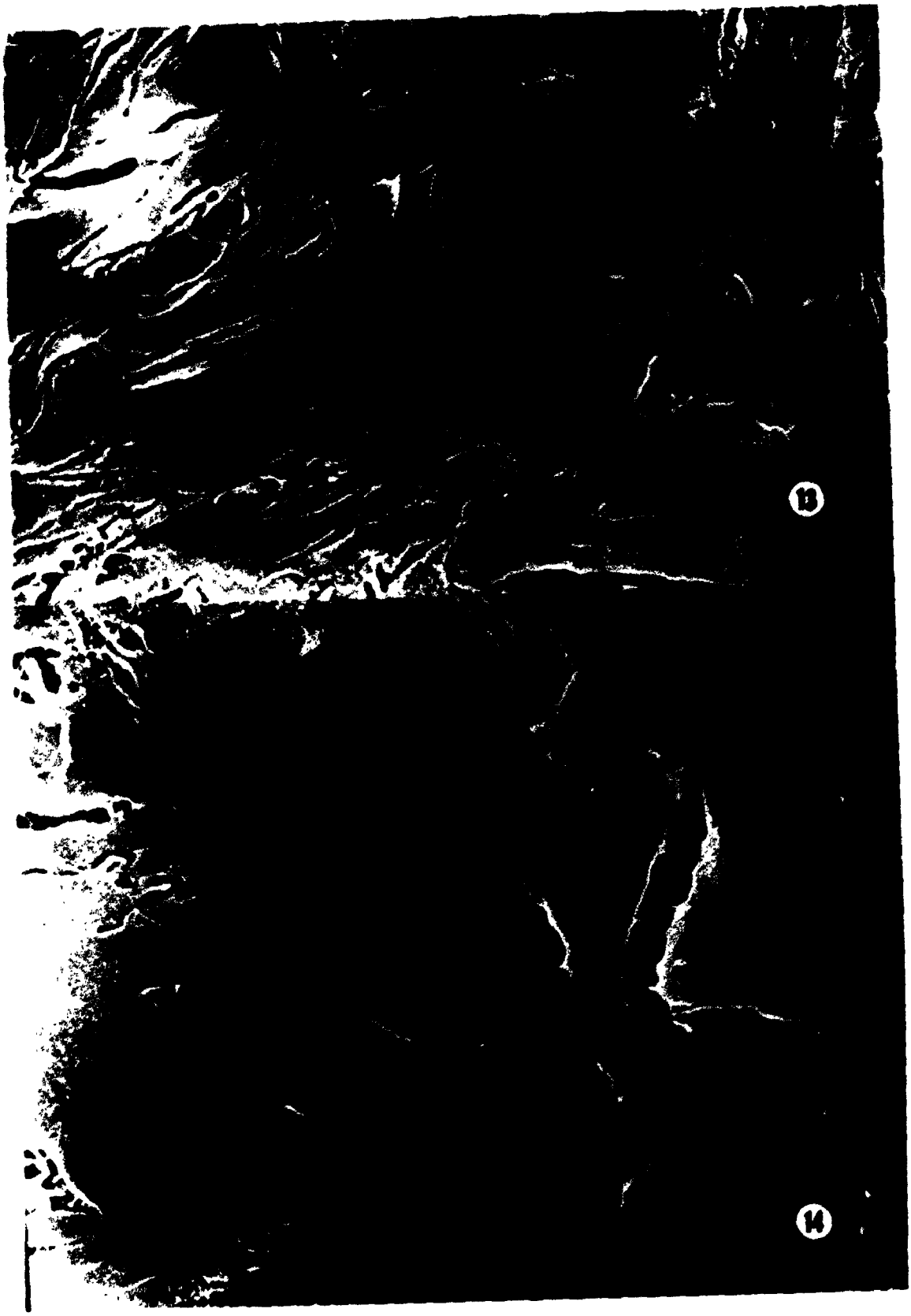
13
14

3.2.2 The growth and orientation of the hemidesmosomes

The appearance of the hemidesmosomes

The basal plasma membrane surfaces of the cell bodies and feet were not smooth but were covered with roughened spots and ridges that corresponded in size, shape and position to hemidesmosomes seen by transmission electron microscopy (fig. 15A and Locke, 1985). The roughness is probably caused by tearing of the links to the basal lamina. They occurred in spots or ridges up to several micrometres long with a uniform width of 0.15-0.2 µm. The hemidesmosomes seen by SEM varied with development in both their shape and distribution.

The development of the hemidesmosomes

Initiation. Early in the stadium from ecdysis until commitment, the hemidesmosomes were either circular or elongated spots not more than 0.5 µm long (figs. 7 & 15B). They occurred all over the exposed surface but were usually missing from the short extensions at the cell periphery. This suggests that only the peripheral extensions are free to move relative to the lamina. Hemidesmosomes rarely occurred at the tips of the feet. This implies that the hemidesmosomes are not directly involved in the extension or perhaps even the orientation of the feet. Once the feet have begun to form, hemidesmosomes may stabilize their positions by anchoring them to the basal lamina, but the tips are free to orient and grow.

Elongation and orientation. In their shape and position the hemidesmosomes initially reflected the lack of orientation of the feet, but at commitment the chains of spot hemidesmosomes fused to form axially aligned ridges even before the feet themselves were axially oriented (fig. 16). The arrangement of the hemidesmosomes is therefore the first recognizable feature showing that the cells know their orientation in the plane of the epidermis. The hemidesmosomes on the feet were mostly spots at this early stage of alignment. They only became elongate and axially aligned when the feet themselves did so (fig. 17).

Contraction. As the larva shortened the feet contracted and reoriented. The hemidesmosomes not only reoriented with the feet but also became

Fig. 15A. Hemidesmosomes (brackets) connect the feet (ef) and the cell bodies to the basal lamina (bl). This thin section was taken from a 5th stadium larva 68 hr after ecdysis. The hemidesmosomes are similar in size and distribution to those seen by SEM, although it is difficult to determine their exact topography. Bar = 0.1 μm.


15
A

Figs. 15B-19. The growth and orientation of the hemidesmosomes (Hd) (fixed with glutaraldehyde followed by osmium tetroxide, tannic acid and uranyl acetate).

Fig. 15B. Early in the stadium the basal cell surface has round or slightly elongate rough surfaced bulges 0.1-0.2 μm across. They correspond to Hd in their size and position. They are rarely seen near the tips of feet (see also fig. 7). The basal lamina is difficult to remove without a short trypsin treatment to break the Hd before critical point drying.

Fig. 16. Prior to elongation, and before the feet are axially oriented, the Hd spots are arranged in rows that are often axially oriented. Some of the Hd are elongated as though Hd spots have fused together.

Bars = 1 μm.

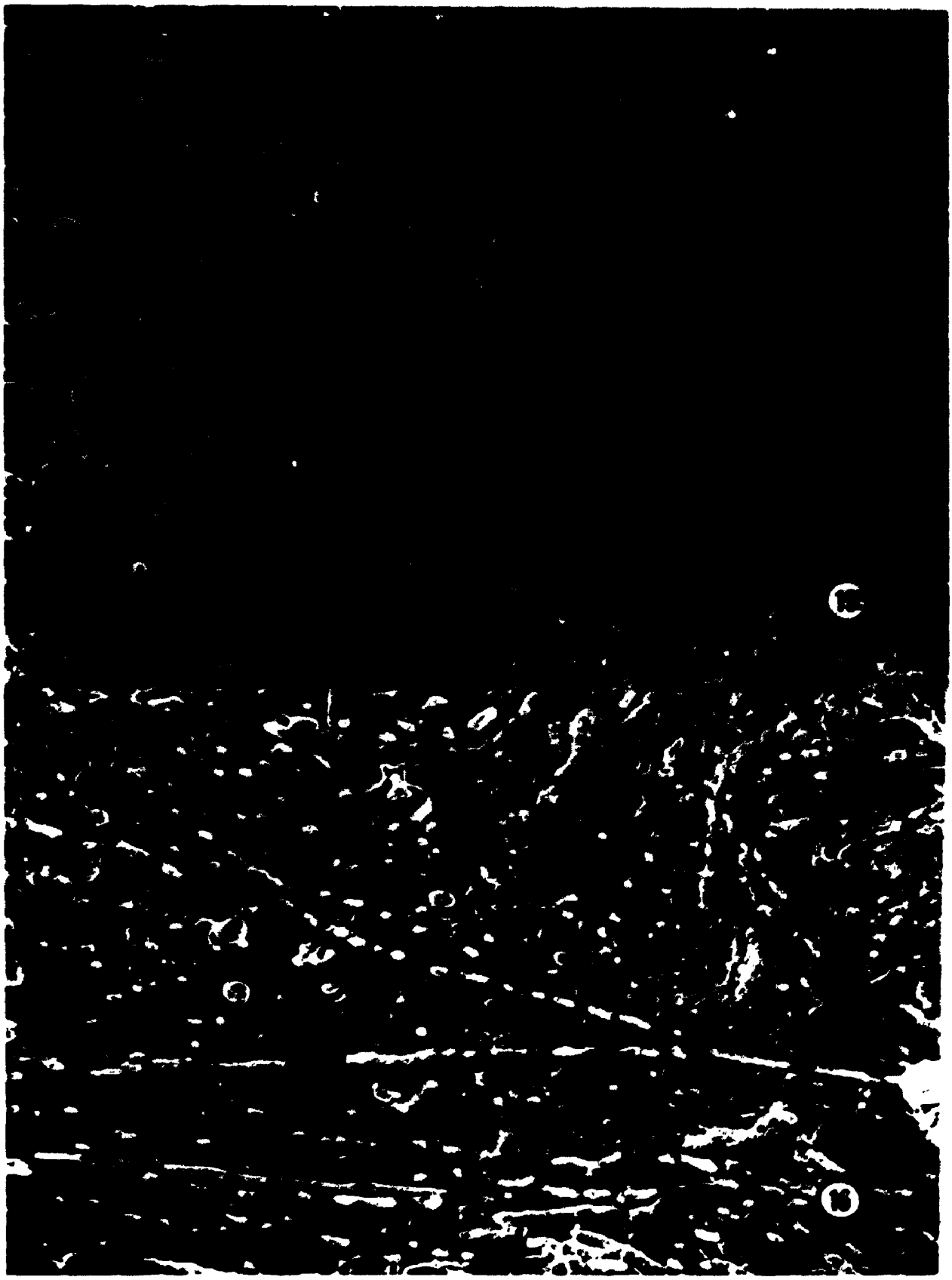
C
O

reoriented on the cell bodies (figs. 17 & 18). They became more branched, perhaps by the fusion of ridges as the basal surface area decreased. Loss of hemidesmosomes must also take place because the density did not increase as the surface area of the cells' bases declined.

At the end of foot contraction the basal lamina could be removed very easily. This is not only because of the loss of hemidesmosomes, because those remaining have about the same density. Presumably the remaining hemidesmosomes form weaker links with the basal lamina. Such weaker links and a loss of connections to the basal lamina would allow the movement relative to the basal lamina needed for both cell rearrangement and the reduction of basal cell surface area.

3.2.3 Basolateral adhesions between cells and feet occur at all stages of development

The mechanical integrity of the integument is maintained mainly by the cuticle and to some extent the basal lamina. Most of the time the epidermis is tightly confluent, with the cells linked especially towards their apical surfaces. There is an adhering apical zonule below which lie septate desmosomes and gap junctions. These have been well described (Fristrom, 1988; Lane, 1982). The basal edges of the cells are united by basolateral adhesions about which much less is known (Locke, 1985). SEM showed that basolateral adhesions outlined all the interdigitating convolutions of the feet and they did so throughout the stadium. They appeared as fine projections between the cells. The projections had a periodicity of about 100 nm and separated the cell surfaces by about 100 nm (figs. 19-21). Since these preparations are subject to much shrinkage the dimensions are only approximate.

SEM visualizes the gold coated surface. It cannot distinguish between plasma membrane and glycocalyx-like surface coats. In order to see if the adhesions with their periodicity were patterns in the plasma membrane or accretions to the surface, gold coated SEM preparations were re-embedded and sectioned for transmission electron microscopy. Sections showed that in regions of adhesion the gold had been deposited over fibrous material external to the plasma membrane (figs. 22 & 23) as has been depicted previously(Locke, 1985). One may therefore picture epidermal cells as being united at their bases as well as at their apices. The basal zonular adhesions are characterized by

Fig. 17. Both spot and elongate Hd are seen when the larva is close to its maximum size. The Hd are elongated in the long axis of the feet. Fine connections hold the feet together.

Fig. 18. The axial orientation of the Hd is lost as the feet and the cells start to rearrange. On the cell bodies the hemidesmosomes are once more strips and circular patches with all orientations. The attachment of the basal lamina to the cells is weak and was easily peeled off after critical point drying even without incubation in trypsin.

Figs. 19 & 20. Fine basal connections (arrowheads) between the cells and their processes occurs at all stages of development of the epidermis during the 5th stadium. Like the hemidesmosomes, these basolateral adhesions are removed easily by the trypsin treatment. The critical point drying used to prepare epidermis for SEM also causes most of the adhesions to separate, unless the cells only shrink a little.

Fig. 21. When the feet are at their maximum length the fine connections (fc) have a periodicity of about 100 nm. They are about 100 nm long and 30-40 nm wide, but these dimensions may be affected by shrinkage.

Bars = 1 µm unless indicated otherwise.

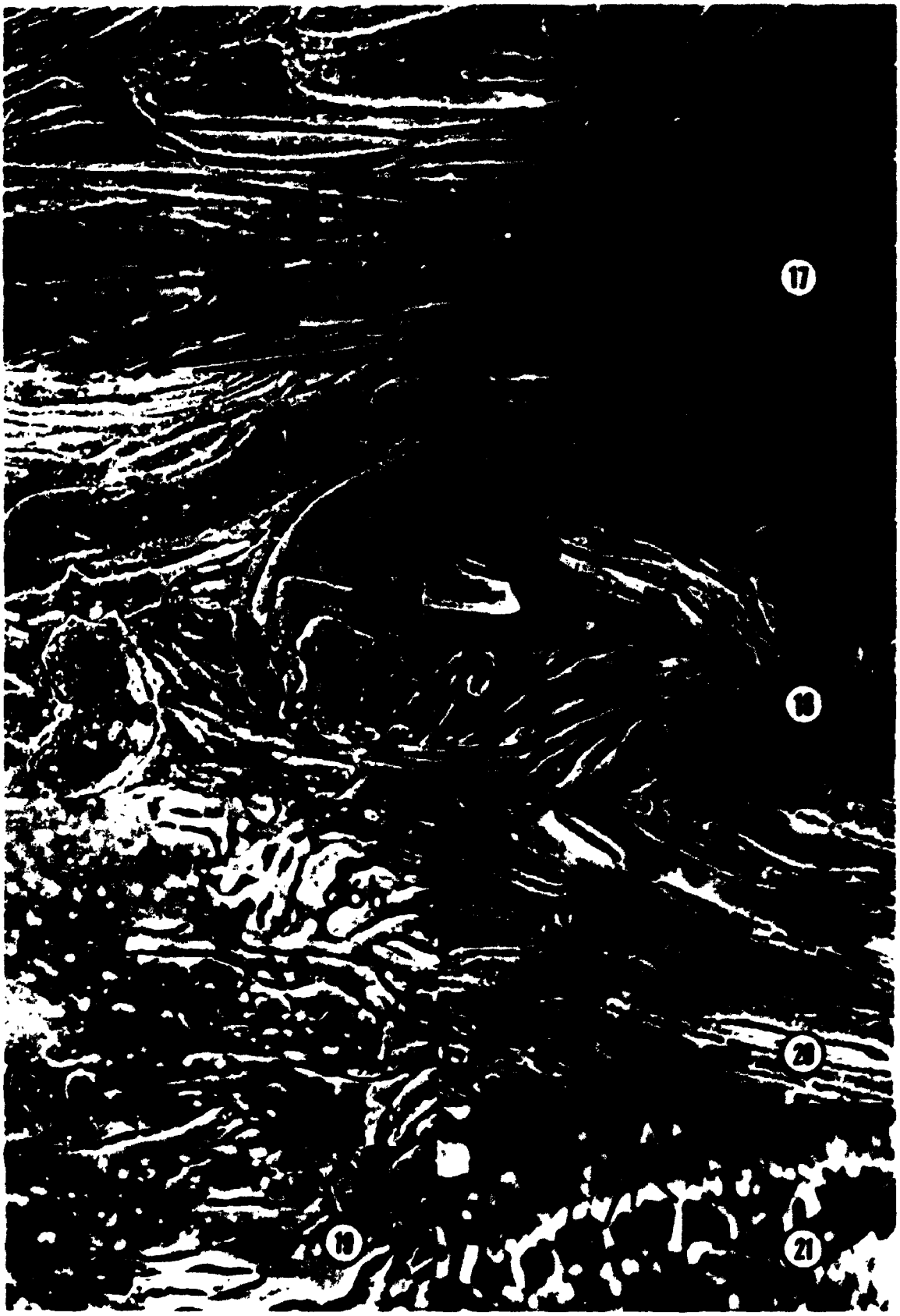
17
18
20
19
21

Figs. 22 & 23. Fine basal connections (fc) between the edges of the cells. This preparation is the same as that used for the scanning electron micrograph in fig. 20. The gold coating shows as an irregular black layer on the surfaces of the cells.

22

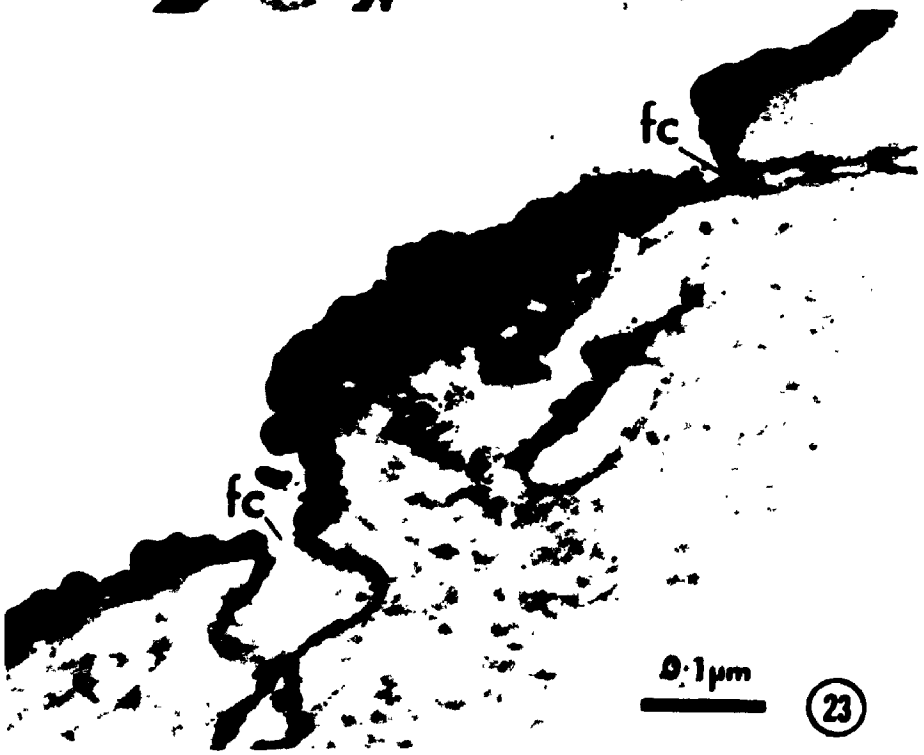

23

being less elaborate than those at the apex, and by outlining all of the tortuous interdigitations of the feet, however complex these become.

3.2.4 The development of lymph spaces between the cells

The demonstration that both apicolateral and basolateral cell margins stick the epidermal cells together, draws attention to the lateral intercellular spaces. In *Rhodnius* and *Calpodes* these spaces have been shown to have some integrity separate from that of the haemolymph (Locke, 1989). Hypotonic media caused the spaces to swell and hypertonic media caused them to shrink. That is, the intercellular lymph spaces behaved like osmometers, swelling and shrinking according to the tonicity of the haemolymph. For this reason the intercellular spaces are referred to as lymph spaces. Their size and shape are greatly affected by growth and development of the feet.

Early in the stadium, when the cells were closely apposed with short feet, the lymph space was relatively small and uncomplicated (figs. 7 & 8). By the time of commitment when the feet had extended, the lymph space became correspondingly complex, following the convolutions of the feet but with little space between the cells (figs. 9-11). During the time from ecdysis to 156 hours the epidermis remained about 5-10 μm thick (fig. 24). There was then a rapid change as cell area decreased, the feet contracted and the cells became columnar. The epidermis was about 25 μm thick by the time ecdysial droplets had formed in the endocuticle. At this time the lateral surfaces of the cells had separated, allowing intercellular spaces as much as 5 μm across to form (fig. 25). The lymph spaces continued to lengthen and broaden basolaterally as the cells became spindle shaped. They were almost completely separate from one another by the time that the ecdysial membrane had formed from the last few lamellae to be secreted (figs. 26 & 29).

By the time that pupal cuticle had begun to be secreted (figs. 27-29), cells were up to 60 μm long and the lymph spaces often extended along most of their length. The bases of the cells had spread out, maintaining their basal contacts but with the nuclei squeezed into tear-drop shapes by the lateral constriction. The epidermis readily fell apart after critical point drying once the premetamorphic ecdysteroid peak had been reached. The greater friability of late as compared with early epidermis after critical point drying is consistent with loss of lateral cell to cell connections as the epidermis ages. Fixation and

Figs. 24-29. Cell apices towards the left.

Figs. 24-27. The development of lymph spaces (from the lab files of M. Locke).

Fig. 24. No lymph spaces are seen in semi-thin araldite sections before the start of the premetamorphic peak although the SEM shows their ramification with the development of the feet (see figs. 7-10; cu, cuticle; ep, epidermis).

Fig. 25. Intercellular lymph spaces (ls) up to 5 μm across form when the feet begin to shorten. Also the epidermis thickens and ecdysial droplets (ecd) form in the inner endocuticular layers.

Fig. 26. The lymph spaces enlarge as the cells become columnar and lose their feet (ecm, ecdysial membrane).

Fig. 27. By the time that pupal cuticle is deposited the lymph spaces extend along much of the height of the cell.

Figs. 28 & 29. The formation of filopodia (fp) upon cell separation. Lateral filopodia up to 5 μm long extend across the spaces between the columnar cells. The separation of the cells is to some extent due to shrinkage, but it shows that the cells are no longer tightly coherent. Earlier in the stadium the cells never separated in this way. Filopodia do not occur until cell separation.

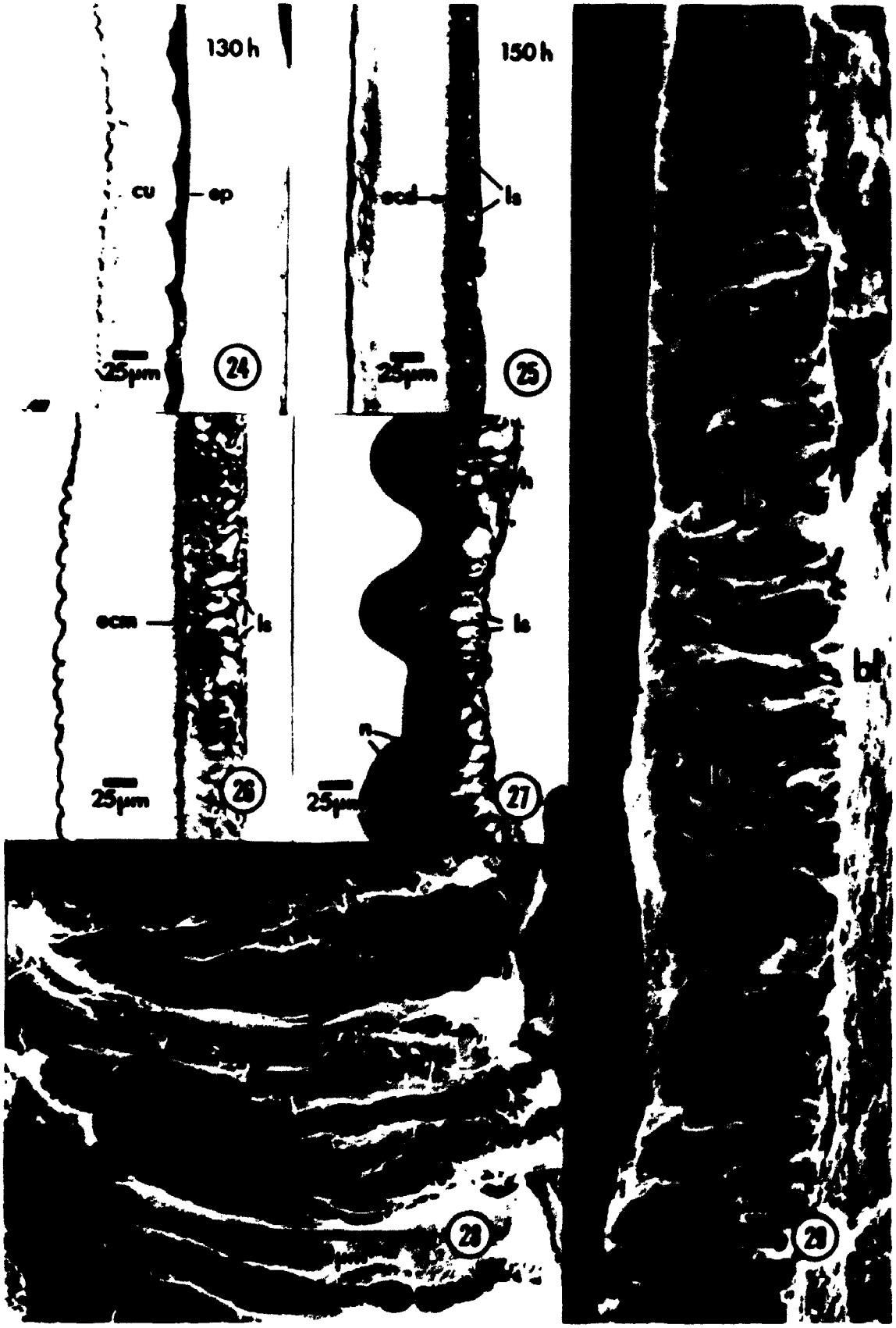
130 h
150 h
cu
ep
ecd
la
25µm
24
25
ecm
la
la
bl
25µm
26
25µm
27
28
28

dehydration probably shrink the cells, widening the space between them so that measurement of its size may be in error, but there can be little doubt that the space exists.

3.2.5 The formation of filopodia and cell separation

As the cells became columnar they remained linked by the feet and the apical junctions although widely separated basolaterally. Filopodia then developed, bridging the gap, to form a new kind of intercellular contact. The newly developed filopodia were up to 5 µm long, confirming the size of the lymph spaces (figs. 28 & 29).

3.3 Discussion

Scanning electron microscopy of the basal surface of the epidermal cells of 5th stage larval *Calpodes* shows that the feet develop in three phases, initiation, elongation and contraction (figs. 2 & 6). The initial growth begins immediately after ecdysis and continues until commitment to pupation 66 hours later. During this phase the feet remain randomly oriented. Elongation and orientation begin after commitment to pupation. Orientation may be achieved by the selective survival and growth of those feet that are axially oriented rather than by reorientation. It is as if there is positive feedback to the growth of axially oriented feet. In the same way microtubules in cultured endothelial cells at the edge of an artificial wound are initially randomly distributed and then become oriented perpendicular to the edge of the wound as they migrate into it (Gotlieb *et al.*, 1981). Kirschner & Mitchison (1986) have developed a model to explain how cells might become oriented, based on the dynamic instability of microtubules (Mitchison & Kirschner, 1984). The essential point about dynamic instability is that only the very ends of these polymers are responsible for maintaining their polymerised state. A small change in this terminus will cause a "catastrophic" depolymerization (Carlier, 1988), meaning that the cell can rapidly change the distribution of its microtubules. Reorientation of the microtubule array could easily be achieved by stabilizing only those microtubules that are in a particular orientation. The others would become unstable with the shift of the tubulin pool into the growing, stabilized microtubules. This may be the mechanism behind the orientation of microtubules in endothelial cells at the edges of wounds. Epidermal feet shortened or were lost in colchicine treated mid-instar larvae which had been

arrested in development by thoracic ligation (Locke & Huie, 1981b). This suggested that microtubules may maintain the shape of the feet. Although the dynamics of microtubules in the epidermal cells has not been investigated, it is possible that they also become oriented by selective stabilisation of the microtubules only in axial feet.

Contraction of the feet occurs late in the stadium coincident with the cells becoming columnar and separating from the old cuticle as the larva shortens to the pupal form. The process is similar to that in the epithelio-muscular cells of *Hydra* ectoderm, or fibroblasts in tissue culture. *Hydra* ectoderm cells change the shape of the body column by extending and contracting basal muscle processes analogous to the feet (Campbell, 1980; Otto, 1977). The feet are not muscles but are like fibroblasts in containing oriented microfilaments and microtubules. Fibroblasts can contract and buckle the rubber sheets on which they are grown (Harris *et al.*, 1980), in much the same way that insect epidermis deforms a newly formed cuticulin surface to create a sculptured epicuticle or puts folds into the basal lamina (Locke, 1985). The feet finally disappear as the cells rearrange themselves into new positions in the pupal epidermis.

The cells might rearrange by sensing and moving along adhesive gradients to a position where they are in an adhesive equilibrium with their neighbours (e.g. Mittenthal & Mazo, 1983; Nardi & Kafatos, 1976a; Nardi & Kafatos, 1976b; Steinberg & Poole, 1982). In the epidermis of *Calpodes* this process may be similar to the way neurons find their way through neural networks of the CNS (Goodman *et al.*, 1984). The termini of neurons have amoeboid growth cones which extend filopodia in all directions to explore the surrounding environment. Goodman *et al.* (1984) have shown that the filopodia may guide the growth cone by adhering differentially to different parts of their surroundings. The growth cone pulls on the filopodia which act like guy ropes, ultimately allowing the neurons to make appropriate synaptic connections. The feet may have a similar function to these filopodia. By adhering to specific cells and regions of the basal lamina, and then contracting, the feet could guide the cells to new positions in the pupal epidermis.

Another main finding is that the lateral margins of the feet continue to be united by adhesions, even when they form complex interdigitations. These adhesions are strikingly similar to those of the apical attachment zone between intestinal epithelial cells seen at high resolution in quick-freeze, deep-etch preparations (fig. 14 in Hirokawa & Heuser, 1981). The filopodia of neuronal

growth cones also have filamentous links 30-100 nm long called adherons (Tsui *et al.*, 1985; Tsui *et al.*, 1988). The periodicity of the adhesions seen by Hirokawa and Heuser would be expected to be close to the natural state because the tissue was fixed by very rapid freezing. However, any viscous material might break up into uniform fragments when dried or when its properties were changed by conventional fixation. The significance of the beaded edges is that they are evidence for something existing at the periphery of the feet which presumably keeps them together. These regions, as well as the basal lamina, bind cationic ferritin when it is used as a tracer for charges at the surfaces of live cells (Locke & Huie, 1983). The basolateral adhesions may form an anionic barrier which haemolymph components would traverse selectively. The intercellular space would then be lymph rather than haemolymph. We are accustomed to thinking about epithelia using vertebrate models, where conspicuous tight apical junctions form a transepithelial barrier and basolateral surfaces are exposed to intercellular fluid derived from blood that has passed through capillary endothelia. This model cannot be transferred directly to insect epidermis.

Many workers have shown intercellular spaces developing in the epidermis before metamorphosis, usually with little or no comment (Diehl *et al.*, 1982; Richards, 1951; Wielgus & Gilbert, 1978; Wigglesworth, 1959). There has always been a suspicion that the cells' untidy appearance might be related more to poor fixation than to their activity. However, there is no doubt that the spaces and irregular outlines exist, indeed would be postulated to exist, knowing that the cells must separate in order to reposition themselves. Large intercellular spaces also form between follicular epithelial cells in *Rhodnius* ovaries allowing passage of yolk proteins from the haemolymph to the developing eggs (Davey, 1981; Huebner & Injeyan, 1980).

The lymph space remains small through most of the stadium, but enlarges with the loss of lateral junctions as the feet contract, eventually extending along most of the length of the columnar cells. This is the time when the cells are no longer firmly fixed apically and basally. They may therefore move relative to one another, leaving the surviving apical junctions stretched out on processes that are slower than the separated lateral surfaces in changing their adhesions to other cells. Filopodia form on the separated lateral surfaces, spanning the gaps as though they have been induced by the separation and loss of lateral cell to cell contact. Filopodia were also seen, but

not initially recognized, in an earlier EM study of the epidermis as it became columnar and formed intercellular spaces (figs. 37 & 38 in Locke, 1985). This points out the need for SEM as an aid in the interpretation of TEM profiles in three dimensions. Filopodia form on *Rhodnius* epidermal cells separated from one another experimentally and on *Calpodes* fat body cells that have separated during pupal development and are about to reunite to form adult tissue (Locke, 1987). In these examples the filopodia probably serve to sense nearby cell surfaces and to draw the cells back together again. It is surely not a coincidence that filopodia only form naturally in *Calpodes* epidermal development at the same time as the cells separate and move relative to one another.

Scanning electron microscopy also shows that hemidesmosomes are linear structures having a constant width of 0.15-0.2 μm and a variable length. The basic subunit may be a small circular hemidesmosome spot having the same diameter as the width of the linear structure (this is the same size as the subunits of fragmented focal adhesions; Woods & Couchman, 1988). They arise in these short sections and lengthen by the linear addition of more spots. Linear hemidesmosomes on the cell body reflect the axial alignment of the cells even before they appear on the feet. Oriented hemidesmosomes are therefore the first overt sign of axial orientation. They are probably similar to the stress fiber focal adhesions that attach tissue culture cells to the substrate (Woods & Couchman, 1988).

The hemidesmosomes act as anchors between the feet and the basal lamina, but they must also move or break as the cells themselves move or the feet change their orientation. Chen *et al.* (1984) have found that some transformed cells probably have membrane associated proteases which locally digest their connections to the substrate. Such local digestion could explain how the "stable" hemidesmosomes allow feet to elongate and change orientation. A less localized production of proteases could cause the loss of adhesion with the basal lamina found late in the stadium. This also fits with the observation that a short incubation in trypsin causes the hemidesmosomes to lose their connection with the basal lamina (fig. 20 in Locke, 1987).

Calpodes epidermis is made up of siamese twin cells, sibling cells that remain united by midbodies persisting from mitosis to mitosis (Locke, 1988; Locke & Leung, 1985b). These twins resemble one another in having identical or mirror image patterns of some nuclear (nucleoli) and cytoplasmic (actin bundles) components (Delhanty & Locke, 1990a and chapter 4). In spite of this,

adjacent cells do not have identical or even similar patterns of feet. The shape of the feet is therefore not inherited like the nucleolar patterns or numbers of actin bundles. There is a dogma derived from vertebrate studies that dividing cells carry out few other activities. For example, many tissue culture cells round up and lose their processes when beginning to divide. This clearly does not apply to *Calpodes* epidermal cells which divide frequently after commitment to pupation without any change in their feet.

CHAPTER 4

THE CONSERVATION OF A CYTOSKELETAL PATTERN IN EPIDERMAL CELL DOUBLETS

Where, like a pillow on a bed,
..A pregnant bank swelled up to rest
The violet's reclining head,
Sat we two, one another's best.

John Donne, 1633

4.1 Introduction

The previous chapter describes the changing shapes of the epidermal cells as they prepare for metamorphosis. Although difficult to analyze exactly, the cells never resemble one another in their outward form. This is probably because cell shape is not inert but continually changes, and is changed by, the shapes of neighbouring cells. However, certain internal structures do resemble those in adjacent cells.

The epidermis of fifth instar *Calpodes ethlius* forms a sheet of Siamese twin cells by the maintenance of midbodies between daughter cells from one mitosis to the next (Locke, 1988; Locke & Leung, 1985b). The nuclei of these epidermal cells and those of other lepidopteran larvae have repeated cycles of nucleolar unravelling and condensation (Locke & Leung, 1985a; Tuck & Locke, 1985). In spite of this, the nuclei of sibling twin cells have paired nucleolar patterns that begin as mirror images after mitosis. A component of the cytoplasm containing actin filaments which also exists in paired patterns is described here. The situation is reminiscent of the paired mirror image patterns of stress fibres in dividing 3T3 cells (Albrecht-Buehler, 1977), and is evidence for the replication and transient inheritance of a cytoplasmic pattern. This chapter describes paired patterns of actin filaments in epidermal cell doublets as they develop in the molt-intermolt cycle of 5th stage larvae of *Calpodes ethlius*. The filaments occur in bundles associated with a particular kind of pore canal. The results suggest that there are somatic determinants of pattern which conserve some aspects of both nuclear and cytoplasmic architecture between mitoses in normal tissue development. However, the number of bundles also correlates

with cell size although not with nuclear area. The pairing of the number of bundles may therefore relate to sibling cells retaining the same ploidy.

4.2 Results

4.2.1 Epidermal cells have apical bundles of F-actin

One day after ecdysis to the fifth stadium, epidermal cells labelled with rhodaminyl phalloin showed sharply defined spots of fluorescence close to their apical surfaces (figs. 30 & 64). Since the reaction is specific for F-actin (Warn & Magrath, 1983; Wieland & Govindan, 1974) and electron microscopy showed the spots to contain microfilaments (fig. 65), they will be referred to as actin bundles. The bundles varied in their shape and number per cell, in their distribution over the integument, and with the time of larval development.

Cells commonly contained one or two bundles, occasionally three or more. Counts on light micrographs in regions selected for the clarity of pairing, and therefore biassed in favour of higher numbers of bundles (fig. 30), showed the following frequencies: 1 per cell, 55.2 %; 2 , 35.2%; 3, 8.8%; 4, 0.7% ; 5, 0.1%. Cells without bundles presented a problem in this study. They might never have had bundles, the bundles may have been lost a few hours after ecdysis (see 4.2.2) or else they are fixation artefacts. I chose to observe the cells 24 hours after ecdysis because this is when most of the bundles are at their most conspicuous, thus any bundles which had been lost just after ecdysis could not be counted. Because of the possibie ambiguity I decided to exclude cells without bundles from the data.

The bundles occurred almost uniformly in the dorsal epidermis but were absent from the ventral surface and muscle insertions. The distribution did not correlate with the tendency of dorsal tubercles to melanize. Regions of melanized integument did not necessarily have epidermal cells with bundles and regions of cells with bundles did not always correspond with areas of melanized cuticle (figs. 31-38). However, the cells which appear to contain no bundles may just have lost them prematurely.

4.2.2 Actin bundles appear transiently after the 4th-5th ecdysis.

The timing of the formation of actin bundles in relation to mitoses and the presence of midbodies during the fourth and fifth stadia is summarized in figure

Fig. 30. The pairing of microfilament patterns in a group of epidermal cells presumed to be connected by midbodies (MB, microfilament bundle; m? profiles of peripheral F-actin, probably mostly consisting of filaments beneath the apical adhering zonules).Bar = 10 μm.


mz

Figs. 31-38. There is no correlation between the occurrence of apical actin bundles (MB) and melanization of the cuticular tubercles (tu) overlying them. Each row represents the same field of view. On the left is the rhodaminyl phalloin labelled epidermis and on the right the corresponding bright field view of the cuticle.

Figs. 31 & 32. An area of cells with few actin bundles overlain with melanized cuticle.

Figs. 33 & 34. An area of cells with many actin bundles overlain with melanized cuticle.

Figs. 35 & 36. An area of cells with few actin bundles overlain with incompletely melanized cuticle.

Figs. 37 & 38. An area of cells with many actin bundles overlain with incompletely melanized cuticle.

Bars = 10 μm.

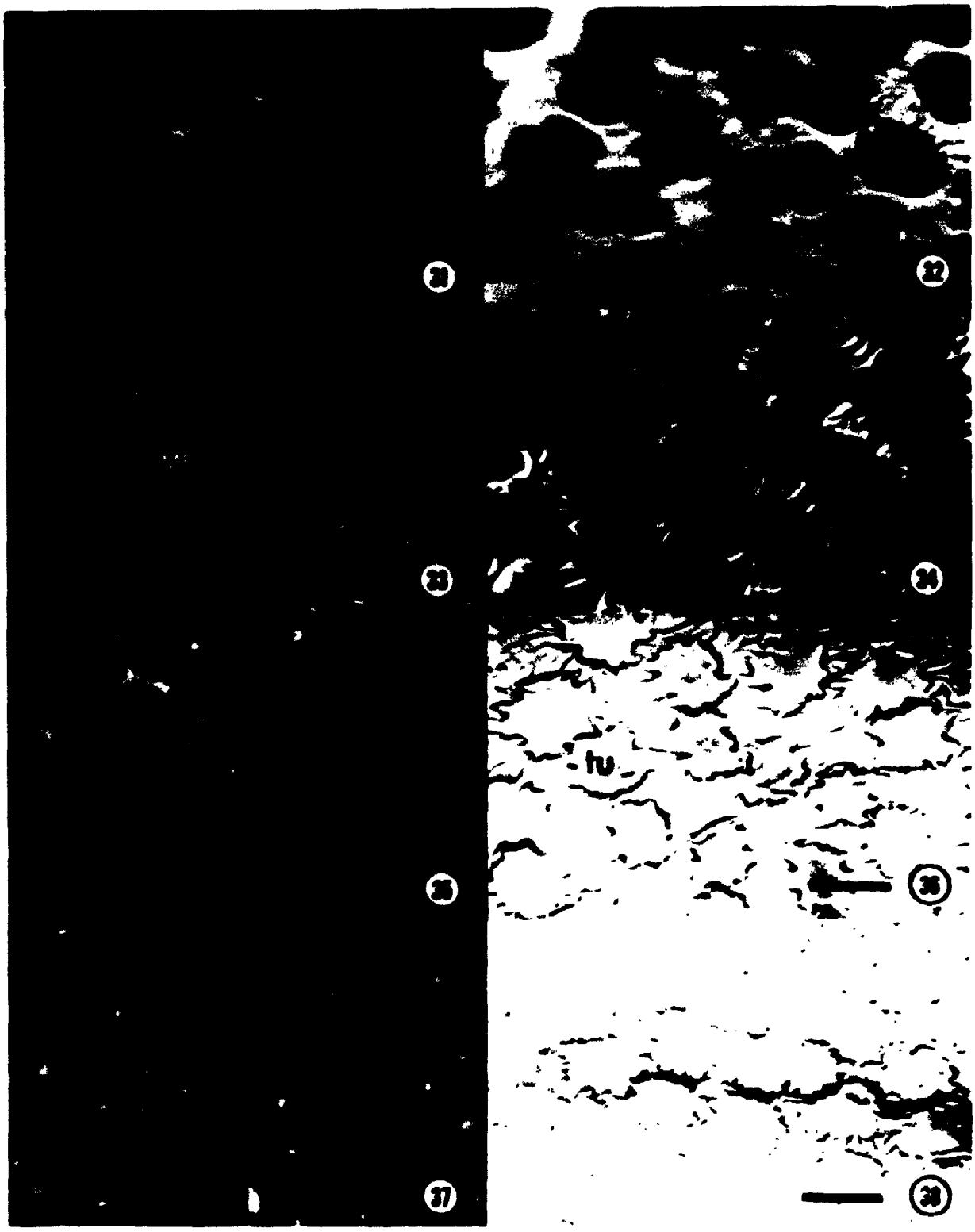
31
32
33
34
tu
35
36
37
38

39. Controls for autofluorescence of the integument and specificity of rhodaminyl phalloin labelling are shown in figures 40 & 41.

Actin bundles do not occur until the fifth stadium.

Actin bundles did not occur in the epidermis during the third to fourth moult, but the fluorescence of other actin components showed binding by rhodaminyl phalloin. The nuclei obscured much of the weak fluorescence from the apical web and microvilli at the apical surface, but both microfilament zonules and contractile rings between newly divided cells fluoresced (fig. 42). No strongly fluorescent spots (figs. 43 & 44) characteristic of apical actin bundles were seen in the 4th stadium epidermis. Therefore the bundles are probably a premetamorphic rather than a moult related activity.

The development of microfilament bundles during the fifth stadium

Actin bundles first appeared at the apical cell face just before ecdysis to the fifth stadium (fig. 45). They remained indistinct and uncountable, mixed with numerous small subapical particles (fig. 46), until a day after ecdysis (fig. 47) when the bundles had matured, appearing as brightly fluorescent spots. Coinciding with this the subapical particles became less distinct suggesting that they may store actin for incorporation into the apical bundles. The bundles were either simple rods or short segments of helices projecting a comma-like profile. They were usually located in the centre of the apical surface, although sometimes they were close to the edge, perhaps pulled there by their attachment to the cuticle.

The bundles persisted until about thirty hours after ecdysis (figs. 48 & 49) disappearing 5 hours later (fig. 50). The bundles did not reappear in the fifth or early pupal stadia (fig. 51).

4.2.3 The number of actin bundles is paired in adjacent cells

A day after ecdysis to the fifth stadium the actin bundles were brilliantly labelled with rhodaminyl phalloin and could be counted in each cell. The only problem lay in the plane of focus being too shallow to include all the bundles in the photographic record. Composite photographs were necessary, especially where the epidermis was not flat over the large area of cells to be surveyed.

Fig. 39. The timing of epidermal mitoses in relation to the presence of midbodies and the formation of microfilament bundles during the fourth and fifth stadia (midbody data from Locke & Leung, 1985; mitosis data from Locke, 1970).

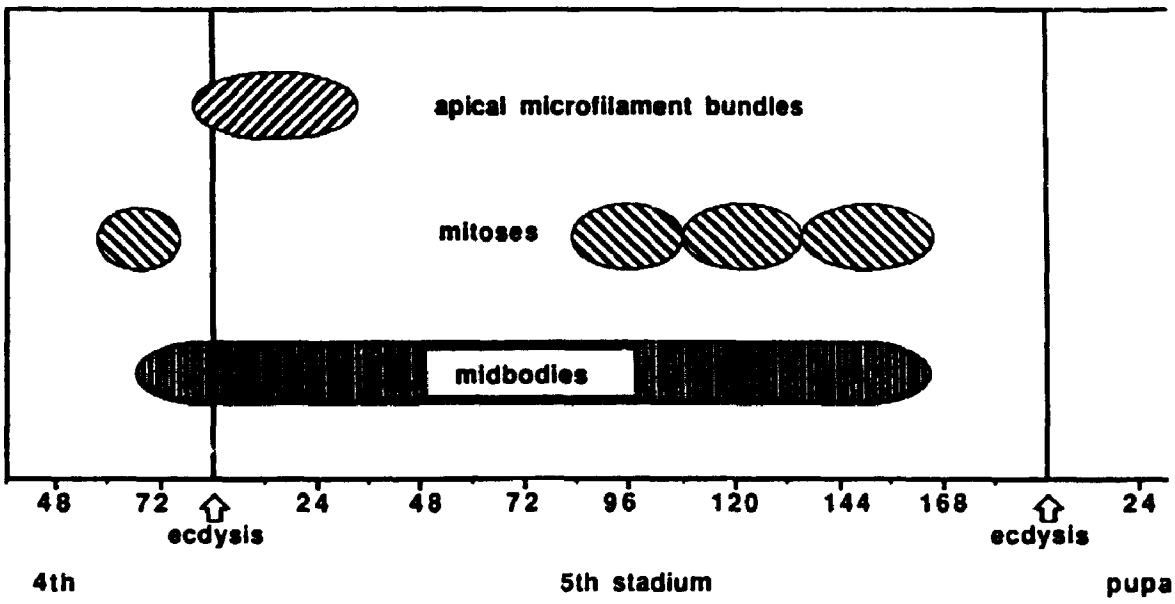
apical microfilament bundles
mitoses
midbodies
48
72
ecdysis
24
48
72
96
120
144
168
ecdysis
24
4th
5th stadium
pupa

Fig. 40. Epidermis without stain has no autofluorescence.

Fig. 41. Preincubation in 10 μg/ml phalloidin blocked labelling of the cells with rhodaminyl phalloin, showing that the staining observed in other preparations locates F-actin.

Figs. 42-44. Microfilament bundles are absent in the fourth stadium.

Fig. 42. Each cell is outlined by its microfilament zonule and some newly divided cells have contractile rings but there are no bundles. Two to three hours before third to fourth ecdysis.

Fig. 43. There are no microfilament bundles at the third to fourth ecdysis although the apical cortex and microvilli show up faintly The nuclei (n) occupy darker areas where they appear to have masked the fluorescence from the apices of the cells.

Fig. 44. There are no microfilament bundles early in the fourth stadium while there are many at the corresponding time in the fifth (see fig. 47).

Fig. 45. Microfilament bundles appear on the apical face just before ecdysis to the fifth stadium. There are also smaller labelled foci (sp) in other parts of the cell.

Bars = 10 μm.

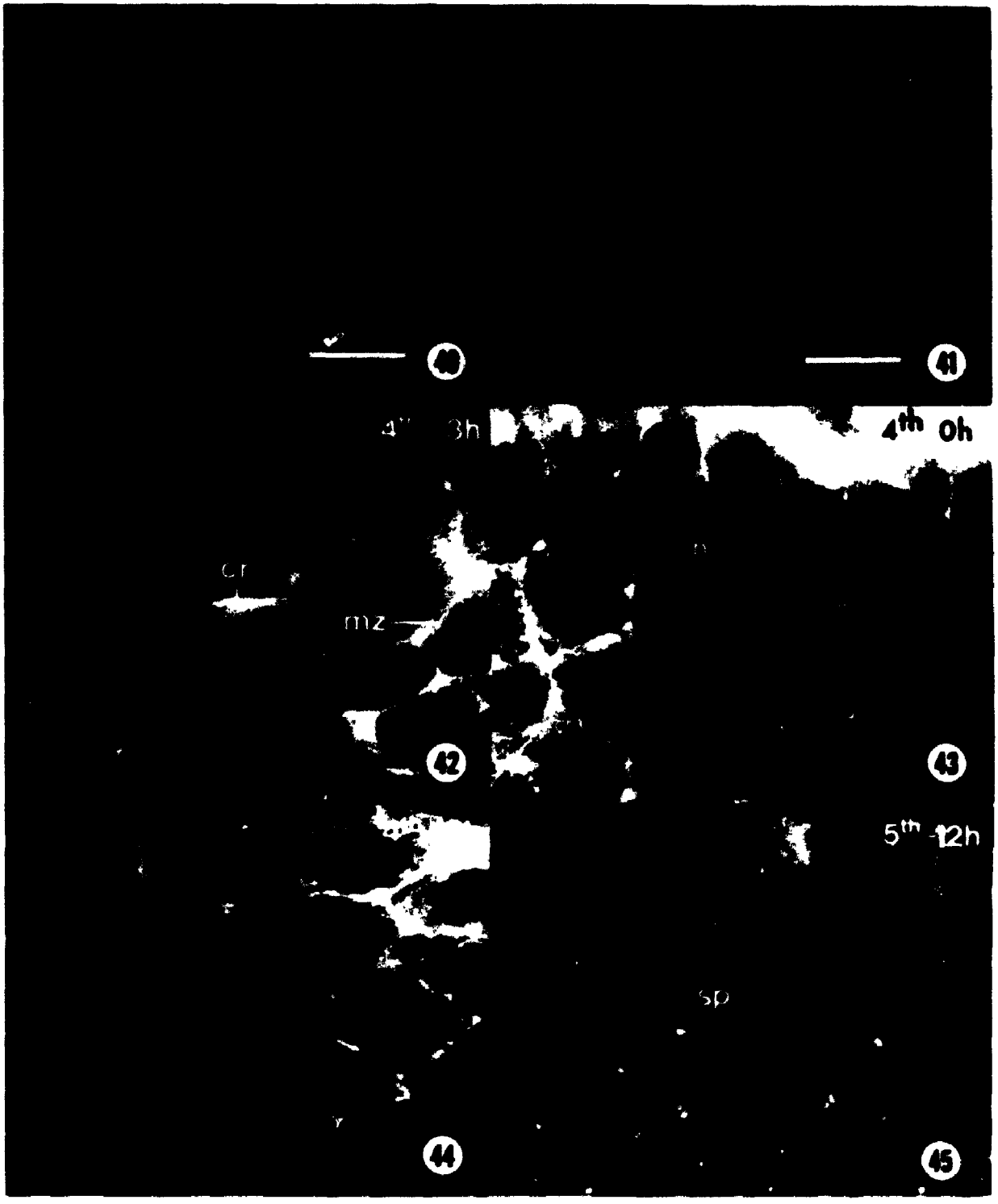
40
41
4th 0h
cr
mz
42
43
5th 12h
sp
44
45

Figs. 46-51. The development of microfilament bundles after ecdysis to the fifth stadium.

Fig. 46. The bundles are indistinct immediately after ecdysis but smaller particles are abundant.

Fig. 47. Twenty hours into the stadium many smaller particles have disappeared and the bundles (MB) have enlarged to become rods or short helices with comma-like profiles.

Fig. 48. By twenty seven hours there are no small particles and the cells have one or two, rarely three or more bundles with distinct outlines.

Fig. 49. By thirty hours the bundles are less distinct as if they are breaking up.

Fig. 50. By thirty five hours the bundles are absent and do not reform.

Fig. 51. Microfilament bundles do not form in the pupa.

Bars = 10 μm.

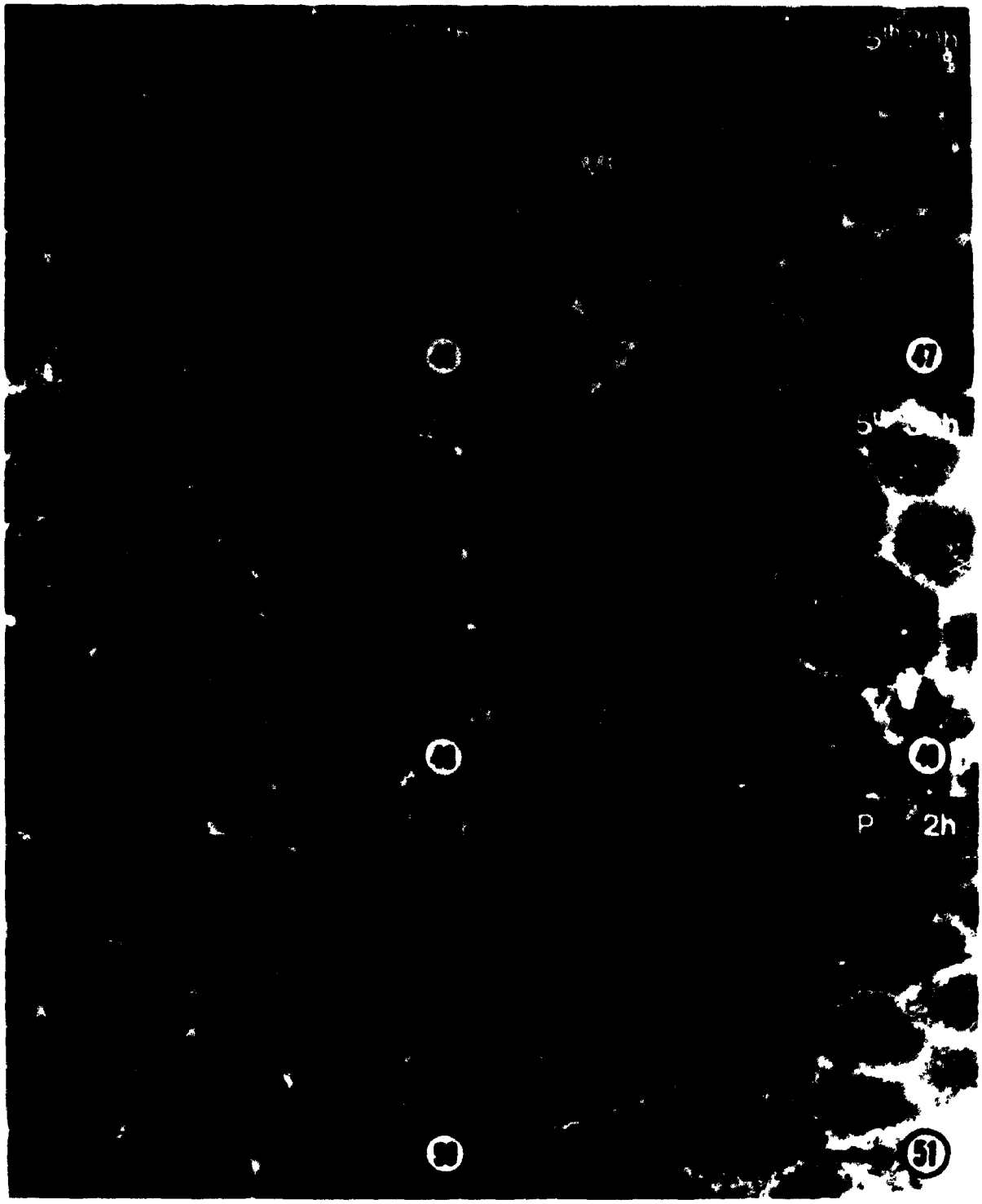
P
2h
51

Each cell resembled one of its nearest neighbours with respect to the number of apical actin bundles that it contained (fig. 30). Because most cells only contain one or two bundles the reality of the pairing is difficult to confirm. However, even the rare cells containing three or more bundles usually had a similar neighbour (e.g. figs. 54-58). The few exceptions could be errors of observation because of the shallow plane of focus or because the cell observed had not recently divided. A statistical analysis of 617 pairs of cells from randomly chosen areas of epidermis showed that the pairing of cells observed is perhaps real, even taking into account the large number of cells with only one or two bundles ($P < 0.005$, see appendix).

The bundles usually had the simple profile expected for a short rod (e.g. figs. 52 & 54). Occasionally more complex shapes could be seen to be conserved in paired cells (fig. 59). The Y-shapes seen by light microscopy of whole mounts also occurred as branched bundles in thin sections of cuticle when examined by electron microscopy.

4.2.4 The relation between ploidy and the number of bundles

Cell and nuclear area, rough indicators of ploidy, were compared with the number of actin bundles in each cell.

Cell area vs. number of bundles

Three categories of cells were used for analysis, those with one, two and three or more bundles. The areas referred to here are those delineated by the apical microfilament zonule (e.g. fig. 30). Analysis of variance of over 500 cells showed that there was a significant difference between the mean areas of the three groups chosen ($P<0.001$, table 1). The mean areas progressively increase with increasing numbers of bundles (fig. 60). Pairs of means from each category also show significant differences using the t–test (table 2).

Nuclear projectional area vs. number of bundles

Epidermis was simultaneously labelled with rhodaminyl phalloin and Hoechst 33258 (e.g. figs. 61-63). Analysis of variance of nearly 192 cells showed that nuclear area was not correlated with the number of bundles of actin ($P>0.1$, table 3). This is not surprising considering that the packing of chromatin varies with its stage in the cell cycle and nuclear area correlates

Figs. 52-58. The pairing of adjacent cells with respect to the number of their bundles.

Fig. 59. Some cells have bundles with paired shapes as well as number.

Bars = 10 μm.

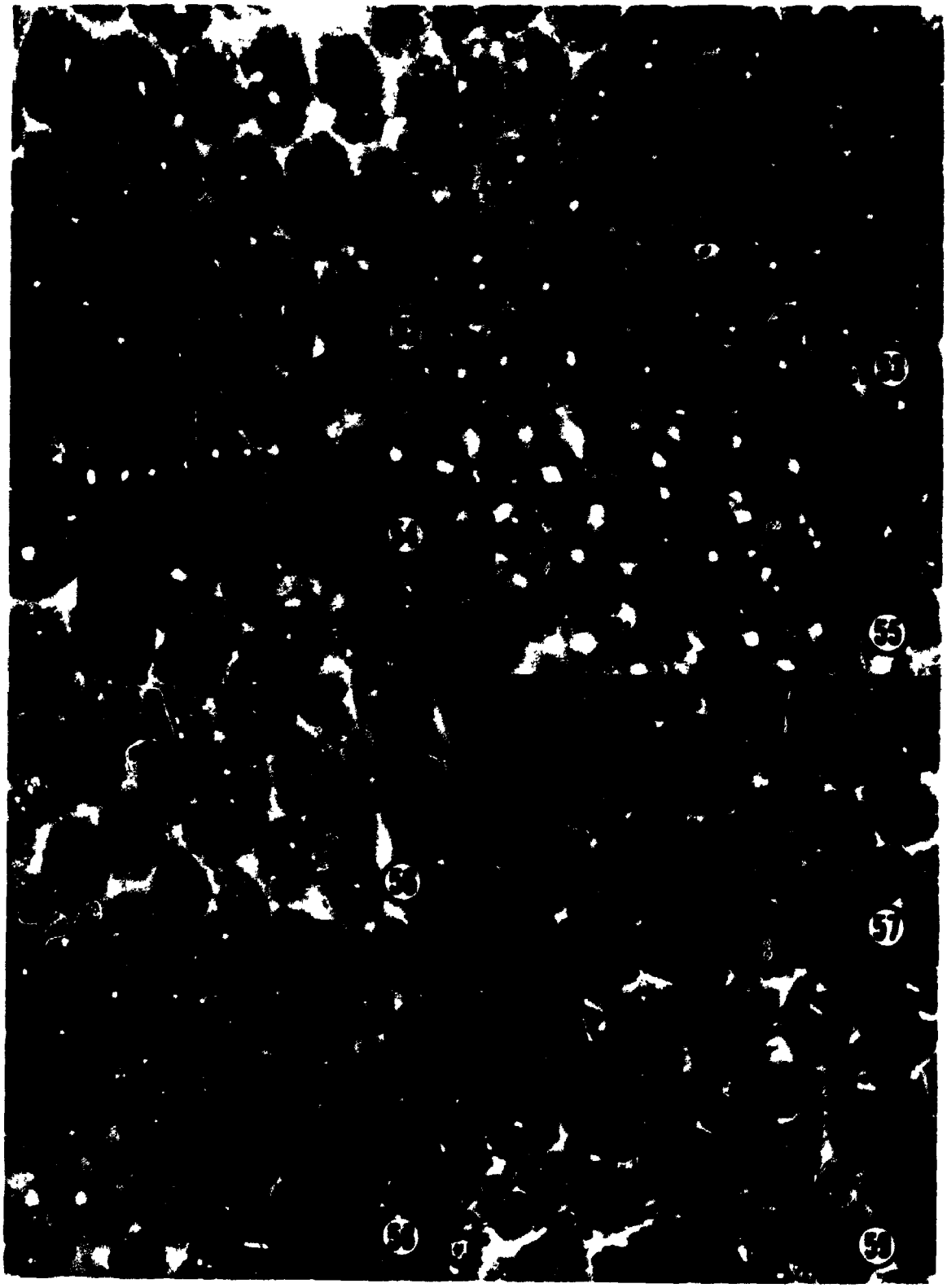

Table 1. Calculation of the probability that cell area varies with the number of actin bundles.

Source	Sum of squares	Degrees of freedom	Mean squares	F-ratio	Probability
Between bundle #	62490.671	2	31245.335	19.663	P<0.001
Error	831064.639	523	1589.034		
Total	893555.310	525			

Data from appendix 3.

Analysis of variance between the mean areas (μm^2) of three groups of cells. The groups are defined by the number of actin bundles the cells contain, in this case 1, 2 and 3 bundles.

Fig. 60. Cells with different numbers of bundles have significantly different mean areas. Cells with more bundles have greater mean areas (vertical bars represent standard error of the mean, SEM for cells with one bundle = ± 2.231, two bundles = ± 2.819, three bundles = ± 6.853). There is a significant difference in mean area between cells with one and two, and between cells with one and three bundles ($P < 0.001$, tables 2a, b). The difference between mean areas of cells with two and three bundles is less obvious ($P=0.027$, table 2c).

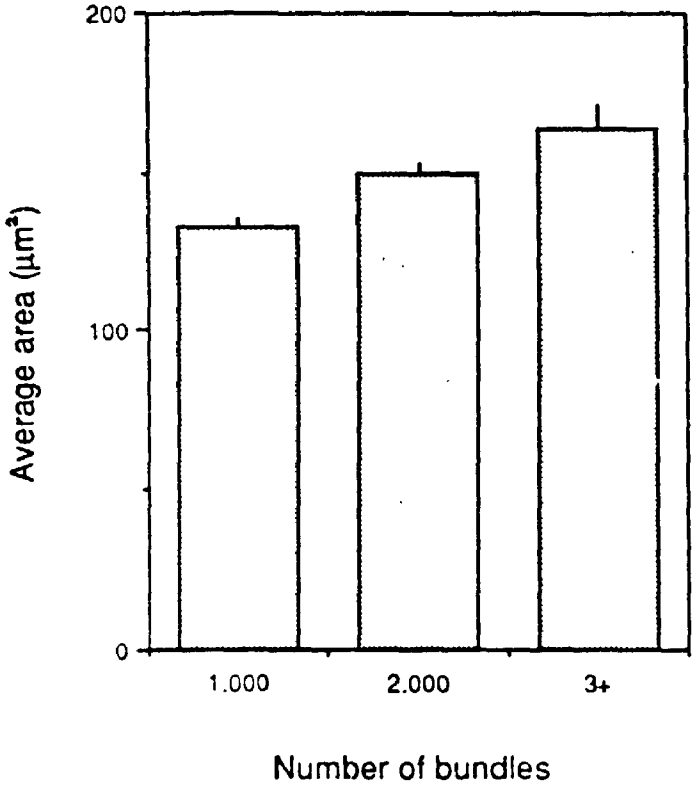
200
100
0
Average area (µm²)
1.000
2.000
3+
Number of bundles

Table 2. Variance between groups with different numbers of bundles examined using the t-test.

Table 2a.

Variable:	1. cells with 1 bundle	2. cells with 2 bundles
Mean:	132.659	149.801
Std. deviation:	35.630	41.436
Observations:	255	216
t-statistic:	-4.827	
Degrees of freedom:	469	
Significance:	P<0.001	Ho: $\mu 1 = \mu 2$

Table 2b.

Variable:	1. cells with 1 bundle	3. cells with 3 bundles
Mean :	132.659	164.418
Std. deviation:	35.630	50.823
Observations:	255	55
t-statistic:	-5.516	
Degrees of freedom:	308	
Significance:	P<0.001	Ho: $\mu 1 = \mu 3$

Table 2c.

Variable:	2. cells with 2 bundles	3. cells with 3 bundles
Mean:	149.801	164.418
Std. deviation:	41.436	50.823
Observations:	216	55
t-statistic:	-2.226	
Degrees of freedom:	269	
Significance:	P=0.027	Ho: $\mu 2 = \mu 3$

Data from appendix 3.

Figs. 61 & 62. Neither the size nor the intensity of staining of the nucleus correlates with the number of actin bundles in cells double-labelled for F-actin and DNA.

Fig. 61. Cells with two bundles of F-actin (A) have nuclei which are neither larger nor more intensely stained (B) than those with only one bundle.

Fig. 62. There is variation in the size of nuclei without a corresponding variation in the number of bundles.

Figs. 63. A few cells are binucleate, single and contain several bundles.

Bars = 10 μm.

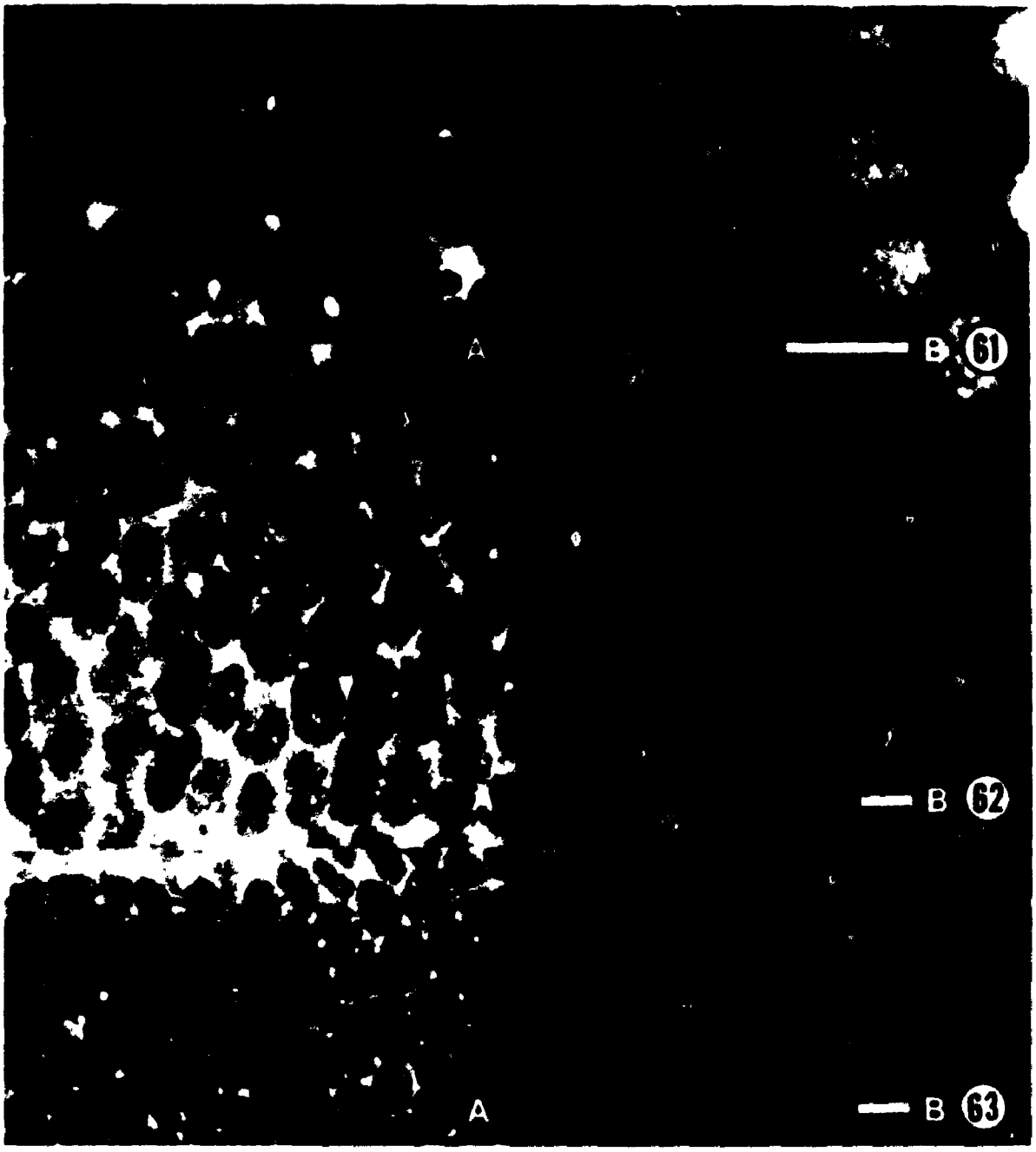
A
B 61
B 62
A
B 63

Table 3. Calculation of the probability that nuclear area varies with the number of actin bundles.

Source	Sum of squares	Degrees of freedom	Mean squares	F-ratio	Probability
Between bundle #	175.523	2	87.762	1.255	P=0.287
Error	13211.580	189	69.903		
Total	13387.103	191			

Data from appendix 4.

Analysis of variance between the mean nuclear areas (μm^2) of three groups of cells. The groups are defined by the number of actin bundles they contain, 1, 2 or 3.

poorly with the ploidy (Nagl, 1978). However, the intensity of staining expected with increasing ploidy was not observed.

Binucleate cells

Binucleate cells were seen occasionally (fig. 63). They had larger numbers of bundles perhaps because, although cytokinesis had not occurred, the cytoplasm had replicated and segregated. This shows that segregation can occur without cytokinesis. This special case of polyploidy may show a direct link between ploidy and bundle number.

4.2.5 The structure of the bundles

The apical location of the bundles suggested that they might have an association with the overlying integument. The epidermis was stripped from the cuticle which was then exposed to rhodaminyl phalloin. Fluorescent spots were still seen in oblique optical sections through the stained integument (fig. 64), showing that the bundles extended into the cuticle. Sections of integument showed cytoplasmic projections like giant microvilli extending for at least one µm into the integument (fig. 65, 69 & 70). Since cells have so few bundles, finding them in thin sections required a lengthy search. Bundles were seen in thicker sections with microfilaments aligned parallel to their long axes (fig. 65).

4.2.6 The bundles are associated with a transverse cuticle component.

Typical pore canals - channels containing a central filament with bundles of finer filaments similar to those traversing the epicuticle (Neville, 1975) - have not been seen in *Calpodes* (Locke, 1961). Nevertheless, the dorsal integument is traversed by a particular kind of helical structure having the same dorsal distribution as the cells with apical actin bundles. These helical structures were easily visible by light microscopy of whole mounts stained with haematoxylin (fig. 66). They were difficult to find in sections prepared for electron microscopy, partly because of their low frequency and partly because their staining properties were similar to the cuticle surrounding them. Toluidine blue stained semi-thin araldite sections showed the bundles extending into the cuticle as helical wisps of material (fig. 67). Electron micrographs showed helical microfilament bundles continuing into the cuticle as helical discontinuities in the

Figs. 64 & 65. The structure of microfilament bundles.

Fig. 64. An oblique optical section through the integument shows that the bundles (MB) project apically into the cuticle (cu). Confocal epifluorescence (ep, epidermis). Bar = 10 μm.

Fig. 65. The bundles extend into the deposition zone of the endocuticle. Thick sections show membrane bound apical processes with parallel microfilaments (Mf) oriented normally to the plane of the cuticle.

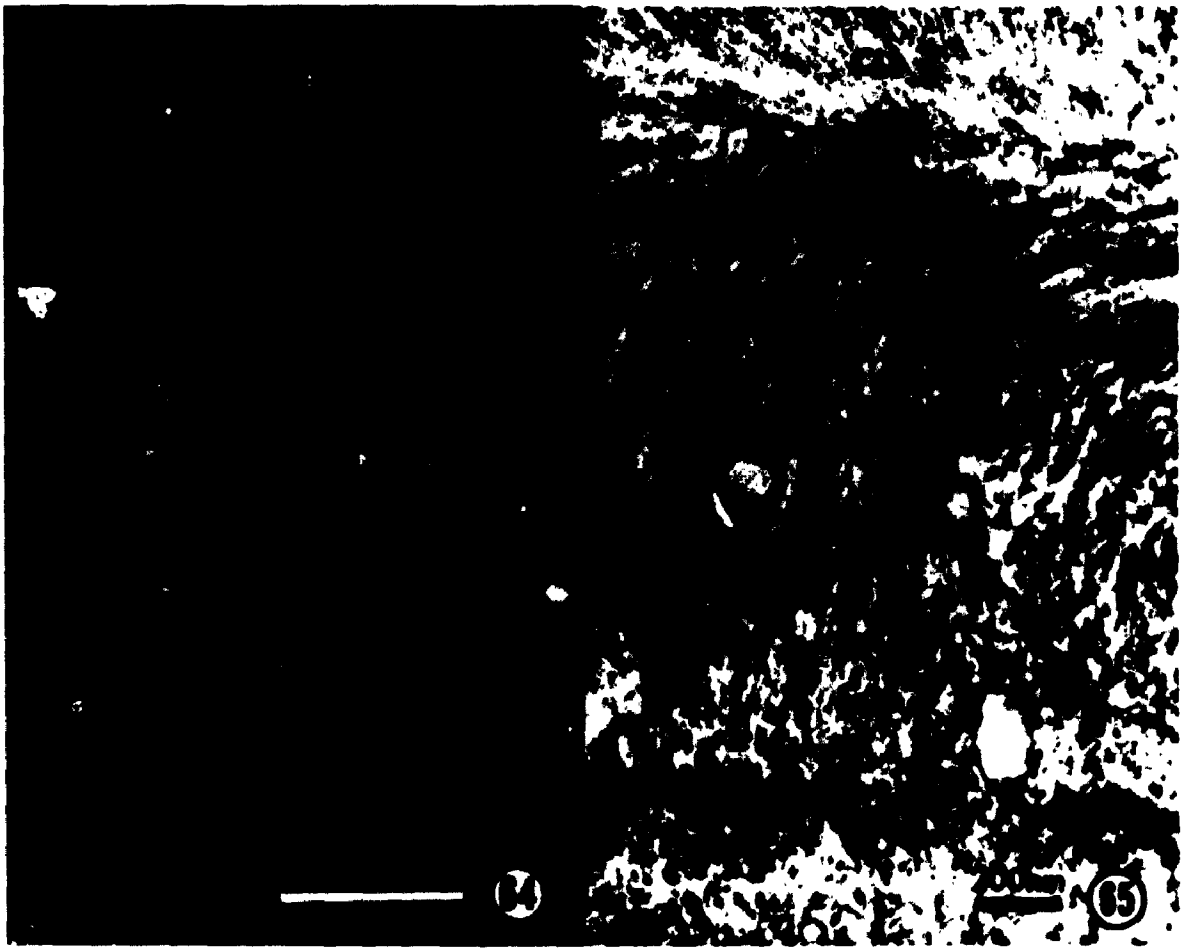
(A)
(B)

Figs. 66-70. The bundles are associated with cuticular structures resembling pore canals.

Fig. 66. Helical cuticular structures resembling pore canals (pc) have the same frequency and distribution as the bundles. Light micrograph of whole integument stained with mercury mordanted haematoxylin (from the lab files of M. Locke).

Fig. 67. Wisps of stained material extend from the epidermis (ep) into the cuticle (cu). Light micrograph of a toluidine blue stained semi-thin araldite section of tissue fixed for electron microscopy.

Fig. 68. The pore canal-like structures show up as disturbances to the helicoidal architecture of the cuticle (arrowheads). Electron micrograph of a near tangential section through unstained cuticle (from the lab files of M. Locke).

Fig. 69. Bundles (MB) extending into the cuticle are often S-shaped, suggesting the helical pattern seen in rhodaminyl phalloin stained preparations (fig. 48) and the mercury stained structures (fig. 66).

Fig. 70. Bundles lie beneath a helical column of cuticle different from that surrounding it (see also figs. 67 & 68).

Bars = 10 µm unless indicated otherwise.


cu
66
67
cu
69
70

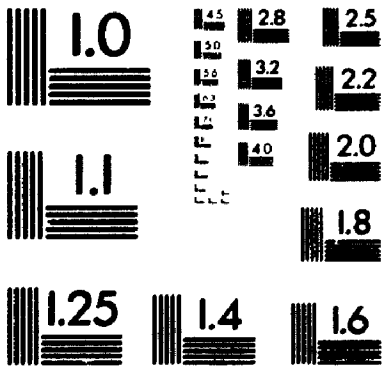

lamellate cuticle (figs 69 & 70). Sections approximately parallel to the cuticle surface showed them to be solid helical structures with about the frequency expected if most of them had arisen from single cells (fig 68). They contained fine fibres normal to the surface, but none of the filaments usually associated with pore canals. They were not osmiophilic, nor did they reduce silver using the silver hexamine stain, suggesting that they are not carrying lipids or polyphenols to the surface, at least at the time of staining. The term pore canal should probably not be applied to them since they appear to be neither pores nor canals.

4.3 Discussion

The main finding is that caterpillar epidermal cells have a cytoplasmic component - the apical actin bundle - that is paired in adjacent cells. The paired cells are assumed to be Siamese twins, implying that the cytoplasmic patterns are similar because they have recently been inherited.

Are the cytoplasmic patterns inherited somatically or genetically?

There are two possible models for positioning the bundles in three dimensions. The first is via a conventional genetic code which is replicated and segregated equally to each sibling cell. The second is a somatic or cytoskeletal memory which would also have to be replicated and equally distributed to each sibling cell during division.

In common with each mechanism is the need for a morphological determinant which is positioned either genetically or somatically (fig. 71), specifically a microfilament organizing centre (see e.g. Herrmann, 1989; Tilney, 1983). Similar morphological determinants are the basal bodies in *Paramecium* (Beisson & Sonneborn, 1965) and presumably microtubule organizing centres (MTOC) in neuroblastoma cells (Solomon, 1980). The orientation of the basal bodies in the progenitor cell of *Paramecium* determines their orientations in the daughter cells Reversing their orientation in the progenitor leads to their reversed orientation in the daughters, showing that there is no direct genetic control. Neuroblastoma cells extend neurites in patterns which are mirrored in daughter cells but which are otherwise unique. Depolymerization of their microtubules with nocodazole causes loss of the neurites, but removal of the nocodazole leads to a recapitulation of their original pattern. This shows the

Fig. 71. An interpretation of the paired bundles found in adjacent cells. Bundle organizing centres or their genetic antecedents are presumed to divide and segregate in sibling siamese twin cells.

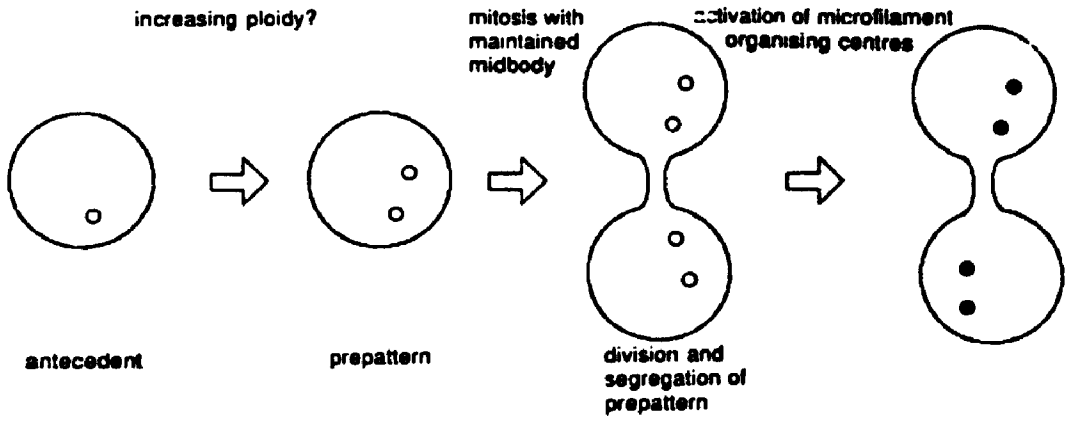
increasing ploidy?
mitosis with maintained midbody
activation of microfilament organising centres
antecedent
prepattern
division and segregation of prepattern

presence of "endogenous determinants", presumably MTOCs, which nucleate MT in specific orientations.

Because the epidermal cells are genetically and developmentally identical, it was originally presumed that variation in the number of bundles between cells would not be determined directly by genes. The pattern pairing seemed to be like that in *Paramecium* and the cell types discussed above. However, this is not certain. Insect epidermal cells vary in their ploidy, so that their genetic makeup may vary quantitatively if not qualitatively. Ploidy at ecdysis in the fifth stadium of *Manduca* varies from 4 to 32 C with the proportion of higher ploidies increasing during the intermoult (Kato *et al.*, 1987). The variation in cell and nuclear size in *Calpodes* suggests that it is like *Manduca* in this. Bundle pairing might therefore merely reflect ploidy. Ploidy may correlate with the number of bundles, but it does not easily explain odd numbers of bundles. A direct relationship with ploidy would predict a geometric distribution of 1, 2, 4, 8 and so on without intermediates. However, there is not always a direct relationship between ploidy and rates of transcription and translation. For example, in the wall cells of the testis in the grasshopper *Chrysochraon dispar* and onion cells increasing ploidy is proportional to increasing incorporation of [^{3}H]-uridine (Brodsky & Uryvaeva, 1977). In hepatocytes incorporation of [^{14}C]-uridine is roughly proportional to DNA content although diploids have a slightly higher level of transcription than polyploids (Hirano *et al.*, 1981). However, although the amount of albumin synthesis correlates with ploidy in hepatocytes (Le Rumeur *et al.*, 1981), the rate of transferrin synthesis does not (Foucrier *et al.*, 1988). This shows that if the actin bundles are genetically regulated then it is possible, but not necessarily true that ploidy level will correlate with their number. If reduction of the mitotic cycle causing polyploidy really does involve metabolic competition between mitosis and other cellular functions (Brodsky & Uryvaeva, 1977), then a simple relationship would be unlikely to exist. It must be concluded that while somatic inheritance of these actin bundle patterns is possible, it remains unproven.

How are the paired patterns maintained ?

The patterns of bundles in the cells are not obvious mirror images or rotations of each other, although there are some similarities in positioning (see for example figures 54 & 55). There are several possible causes, in addition to

the patterns not originally being symmetrical. There are few bundles in each cell, all with simple shapes, so that it is difficult to distinguish mirror images. The 24 hours from division would be sufficient time for patterns to shift. The cuticle is very plastic, transmitting its distortions to the bundles embedded in it (figs. 64 & 65). That paired patterns survive at all may be due to their common abode in a cell doublet with retained midbodies.

Midbodies are seen more commonly in the epidermis than would be expected if they were only short-lived structures (Locke & Leung, 1985b). They probably bridge all sibling cells for several days after division and form a minimal syncytium of Siamese twin cells within the epidermis (fig. 39). The persistence of the midbodies coincides with the pairing of cells with respect to microfilament bundles, nucleoli (Locke & Leung, 1985b) and female heterochromatin (Locke, 1988). Communication through such direct structural links between daughter cells may conserve patterns. Injected rhodaminyl phalloin moves freely through these midbodies (fig. 72) and various dyes cross the bridges between post-mitotic daughter HeLa cells (Schulze & Blose, 1984). Although the nuclear and actin patterns appear to be paired, it is possible that the syncytia consist of more than two cells. In *Manduca* the cells are thought to go through several rounds of division at the end of the 5th stadium, reducing their ploidy from up to 64C to about 4-8C (Kato *et al.*, 1987). If 4th stadium *Calpodes* epidermis is like this the syncytia may contain of 4, 8, 16 or more cells, assuming midbodies are retained after each division. The size of these syncytia could be determined by microinjecting cells with markers large enough that they will only pass through the midbodies.

Contractile rings of microfilaments can be seen for a short time after division in the fourth stadium using rhodaminyl phalloin as a label (fig. 5). Unfortunately, they did not persist to show the pairing of daughter cells a day after ecdysis. Microtubules are not present in the midbodies at the time when the bundles can be labelled with rhodaminyl phalloin (Locke & Leung, 1985b), therefore antibodies to microtubules could not be used to show cell pairing. Unsuccessful attempts were made to label the epidermal cells with antibodies to the midbodies from CHO1 cells (from Dr C. Sellitto, University of Minnesota) and *Drosophila* (from Dr D. Kellogg, University of California, San Francisco).

Fig. 72. Rhodaminyl phalloin (1.2 mM) microinjected into cell 1 (orientation of microsyringe indicated by >) flowed into cell 2 presumably through the midbody. The epidermis in this preparation was incubated in 1 mM chlorpromazine for 45 minutes to try to block the gap junctions. Without incubation in chlorpromazine the rhodaminyl phalloin spread concentrically away from the injected cell, as would be expected if it was passing to all the neighbouring cells through gap junctions.

Fig. 73. Haemocytes (possibly plasmatocytes, see Gupta, 1979) have bundles (Fb) of F-actin (cells labelled with rhodaminyl phalloin). Stores of actin may be necessary for cell spreading.

Bars = 10 μm.

The function of Calpodes epidermal actin bundles

The increased rate of cuticle deposition in the intermoult of fifth stage *Calpodes* is brought about by adding more lamellae and by intussusception into preexisting lamellae (Condoulis & Locke, 1966). In *Manduca* the endocuticle probably grows by stretching. This is helped by columns of cuticle with chitin fibrils oriented normally to the plane of the integument (Wolfgang & Riddiford, 1981). The cuticular columns in *Manduca* originate from bunches of very long microvilli which insert into the cuticle from the apical faces of the epidermal cells. The cuticular columns in *Calpodes* are similar and could allow for deformation of the endocuticle. They may also act as mechanical links to keep cells below the surface that they originally secreted as do similar transverse structures in the extensible intersegmental membranes of the female migratory locust (Vincent, 1981).

The generality of actin bundles

Actin bundles also occur in *Calpodes* haemocytes (fig. 73) and dermal glands (Delhanty & Locke, 1990b), where they appear at the same time as in the epidermis. Actin bundles occur naturally in other cells such as pollen grains (Heslop-Harrison *et al.*, 1986) and the macrociliary cells of *Beroë* (Tamm & Tamm, 1988). Bundles in the lens epithelium of mice are especially similar to those in *Calpodes* (Rafferty & Scholz, 1985). They can also be induced to form in a variety of cells by incubation in dimethyl sulphoxide (Fukui & Katsumara, 1979; Sanger *et al.*, 1980).

CHAPTER 5

CYCLES OF F-ACTIN REDISTRIBUTION IN THE DERMAL GLANDS RELATE TO SECRETION

"Ecdysis in insects is the homologue of metamorphosis, and there can be small prospect of understanding the complex process of metamorphosis until the physiology of ecdysis has been adequately described."

Wigglesworth, 1933

5.1 Introduction

The secretory cells of the dermal glands (Verson's glands) are another example of the effect that actin can have on a cell's shape.

The secretory cells of dermal glands in Lepidoptera are very large. In late 4th stage *Calpodes ethlius* they may be up to 1.6 mm long (Lai-Fook, 1973), and as long as 6 mm by the end of the fifth stadium. Dermal glands in *Calpodes* correspond to the class 3 glands of Noirot & Quennedey, 1974. They consist of three cells, two of which, the duct cell and the saccule cell, have a cuticulin lining continuous with that of the surface epicuticle (fig. 74). The duct cell forms a passage through the cuticle. The saccule cell contributes a small amount of material to the secretion from the much larger secretory cell (Lai-Fook, 1973). Just before ecdysis, the secretory cell is replete with vacuoles presumably containing secretion from the numerous Golgi complexes. The vacuoles empty just after ecdysis when the cells decrease in size. The glands reform and grow, becoming larger and more polyploid at every moult (Lai-Fook, 1972) until they are lost after the larval/pupal transformation.

Despite their size and relative ease of manipulation, the function of their secretory product is still uncertain, perhaps because dermal glands from different orders of insects have incorrectly been considered exactly homologous. In *Calpodes*, the glands only empty their contents just before ecdysis, which means that they probably do not secrete a component of the moulting fluid (Lai-Fook, 1973). The glands in *Manduca* have been presumed to produce a shellac-like cement layer which spreads over the surface of the cuticle as the exuvium falls away during ecdysis (Truman, 1985). In *Rhodnius*

Fig. 74. The structure of a dermal gland in *Calpodes*. The gland is formed from three cells. The duct cell and saccule cell are lined with cuticulin. The large secretory cell fills with vacuoles whose coalescence at ecdysis is followed by discharge of secretion through the saccule and duct cells (after Lai-Fook, 1973, not drawn to scale).

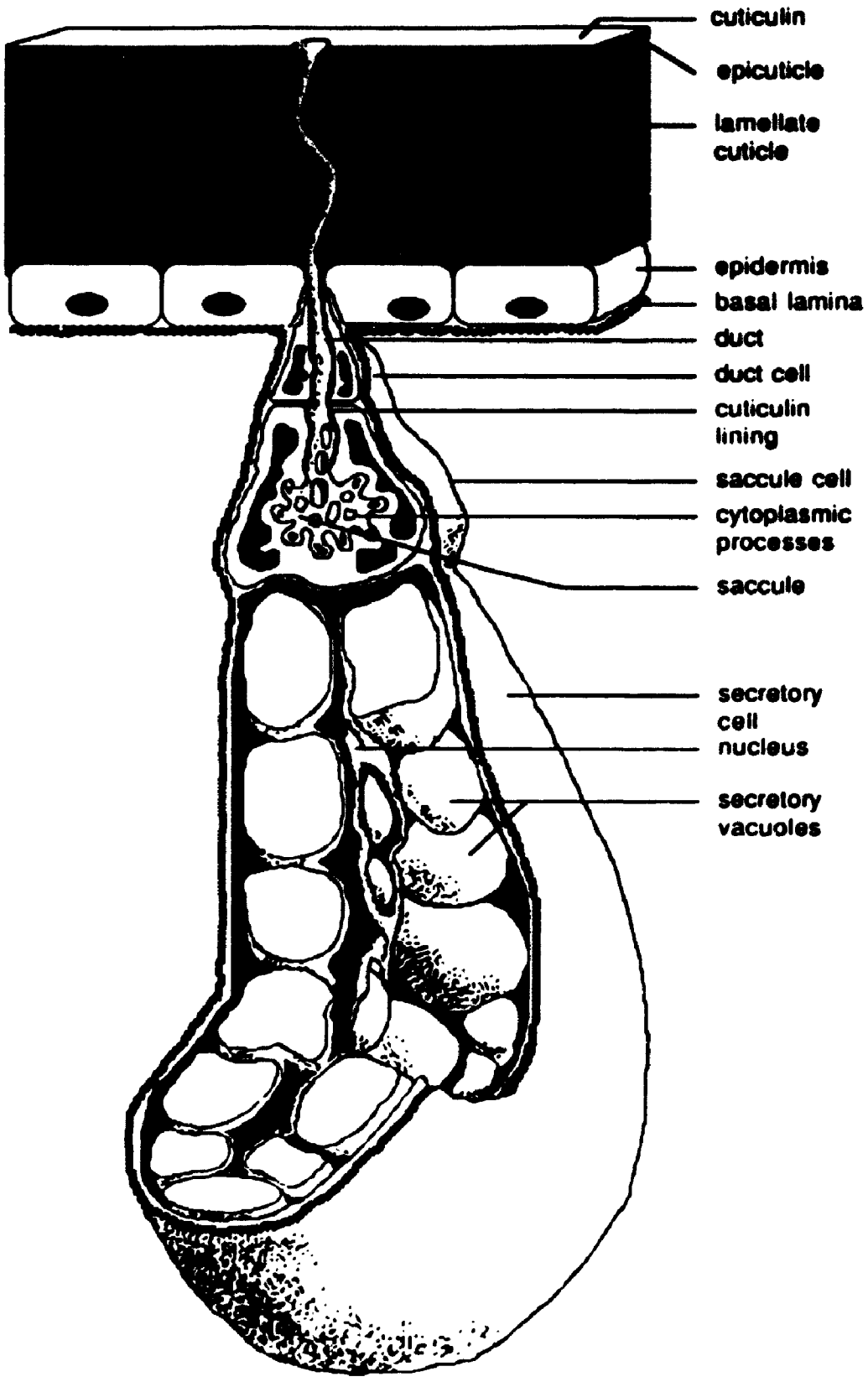
cuticulin
epicuticle
lamellate cuticle
epidermis
basal lamina
duct
duct cell
cuticulin lining
saccule cell
cytoplasmic processes
saccule
secretory cell nucleus
secretory vacuoles

the dermal glands also discharge after ecdysis at the same time as the cuticle becomes more hydrophilic. This is presumed to be a result of the cement layer spreading over the cuticle surface (Wigglesworth, 1947). A clue to their function may be that the secretory components themselves vary segmentally and temporally, perhaps causing the different mechanical properties of cuticle in each pupal segment (Horwath & Riddiford, 1988). A more general possibility is that the secretion acts as a lubricant, easing the sloughing of the exuvium (see Wigglesworth, 1933).

The development of the gland during the intermoult is regulated by ecdysteroid (Lane *et al.*, 1986). Injection of eclosion hormone into pharate *Manduca* pupae leads to early secretion by the dermal glands (Truman, 1985) and in untreated larvae and pupae the timing of secretion correlates with the release of eclosion hormone from the ventral ganglia initiating ecdysis.

It has been found that F-actin changes its distribution in relation to the stage of the secretory cell. The distribution of F-actin before and just after ecdysis suggests that it may be involved in the mechanism of secretion. This paper describes the cyclical changes in F-actin distribution from the second larval to the pupal stadium of *Calpodes*.

One of my original objectives was to find out if actin gives the secretory cell its shape. Since it grows relatively freely in suspension it would be expected to become spherical. However, if the gland increased in size isometrically its surface area-to-volume ratio would be unavoidably decreased. The cell lessens this effect by remaining flat with an extensive plasma membrane reticular system. Such anisometric growth is functionally similar to that of the fat body which also floats freely in the haemolymph but never exceeds two cells in thickness. Cytoskeletal restraints to growth presumably prevent thickening while allowing lateral expansion. Although my studies show that F-actin may not be directly involved in shaping the cell, it does influence the shape of the nucleus.

5.2 Results

5.2.1 During larval and pupal stadia F-actin redistributes in repeating cycles that correlate with secretion at ecdysis

My observations agree with those in the literature (e.g. Lai-Fook, 1973), that from the first larval moult until transformation to the pupa the dermal glands

pass through repeating cycles of preparation and secretion. They are not lost until after the larval/pupal ecdysis. During moulting the glands are distended by their secretion but shrink at ecdysis. Vacuoles in the secretory cell coalesce, their contents move into the lumen of the saccule cell and pass through the duct to the cuticle surface. The changes in gland size indicate that secretion occurs at each ecdysis.

The changing distribution of cytoplasmic microfilaments correlated with this repeating secretory cycle is outlined in fig. 75. The microfilaments are believed to be F-actin because they have the appropriate dimensions in electron micrographs, they can be decorated with heavy meromyosin and they bind rhodamine labelled phalloin. In each larval stadium just before ecdysis, cortical F-actin formed capsules around the secretory vacuoles (figs. 80, 82, 84, 89 & 100). The capsules sometimes had small bundles of F-actin (e.g. figs. 80 & 100) which were probably cores of the short microvilli known to extend into the lumina of the vacuoles (Lai-Fook, 1973). The vacuoles were separated by cytoplasm which labelled only weakly, if at all, for F-actin. The nucleus formed a central network separating the vacuoles into two layers (figs. 74 & 77-79). It may be functionally significant that the nucleus, because of its shape, remains close to both vacuoles and cytoplasm in all parts of the cell. This would maintain the shortest route for mRNA to travel from the nucleoplasm to the RER, and a short route from the RER through the cisternae to the secretory vacuoles thus increasing the efficiency of secretion in this very large cell.

Immediately after ecdyses the F-actin formed stellate patterns or clumps distributed in the gland as if they were the remnants of the capsules (e.g. figs. 85 & 93). The shapes suggested that the capsules of F-actin had either contracted or collapsed as the contents of the secretory vacuoles coalesced. A cloudy staining pattern of rhodaminyl phalloin remained after dissolution of the capsules (e.g. figs. 81 & 97), suggesting that some of the F-actin itself may be rearranged without depolymerizing into a large pool of subunits. The F-actin then aggregated into bundles for storage during the intermoult (e.g. figs. 83, 86 & 96). The bundled F-actin disappeared late in each stadium as new capsules formed around the new generation of secretory vacuoles.

Fig. 75. Cycles of F-actin redistribution (see fig. 114) in relation to dermal gland secretion. Events in the 2nd and 3rd stadia duplicate those in the 4th (ecdysteroid data from Dean *et al.*, 1980; the time of secretion at ecdysis agrees with data in Lai-Fook, 1973).

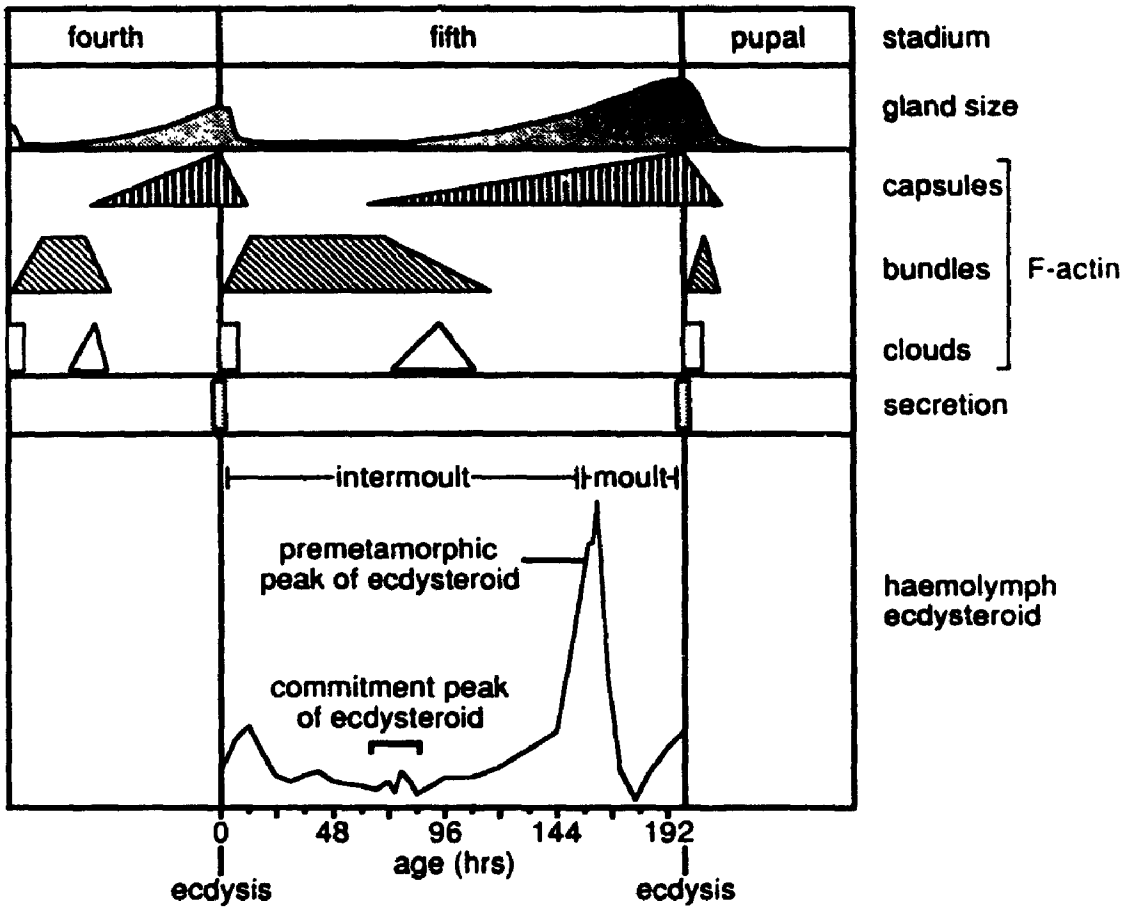
fourth
fifth
pupal
stadium
gland size
capsules
bundles
clouds
F-actin
secretion
intermoult
moult
premetamorphic peak of ecdysteroid
commitment peak of ecdysteroid
haemolymph ecdysteroid
0
48
96
144
192
age (hrs)
ecdysis
ecdysis

Fig. 76. The nucleus (n) of the secretory cell formed a flat fenestrated network through the centre of the cell. Strands of the nuclear network surrounded groups of vacuoles. A, anti nuclear antibody (autoantibody control ANA positive, speckled; Sigma diagnostics, Sigma Chemical Co., St. Louis, MO) labelling of the nucleus. B, rhodaminyl phalloin labelling of the F-actin. A and B are optical sections at the same plane of focus made using a confocal microscope. Profiles of F-actin capsules (Fc) appeared as a reticulum (B) within the much larger nuclear reticulum(A).

Fig. 77-79. The nucleus lay between two layers of F-actin capsules (see fig. 74). The 3 figures have the same field of view but are at different levels of focus. The A series was photographed using a fluorescein filter to detect labelling with an anti-nuclear antibody. The B series used a rhodamine filter to detect the F-actin stain. The nucleus only appeared in the centre of the cell. The cytoplasmic space projecting into the nucleus contained several actin capsules.

Fig. 77. The plane through actin capsules of the lower layer of vacuoles had no nuclear reticulum. Fluorescent spots in the centres of the vacuoles viewed with the rhodamine filter were probably due to the Evan's blue counterstain because they were absent when rhodaminyl phalloin was used alone.

Fig. 78. In the centre of the cell two layers of vacuoles overlapped in the spaces through the nucleus .

Fig. 79. On the upper surface there was a layer of vacuoles and no nucleus.

Figs. 80-86. F-actin formed capsules (Fc) around the secretory vacuoles during moulting to the third, fourth and pupal stadia, but redistributed into storage bundles after each ecdysis.

Fig. 80. Capsules of F-actin around the secretory vacuoles about an hour before ecdysis to the third stadium.

Fig. 81. At ecdysis to the third stadium the F-actin is disordered and the secretory vacuoles have collapsed. Rhodaminyl phalloin labelling is diffuse except for a few short bundles (Fb).

Fig. 82. Before moulting to the fourth stadium F-actin again forms capsules around the secretory vacuoles. There is little or no phalloin labelling between the capsules.

Fig. 83. After ecdysis to the fourth stadium the F-actin had redistributed into short bundles and rings throughout the cytoplasm.

Fig. 84. Shortly before the larval/pupal ecdysis the secretory cells were in all stages from destruction of the capsules to reticulate patterns where the F-actin had begun to rearrange.

Fig. 85. During ecdysis to the pupa the capsules were stellate as though they had contracted around or collapsed with the coalescing secretory vacuoles.

Fig. 86. Twenty hours after ecdysis to the pupa F-actin is patchily distributed in bundles or small clouds.

Fig. 87. Without rhodaminyl phalloin there was no fluorescence, showing that autofluorescence did not contribute to the patterns observed.

Fig. 88. Preparations incubated in an excess of phalloidin before rhodaminyl phalloin had no fluorescence, showing that the rhodaminyl phalloin labels only F-actin.

Bars = 50 μm.

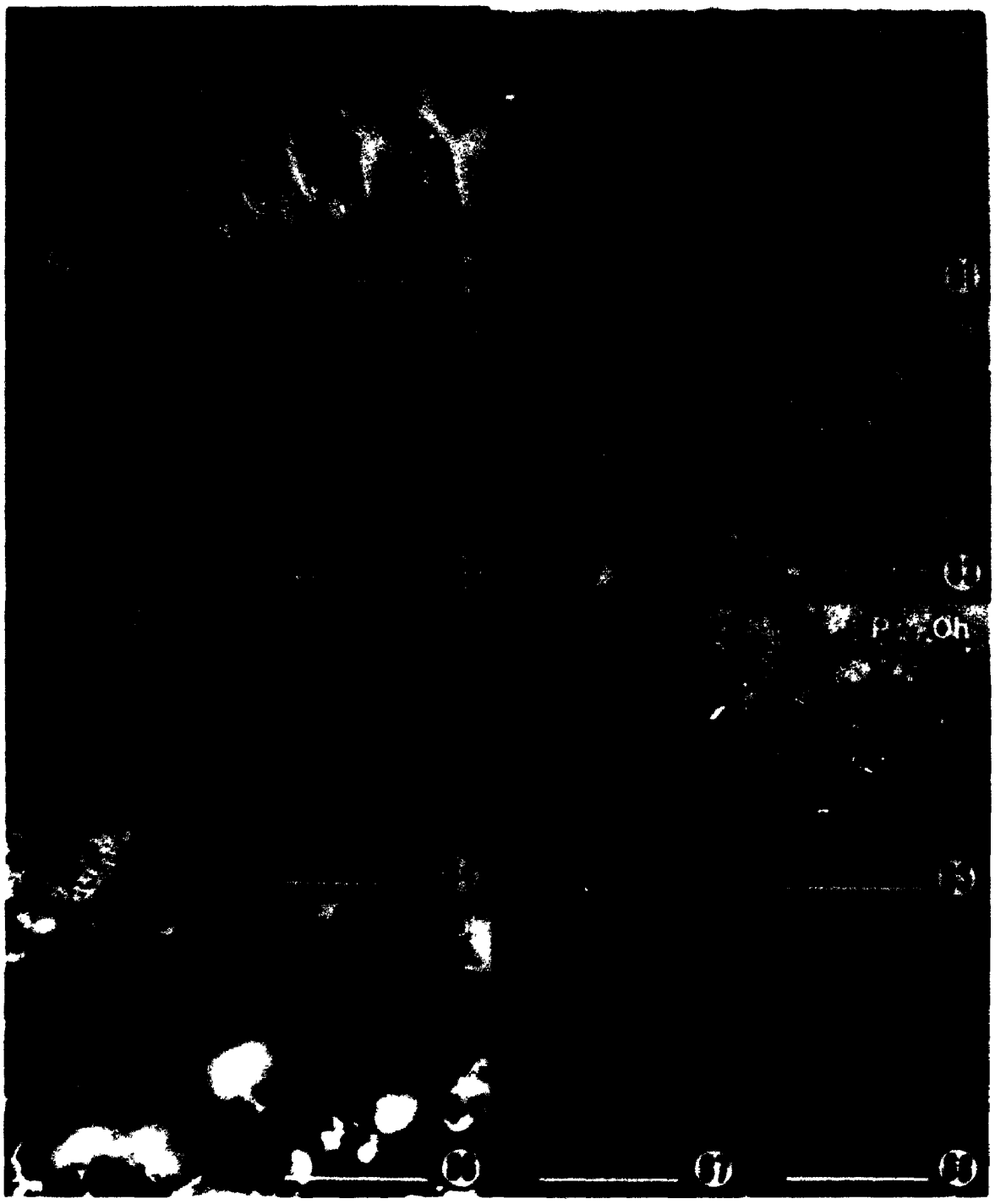
(1)
(2)
(3)
(4)
(5)
(6)

5.2.2 The distribution of F-actin in preparation for ecdysis and its subsequent redistribution in the fifth stadium

Just before ecdysis to the fifth stadium the secretory cells were replete with secretory vacuoles within their F-actin capsules (figs. 89 & 90). Two hours after ecdysis all that remained of the capsules were clumps interspersed with fine strands (fig. 91). The secretory cell was shrunken and the basal lamina shriveled as if an inelastic shell connected to the plasma membrane had been drawn in with the shrinkage due to secretion (fig. 92). For a day after ecdysis the F-actin formed clumps and rings, or discs with uniform diameters of about 2.5 μm (figs. 93 & 94). These are similar to F-actin rings in adult female accessory glands of *Ceratitis* (Dallai *et al.*, 1988). Twenty eight hours after ecdysis most of the fine actin wisps and clumps had condensed into thick bundles (figs. 96 & 103-106). The cell remained shrunken during the formation of these actin bundles.

Just before commitment to pupation (66 hrs into the stadium, fig. 75) the bundles of F-actin became smaller and phalloin labelled the cytoplasm diffusely (fig. 97). By the time of commitment the gland had enlarged to fill the basal lamina which once more smoothly covered the secretory cell surface (fig. 95).

By a day after commitment, vacuoles with actin capsules around them had reformed, although there was still some labelling in the cytoplasm (fig. 98). The enlarged secretory vacuoles caused bulges in the basal lamina (fig. 99). By 130 hours after ecdysis each capsule was separated by F-actin free cytoplasm, as though all the actin had been relocated (fig. 100). At this stage the outlines of vacuoles at the surface of the secretory cell showed through the basal lamina (fig. 101).

5.2.3 The structure of the F-actin storage bundles

At a day after ecdysis when phalloin labelling showed actin storage bundles, thin sections contained oval profiles (fig. 102). Although these are probably the F-actin bundles their filaments were not clearly ordered. The profiles were of rods, tubes, rings and hollow fenestrated spheres, as expected from the shape of the storage bundles seen in whole mounts (figs. 103-105). Such hollow shapes would be expected if they had originated directly from the shells around secretory vacuoles. However, the bundles were not ordered in

Figs. 89-101. F-actin was in capsules (Fc) around the secretory vacuoles before ecdysis to the fifth stadium, and redistributed into bundles afterwards. The bundles then disappeared as the F-actin reformed into capsules.

Fig. 89. F-actin formed capsules around the secretory vacuoles just before ecdysis.

Fig. 90. The dermal gland distends into a flattened pear shape just before ecdysis. The saccule cell is at the neck of the gland and joins with the duct cell in the epidermis (see fig. 74). The thin basal lamina covering the cell is sometimes dimpled as it follows the contours of the underlying reticular system over the vacuoles (see fig. 106 & 112).

Fig. 91. Two hours after ecdysis the capsular F-actin changes to wisps, clumps and hollow spheres.

Fig. 92. After secreting its contents at ecdysis the gland remains shrunken until the commitment peak of ecdysteroid (fig. 75).

Figs. 93 & 94. During the first hours after ecdysis many of the hollow spheres disappeared with their F-actin aggregating into bundles or rings (Fr) between the clumps and few remaining capsules.

Fig. 95. After commitment to pupation the gland is about 500 µm in diameter. Wrinkles in the basal lamina had been taken up by the newly distended secretory vacuoles.

Fig. 96. About a day after ecdysis the cytoplasm lacked diffuse rhodaminyl phalloin labelling and the actin was in bundles 5 µm thick and 30 µm long showing that the F-actin was now stored.

Fig. 97. By the time of commitment the bundles were smaller and the cloudy material between them had reappeared.

Bars = 50 µm unless indicated otherwise.


(b)
(c)
(d)
(e)

Figs. 98 & 99. The secretory cell had begun to refill with vacuoles and the F-actin reformed into capsules by about a day after commitment.

Figs. 100 & 101. At 133 hours after ecdysis the F-actin capsules were complete around the vacuoles which became distended to make rounded impressions in the thin basal lamina.

Figs. 102. The structure of an F-actin storage bundle (Fb). A day after ecdysis sections show spindle shaped and hollow profiles 0.5-1.0 μm wide, as expected from the light microscopy (GC, Golgi complex).

Figs 103-105. The hollow appearance of actin bundles (figs. 103 & 104) expected if they were direct condensations of the capsules, was confirmed in a stereo pair made using 20 optical sections taken at 0.2 μm intervals on a Biorad confocal microscope (fig. 105).

Bars = 50 μm.


C
C
C
C
C
C

two layers like the capsules but were randomly distributed through the cytoplasm (fig. 106).

In detergent and glycerol extracted secretory cells (fig. 107 & 108) heavy meromyosin labelled dense masses of F-actin that are presumed to correspond to the F-actin storage bundles labelled by phalloin. Many of the filaments were anti-parallel with their neighbours. The lack of uniform polarity (fig. 108) may account for the lack of order in electron micrograph profiles (fig. 102). The filaments were not associated with membranes, which may explain their lack of unidirectional polarity (Tilney, 1983). The filamentous nature of the bundles was more easily seen after detergent and glycerol extraction perhaps because of the removal of material from between the fibres (fig. 109).

5.2.4 Secretory vacuoles in thin sections have a zone of exclusion corresponding to the position of the F-actin capsule

Microfilaments were not resolved around secretory vacuoles in thin sections (fig. 110) although filaments often occurred around vacuoles in detergent and glycerol extracted preparations (fig. 111). Osmication for optimal preservation of most tissue components in conventional electron microscopy is known to remove actin (Maupin-Szamier & Pollard, 1978) and ethanol dehydration can have the same effect (Small, 1984). For this reason cortical cytoplasm containing microfilaments often appears as a zone of exclusion, a region bereft of organelles that cannot penetrate the filamentous meshwork present in the live cell. Such zones of exclusion containing ribosomes and microtubules but no larger organelles occurred around the vacuoles, as would be expected if the F-actin capsules were meshworks of microfilaments.

5.2.5 The plasma membrane reticular system of the secretory cell

Like the fat body (Locke, 1986), oenocytes (Jackson & Locke, 1989) and several other tissues (Locke & Huie, 1983), the dermal gland has a complex plasma membrane reticular system (see also fig. 22 in Lai-Fook, 1973). Profiles showed that the secretory cell plasma membrane reticular system was separated from the haemolymph by a relatively thin (50 nm) basal lamina with wide spaces between the entrances to the infolds (fig. 112). SEM after the basal lamina had been removed showed the reticular system to be formed by microvillus-like projections from the cell surface (fig. 113). The structure is

Fig. 105. A stereo pair showing the hollow appearance of the F-actin bundles.

Fig. 106. The stereo pair of a 26 μm deep section of the cell shows actin bundles randomly dispersed throughout its depth.

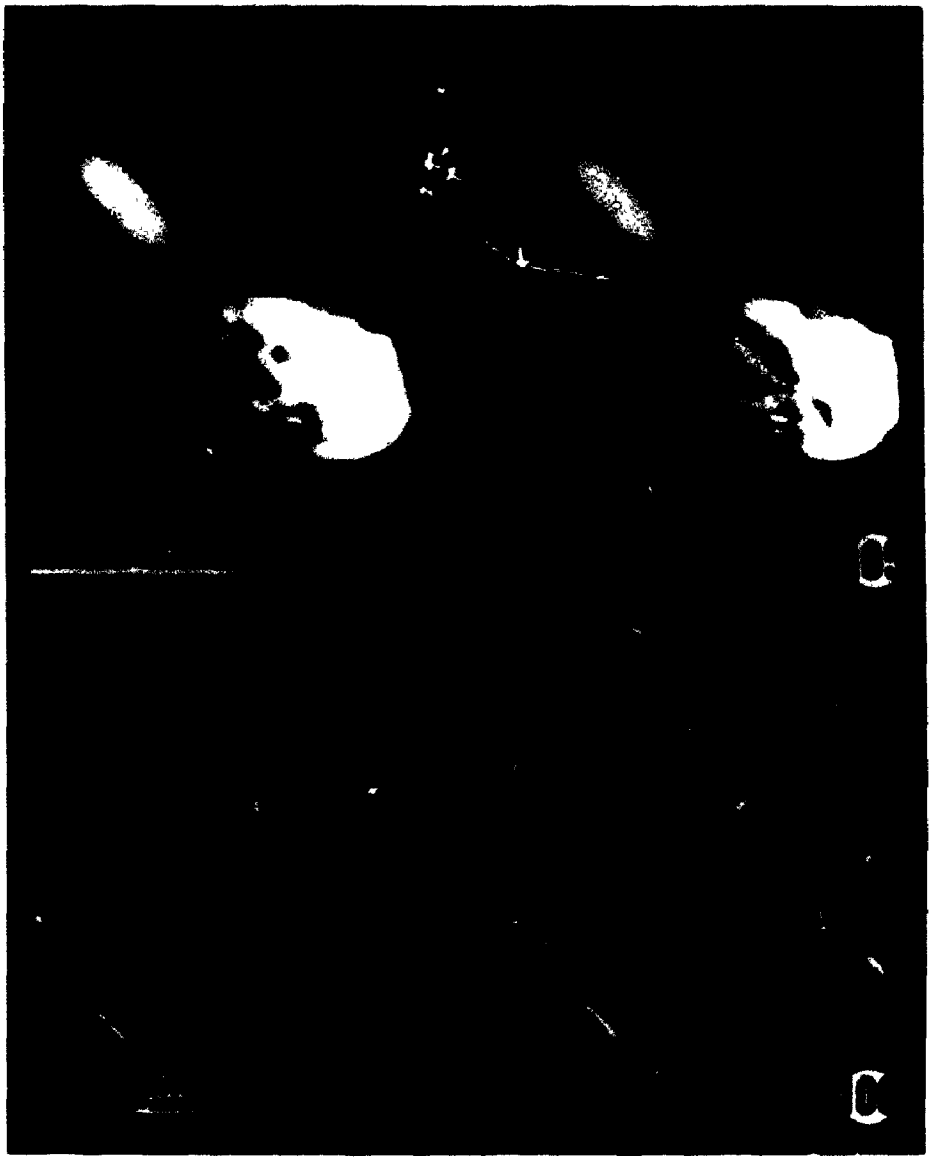
C
C

Figs. 107 & 108. Dermal glands extracted with glycerol and nonionic detergent had bundles of filaments which labelled with heavy meromyosin. Labelled filaments were not all parallel to one another (arrows).

Fig. 109. Bundles treated with glycerol and nonionic detergent have an amorphous matrix between their microfilaments.


5th 24h
5th 24h
0.2μm

Figs. 110 & 111. Zones of exclusion (Ze) of organelles from around the secretory vacuoles (Sv) corresponded to the F-actin capsules (see fig. 100). The capsule of F-actin seen around vacuoles after phalloin labelling was poorly preserved in thin sections, often only surviving as a zone of exclusion (fig.110). Extracted cells had microfilaments (MF) in this region (fig. 111).

Figs. 112 & 113. The plasma membrane reticular system (PMRS) of the secretory cell (bl, basal lamina).

Fig. 112. During formation of the vacuoles the plasma membrane had a reticular system similar to those seen in fat body, oenocytes and the epidermal trichogen-tormogen cell doublets.

Fig. 113. The reticular system consisted of columnar-like microvilli, projecting from the surface of the cell.


Z
Sv
MF
0·2 μm
Sv
Sv
0·2 μm

similar to that seen in the lenticle, another type of epidermal cell (Franzl *et al.*, 1984).

5.3 Discussion

The main finding is that filamentous actin is continuously present in the dermal gland but changes its pattern of distribution during the moult cycle (figs. 75 & 114). Before ecdysis the F-actin forms capsules around the secretory vacuoles. After secretion it is stored in bundles which persist in the fifth stadium until the time when the larva is committed to pupation. Bundles are probably the most space efficient way for the cell to store its actin to meet the repeated involvement in secretion at ecdysis. At commitment the bundles disappear and the secretory vacuoles again become encapsulated in actin as part of the process of secretion at the pupal ecdysis. Although the extent of turnover between G and F-actin is not known, some features suggest that the F-actin is itself redeployed without complete depolymerization. The hollow ball-shaped bundles suggest that they are derived directly from capsules around secretory vacuoles, the condensed shapes being either collapsed or contracted F-actin networks from around the vacuoles. Phalloin only binds to F-actin and diffuse rhodamine phalloin labelling of the cytoplasm persists between loss of the capsules and appearance of the bundles.

Actin cytoskeletons have also been implicated in secretion in silk glands of *Bombyx mori* (Couble *et al.*, 1984; Sasaki *et al.*, 1981; Tashiro *et al.*, 1982) and in mammalian chromaffin (Aunis *et al.*, 1987; Burgoyne & Cheek, 1987) and gastric parietal cells (Cuppoletti & Malinowska, 1988). Cytochalasin treatment of silk glands has given conflicting results, causing both inhibition (Couble *et al.*, 1984) and stimulation (Sasaki *et al.*, 1981) of secretion. Solation of the cortical, membrane-associated, actin network of chromaffin cells is probably necessary for secretion to proceed (Cheek & Burgoyne, 1987). Dermal glands are different in that reorganization of F-actin in the cortex around the secretory vacuoles, rather than in the cortex at the apices of the cells, may be necessary for their discharge. The fully formed F-actin capsules presumably regulate further fusion of secretory vesicles with the vacuoles.

A feature of dermal glands is the rapidity with which they discharge all the product that they have manufactured and stored. This is characteristic of regulated secretion (Burgess & Kelly, 1987). The actin capsules may be a part of this rapid discharge mechanism (see also Dallai *et al.*, 1988). A uniform

Fig. 114. A model for the redistribution of actin in the secretory cell during its repeating cycle of development. After ecdysis the secretory vacuoles discharge, perhaps induced by eclosion hormone. The F-actin forms clumps and strands which eventually condense into larger storage bundles. Midway through the stadium the bundles break up and then reform into capsules around newly forming vacuole. The vacuoles coalesce and the cycle repeats.

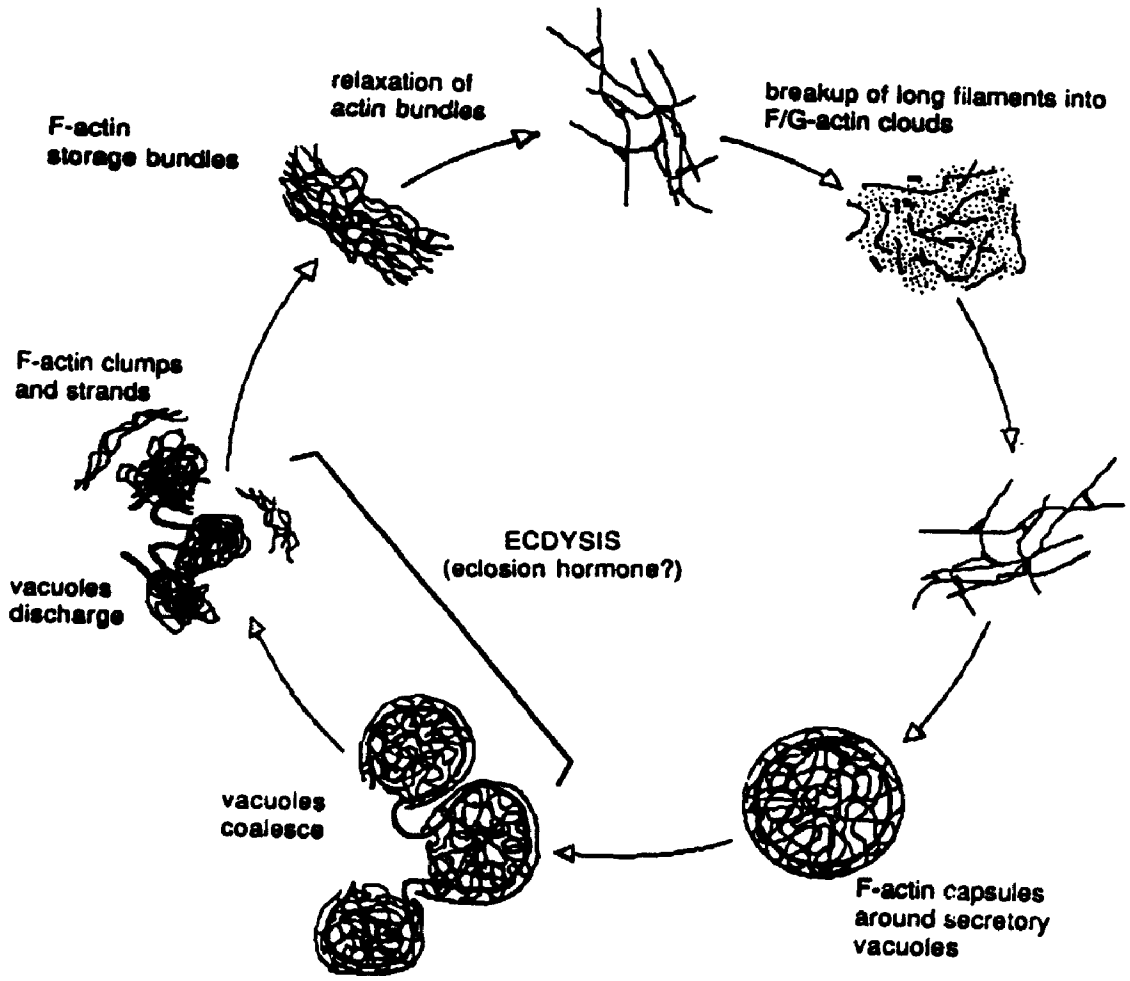
F-actin
storage bundles
relaxation of
actin bundles
breakup of long filaments into
F/G-actin clouds
F-actin clumps
and strands
ECDYSIS
(eclosion hormone?)
vacuoles
discharge
vacuoles
coalesce
F-actin capsules
around secretory
vacuoles

reduction in area of the capsule to cause the discharge requires that the filaments not be parallel to one another. The irregular pattern observed may therefore have significance and would explain why single filaments are difficult to see. A similar situation was found in *Physarum* (Nagai *et al.*, 1978). F-actin forms long plasmodial strands which cyclically elongate and contract, moving cytoplasm in pulses across the cell. While the strands contracted the microfilaments were parallel but when the strands were at their shortest the microfilaments became kinked and formed networks. This was interpreted as a change in the aggregation pattern of F-actin, presumably thrcugh actin binding proteins.

Regulated secretion is induced by a secretagogue. Dermal glands are not innervated (Lai-Fook, 1973) and secretion is probably effected hormonally. Salivary glands in blowfly larvae can be induced to secrete by 5-hydroxytryptamine which causes a rise in calcium concentration inside the gland cells (Fain & Berridge, 1979). Calcium concentration is one of the important regulators of both actin gelation and severing proteins (Weeds, 1982). Such proteins at the site of exocytosis in chromaffin cells may be involved in the mechanism of secretion (Aunis & Bader, 1988). The actin matrix is therefore a probable site for the control of secretion by dermal glands.

A second finding in this work concerns the relation between the cytoskeleton and nuclear shape. Profiles of the nucleus and capsules around vacuoles about to be secreted both appear like cross sections of a sponge. I at first misinterpreted this, supposing that each vacuole fitted into a corresponding space in the nucleus, with the actin capsules determining both nuclear and vacuolar shape. Later it became clear that several capsules may occupy each space in the nuclear network. This indicates that nuclear shape and the deployment of vacuoles are under separate control.

SUMMARY AND CONCLUSIONS

The development of epidermal feet in preparation for metamorphosis in an insect

Basal epidermal feet develop in three phases, initiation, elongation and contraction, which correlate with the larval/pupal transformation.

Initially the feet are randomly oriented.

Elongation coincides with axial orientation after commitment to pupation. Orientation is probably achieved by selective survival and growth of those feet which are already axially aligned.

As the larva shortens to the pupal form the feet contract. They eventually disappear as the cells rearrange.

The lateral margins of the cells carry fine adhesions throughout development.

The adhesions separate a lymph space from the haemolymph. The lymph space enlarges towards the end of the fifth stadium as the feet contract to extend along most of the length of the now columnar cells.

Filopodia form and span the gaps between cells now separated by lymph space.

Hemidesmosomes examined by scanning electron microscopy were shown to be axially aligned even before the feet had become oriented. Late in the stadium they lose their axial alignment and may become branched.

The hemidesmosome plaques are linear having a constant width of 0.15-0.2 μm and variable length. They probably arise by linear addition of a circular subunit.

The conservation of a cytoskeletal pattern in epidermal cell doublets

The epidermis is a minimal syncytium of Siamese twin cells

The twin cells have paired cytoskeletal patterns ($P < 0.005$; $n=617$).

The paired patterns survive for only a day and a half after ecdysis to the fifth stadium.

The retention of midbodies may preserve the paired patterns long enough for them to be observed.

Pairing in the cytoplasm occurs in the number of F-actin bundles.

The number of bundles correlates with the area of the cell ($P<0.001$; $n=526$) but not with the area of the nuclei ($P > 0.1$; $n=192$).

The paired patterns of F-actin bundles, and nucleoli and female heterochromatin, suggest that some aspects of cytoplasmic and nuclear three dimensional architecture are conserved between mitoses.

The actin bundles are associated with a transverse cuticular component which is not a pore canal.

Cycles of F-actin redistribution in the dermal glands of an insect are related to secretion

F-actin redistributes in cycles which relate to cycles of secretion in the secretory cell.

These cells accumulate large vacuoles which are encapsulated by F-actin, shown by rhodaminyl phalloin labelling, just before discharge of the gland at ecdysis.

After ecdysis the F-actin from the capsules is redistributed into clumps and strands.

The strands aggregate into thick bundles for storage during intermoult.

Heavy meromyosin labels the filaments in these thick bundles.

The F-actin capsules reform at the next moult as the cell goes through its secretory cycle which ends at the larval/pupal transformation.

The nucleus is distributed evenly throughout the cell just before ecdysis and is sandwiched between two layers of vesicles. This arrangement may enhance the process of secretion.

APPENDIX 1

by

D.R. Bellhouse

(Dept. of Statistics & Actuarial Science, University of Western Ontario)

and

P. Delhanty

Statistical analysis for paired cells

Notation

Let Pr (cell with a single bundle) = p

Let Pr (cell with two bundles) = q

Let Pr (cell with three or more bundles) = r

$p + q + r = 1$ or $r = 1 - p - q$

Data collection

Pick a cell at random and look at the neighbour in a particular orientation from that home cell:

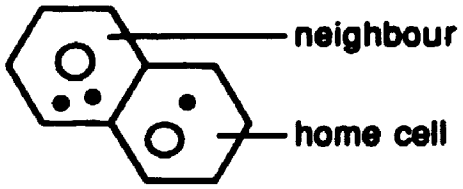

Data notation:

		Neighbour cell (number of bundles)			
		1	2	3	
Home cell (number of bundles)	1	n_{11}	n_{12}	n_{13}	$n_{1.}$
	2	n_{21}	n_{22}	n_{23}	$n_{2.}$
	3	n_{31}	n_{32}	n_{33}	$n_{3.}$
Total		$n_{.1}$	$n_{.2}$	$n_{.3}$	n

Data are:

		Neighbour cell (number of bundles)			
		1	2	3	
Home cell (number of bundles)	1	176	112	14	302
	2	132	106	13	251
	3	26	20	18	64
Total		334	238	45	617

Hypothesis : Cells are paired and randomly oriented

Data analysis

1. Calculation of the likelihood

Let the events H1, H2 and H3 be the home cell chosen having 1, 2 or 3 bundles respectively.

Let the events N1, N2 and N3 be the neighbour cell having 1, 2 or 3 bundles respectively.

The probabilities of each event in the table are needed to calculate the likelihood.

e.g. Pr (H1, N1) = Probability that both the home cell and the neighbour cell has one bundle.

Pr (H1, N1) = Pr (H1). Pr (N1/H1)

= Probability of choosing the home cell with one bundle X Probability that the neighbour has one bundle given that the home cell has one

$= p\,(1/6 \cdot 1 + 5/6 \cdot p)$

Note that p = Pr (H1) and $1/6 \cdot 1 + 5/6 \cdot p$ = Pr (N1/H1)

Assuming a random orientation, there is a 1/6 probability that the neighbour cell will be the paired companion and 5/6 that it will not. If it is the pair then there is a probability of 1 of a match. If it is not then there is a probability p of a match.

By the same arguments:

$\Pr(H1, N2) = p(1/6.0 + 5/6 \cdot q) = 5pq/6$

$\Pr(H1, N3) = 5pr/6$

$\Pr(H2, N1) = 5pq/6$

$\Pr(H2, N2) = q(1 + 5q)/6$

$\Pr(H2, N3) = 5qr/6$

$\Pr(H3, N1) = 5pr/6$

$\Pr(H3, N2) = 5qr/6$

$\Pr(H3, N3) = r(1 + 5r)/6$

The likelihood is proportional to:

$$\prod_{i=1}^{3} \prod_{j=1}^{3} [\Pr(H_i, N_j)]^{n_{ij}}$$

Dropping all constants, by absorbing them into the constant of proportionality, the likelihood reduces to:

$L(p, q, r)$ is proportional to $p^{m1}.(1+5p)^{n11}.q^{m2}(1+5q)^{n22}.r^{m3}.(1+5r)^{n33}$

where:

$$m_1 = n_{1.} + n_{.1} - n_{11}$$
$$m_2 = n_{2.} + n_{.2} - n_{22}$$
$$m_3 = n_{3.} + n_{.3} - n_{33}$$

2. Calculation of the estimates

On using the restriction $p + q + r = 1$ or $r = 1 - p - q$ the likelihood equations were obtained:

$f_1 = \partial / \partial p \ln L(p, q, r) = 0$

$f_2 = \partial / \partial q \ln L(p, q, r) = 0$

or :

$f_1 = m_1/p + 5n_{11}/(1+5p) - m_3/(1 - p - q) - 5n_{33}/(1 + 5(1 - p - q)) = 0$

$f_2 = m_2/q + 5n_{22}/(1+5q) - m_3/(1 - p - q) - 5n_{33}/(1 + 5(1 - p - q)) = 0$

The solutions to these equations give $\hat{p}$ and $\hat{q}$, the maximum likelihood estimates of p and q, and $\hat{r} = 1 - \hat{p} - \hat{q}$.

There is no closed form solution so it must be obtained iteratively.

3. Newton-Raphson iteration (see appendix 2)

A value for the vector $\begin{pmatrix} p \\ q \end{pmatrix}$ was picked and updated to $\begin{pmatrix} p' \\ q' \end{pmatrix}$ by the equation:

$$\begin{pmatrix} p' \\ q' \end{pmatrix} = \begin{pmatrix} p \\ q \end{pmatrix} - H^{-1} \begin{pmatrix} f_1 \\ f_2 \end{pmatrix}$$

where H is the matrix:

$$\begin{bmatrix} \frac{\partial f_1}{\partial p} & \frac{\partial f_1}{\partial q} \\ \frac{\partial f_2}{\partial p} & \frac{\partial f_2}{\partial q} \end{bmatrix}$$

and

$$\frac{\partial f_1}{\partial p} = -\frac{m_1}{p^2} - \frac{25n_{11}}{(1+5p)^2} - \frac{m_3}{(1-p-q)^2} - \frac{25n_{33}}{[1+5(1-p-q)]^2}$$

$$\frac{\partial f_1}{\partial q} = -\frac{m_3}{(1-p-q)^2} - \frac{25n_{33}}{[1+5(1-p-q)]^2}$$

$$\frac{\partial f_2}{\partial p} = -\frac{m_3}{(1-p-q)^2} - \frac{25n_{33}}{[1+5(1-p-q)]^2}$$

$$\frac{\partial f_2}{\partial q} = -\frac{m_2}{q^2} - \frac{25n_{22}}{(1+5q)^2} - \frac{m_3}{(1-p-q)^2} - \frac{25n_{33}}{[1+5(1-p-q)]^2}$$

A starting value was chosen using a method of moments estimate. These were obtained by setting

$n_{11} = n.\ Pr(H1, N1) = n\ (p(1+5p)/6)$ and
$n_{22} = n.\ Pr(H2, N2) = n\ (q\ (1+5q)/6)$

The starting values are the solutions to two quadratic equations:

$5np^2 + np - 6n_{11} = 0$ where $p = (-n \pm \sqrt{(n^2 + 120.\, n.\, n_{11})}) / 10.\, n$

$5nq^2 + nq - 6n_{22} = 0$ where $q = (-n \pm \sqrt{(n^2 + 120.\, n.\, n_{22})}) / 10.\, n$

The updated value was used as a new value for $\begin{pmatrix} p \\ q \end{pmatrix}$ and the process was repeated.

This was continued until $\begin{pmatrix} p' \\ q' \end{pmatrix} - \begin{pmatrix} p \\ q \end{pmatrix}$ was 10^{-6}.

At convergence $-H^{-1}$ gives the variance-covariance matrix estimate $\begin{pmatrix} \hat{p} \\ \hat{q} \end{pmatrix}$

From the data $\hat{p} = 0.51622374$

$\hat{q} = 0.39901540$

$\hat{r} = 0.08476090$

4. <u>The test statistic</u>

The expected frequencies in the table were calculated using $\hat{p}$, $\hat{q}$ and $\hat{r}$. E_{ij} must be ≥ 5, otherwise more data is needed.

The test statistic is:

$$\chi_0^2 = \sum_{i=1}^{3} \sum_{j=1}^{3} \frac{(E_{ij} - n_{ij})^2}{E_{ij}}$$

This was compared to a chi-square distributor on 4 degrees of freedom (table 4).

i.e. 9 cells – 2 parameters estimated (p, q) – 3 restrictions.

The restrictions are:

i) $p + q + r = 1$

ii) Pr of getting one bundle in home same as getting one in neighbour.

iii) Pr of getting two bundles in home same as getting two in neighbour.

Table 4. Chi-squared test for the association of adjacent cells with the same number of apical actin bundles.

neighbours	expected (E) - observed (O)	$(E - O)^2$	$(E - O)^2 / E$
1-1	190.10362-176= 14.10362	198.91209	1.04633
1-2	105.90866-112= -6.09134	37.10442	0.35034
1-3	22.49766 - 14= 8.49766	72.21024	3.20968
2-1	105.90866-132=-26.09134	680.75802	6.42778
2-2	122.89424-106= 16.89424	285.41534	2.32245
2-3	17.38958 - 13= 4.38958	19.26841	1.10804
3-1	22.49766 - 26= -3.50234	12.26637	0.54523
3-2	17.38958 - 20= -2.61042	6.81429	0.39186
3-3	12.41021 - 18= -5.58979	31.24575	2.51774
		χ^2	17.91945

$P < 0.005$ (4 degrees of freedom)

APPENDIX 2

Program for the Newton-Raphson iteration

		Neighbour cell (number of bundles)			
		1	2	3	
Home cell (number of bundles)	1	n_{11} (A1)	n_{12} (A2)	n_{13} (A3)	$n_{1.}$ (A)
	2	n_{21} (B1)	n_{22} (B2)	n_{23} (B3)	$n_{2.}$ (B)
	3	n_{31} (C1)	n_{32} (C2)	n_{33} (C3)	$n_{3.}$ (C)
Total		$n_{.1}$ (D)	$n_{.2}$ (E)	$n_{.3}$ (F)	n (N)

```
100     HOME
110     INPUT "A1=";A1;;
120     INPUT "A2=";A2;;
130     INPUT "A3=";A3
140     INPUT "B1=";B1;;
150     INPUT "B2=";B2;;
160     INPUT "B3=";B3
170     INPUT "C1=";C1;;
180     INPUT "C2=";C2;;
190     INPUT "C3=";C3
200     A=A1+A2+A3
210     B=B1+B2+B3
220     C=C1+C2+C3
230     D=A1+B1+C1
240     E=A2+B2+C2
250     F=A3+B3+C3
260     N=A+B+C
270     M1=A+D-A1
280     M2=B+E-B2
```

```
290     M3=F+C-C3
300     P=(-N+SQR((N^2)+(120*N*A1)))/(10*N)
310     Q=(-N+SQR((N^2)+(120*N*B2)))/(10*N)
315     FOR L=1 TO 10
320     F1=M1/P+(5*A1/(1+5*P))-(M3/(1-P-Q))-(5*C3/(1+5*(1-P-Q)))
330     F2=M2/Q+(5*B2/(1+5*Q))-(M3/(1-P-Q))-(5*C3/(1+5*(1-P-Q)))
340     X=-M1/(P^2)-(25*A1/((1+5*P)^2))-(M3/((1-P-Q)^2))-
        (25*C3/((1+5*(1-P-Q))^2))
350     Y=(-M3/((1-P-Q)^2))-(25*C3/((1+5*(1-P-Q))^2))
360     Z=-M2/(Q^2)-(25*B2/((1+5*P)^2))-(M3/((1-P-Q)^2))-
        (25*C3/((1+5*(1-P-Q))^2))
370     P1=P-(F1*Z-F2*Y)/(X*Z-Y^2)
380     Q1=Q-(F2*X-F1*Y)/(X*Z-Y^2)
400     P=P1
410     Q=Q1
420     NEXT L
430     IF SQR((P1-P)^2)<0.000001 AND SQR((Q1-Q)^2)<0.000001
        THEN 500
440     L=1
450     GOTO 315
500     PRINT "P=";P1
510     PRINT "Q=";Q1
520     END
```

APPENDIX 3

The following data are the cell areas (μm^2) for cells containing 1, 2 and 3 bundles. See materials and Methods for technique for area calculation.

Area	Bundles	Area	Bundles	Area	Bundles	Area	Bundles
69	1	95.5	1	105.5	1	114	1
71.5	1	96	1	105.5	2	114	2
72.5	1	96	2	106	1	114	2
76	1	96	2	106	1	114.5	1
76.5	1	96.5	1	106	2	114.5	1
78	1	96.5	1	106	2	114.5	2
78.5	1	96.5	2	106	2	114.5	2
79	1	97	1	106.5	1	115	1
80	1	97	1	106.5	2	115	2
80	1	97	2	106.5	2	115	3+
80	2	97.5	1	107	1	115.5	1
80.5	3+	97.5	2	107.5	1	115.5	1
81	1	97.5	2	108	1	115.5	1
82	2	97.5	2	108	1	116	1
83	1	98	1	108	1	116.5	1
84	2	98	1	108	2	116.5	1
84	2	98	2	108	2	116.5	2
87	1	98.5	1	108.5	1	117	2
87	1	98.5	1	108.5	1	117	2
87	1	99	1	108.5	1	117.5	1
88	1	99	1	108.5	1	117.5	1
88	1	99	1	109	1	118	1
89	1	99.5	1	109.5	1	118	1
89	2	99.5	1	109.5	2	118	2
89.5	3+	100	1	109.5	2	118	2
90	1	100	1	110	2	118.5	2
90.5	1	100.5	1	110	2	119	1
91	1	100.5	1	111	2	119	1
91	1	100.5	1	111	2.	119	2
91	2	100.5	2	111.5	3+	120	1
91.5	2	101	1	112	1	120	2
92	1	101	1	112	1	120	2
92	2	101	2	112	1	120	3+
92.5	1	102	1	112	1	120.5	1
92.5	2	102	1	112	1	120.5	1
93	1	102	2	112	1	120.5	2
93	3+	102.5	2	112	2	120.5	2
93.5	1	103	1	112	2	120.5	2
93.5	1	103.5	2	112	3+	120.5	2
93.5	1	104	2	112.5	1	121	2
93.5	1	104.5	1	112.5	1	121.5	2
93.5	1	104.5	1	112.5	2	122	1
93.5	2	104.5	1	113	1	122	2
94	1	104.5	2	113	1	122.5	1
94	2	105	1	113.5	1	122.5	1
94.5	1	105	1	113.5	1	122.5	2
94.5	1	105	1	113.5	1	122.5	2
95	2	105	1	114	1	123	1

Area	Bundles	Area	Bundles	Area	Bundles	Area	Bundles
123.5	1	133.5	1	144.5	1	154.5	2
124	2	133.5	2	145	1	155	2
124	2	134	1	145	2	155	3+
124.5	1	134	2	145	2	155.5	2
125	1	134	2	145.5	1	155.5	3+
125	1	134	2	145.5	2	156	2
125	3+	134.5	1	145.5	2	156	2
125.5	1	134.5	2	146	1	156	3+
125.5	1	135	2	146	1	157.5	1
125.5	1	135.5	1	146.5	1	157.5	1
126	3+	135.5	1	146.5	1	157.5	3+
126.5	1	136	1	146.5	2	158	1
126.5	1	136	1	146.5	2	158	1
126.5	1	136	1	146.5	3+	158	2
126.5	2	136	1	147	1	158	3+
126.5	2	136	1	147	2	158.5	1
126.5	2	136	2	147.5	2	158.5	1
126.5	3+	136	2	148	1	158.5	1
127	2	136	3+	148	1	158.5	2
127.5	1	136.5	1	148.5	3+	159	1
127.5	2	137	1	148.5	3+	159	1
127.5	2	137	2	149	1	159	1
128	1	137.5	1	149	1	159	3+
128	2	137.5	3+	149	2	159.5	2
128	2	138	1	149	3+	161	1
128	3+	138	1	149	3+	161	1
128.5	2	138.5	3+	149.5	1	161	1
128.5	2	139	1	149.5	2	161	1
129	1	139	1	149.5	2	161.5	1
129	1	139	2	150	1	161.5	2
129	1	139.5	2	150	2	162	1
129	2	140	1	150	2	162	1
129	3+	140	1	151	1	162	2
129.5	1	140	2	151	1	162	2
129.5	2	140.5	1	151	1	162	2
130	1	140.5	2	151	1	162.5	1
130.5	2	141	1	151	3+	162.5	1
130.5	2	141.5	1	151	3+	162.5	1
130.5	2	141.5	1	151.5	1	162.5	2
130.5	3+	141.5	2	152.5	2	162.5	2
131.5	2	142.5	1	153	1	163	1
132	1	143	1	153	2	163	2
132.5	1	143	2	153	2	163	2
132.5	1	143	2	153.5	2	163.5	1
132.5	3+	143.5	2	153.5	2	163.5	2
133	1	143.5	2	154	1	163.5	2
133	1	144	1	154	2	164	1
133	2	144	2	154.5	1	164	3+

Area	Bundles	Area	Bundles	Area	Bundles
164	3+	178	2	202.5	2
164.5	1	178	2	203.5	3+
164.5	2	178.5	2	206	1
165	1	178.5	2	206	2
165	2	178.5	2	206	2
165.5	1	179	1	206.5	1
165.5	2	179	1	207	2
165.5	2	179	2	208.5	1
166	1	179.5	1	209	1
166	1	179.5	2	209.5	2
166	2	180	1	210	2
166.5	1	180.5	2	210.5	1
167	1	180.5	2	210.5	3+
167	3+	180.5	2	210.5	3+
168	1	181	2	211	2
168.5	2	182.5	1	211	2
168.5	2	182.5	2	213.5	1
168.5	3+	182.5	2	213.5	1
168.5	3+	183	1	214.5	1
169	2	184.5	2	215.5	1
169	3+	184.5	2	218	1
169.5	2	184.5	2	218	2
170	1	185.5	2	219	2
170	1	185.5	2	219.5	2
170	1	186.5	2	220	3+
170	2	187	2	220.5	3+
170.5	2	187.5	2	221.5	1
171	3+	188	2	222.5	2
172	2	188.5	1	224.5	2
172	2	188.5	3+	225.5	1
172	3+	189	1	226	2
172.5	3+	189	3+	228	3+
173	1	190.5	2	230.5	1
173	2	190.5	3+	230.5	1
173	2	191	3+	232.5	1
173	3+	191.5	1	234	2
173.5	1	193	2	235	2
174	1	193	2	236	2
174	2	193	3+	238.5	2
174.5	2	195	2	239	3+
175.5	1	195.5	1	239.5	2
175.5	1	195.5	2	239.5	2
175.5	2	196	2	261	3+
176.5	3+	196.5	2	330	2
177	2	197	2	333	2
177.5	1	199.5	1	416.5	3+
177.5	2	200	2		
177.5	2	201.5	1		

APPENDIX 4

The following data are the nuclear projectional areas (μm^2) for cells containing 1, 2 and 3 bundles. See materials and Methods for technique for area calculation.

Area	Bundles	Area	Bundles	Area	Bundles	Area	Bundles
14.13	1	28.27	1	34.9	1	35.78	1
14.13	1	28.27	1	34.9	1	35.78	2
18.46	1	28.27	1	34.9	1	35.78	2
18.46	1	28.85	1	34.9	1	38.48	1
18.46	1	28.85	1	34.9	1	38.48	1
18.46	1	28.85	1	34.9	1	38.48	1
18.46	1	28.85	1	34.9	1	38.48	1
18.46	1	28.85	1	34.9	1	38.48	1
18.46	1	28.85	1	34.9	1	38.48	2
18.46	1	28.85	1	34.9	1	41.28	1
18.46	1	28.85	1	34.9	1	41.28	1
18.46	1	28.85	1	34.9	1	41.28	1
18.46	2	28.85	1	34.9	1	41.28	2
18.46	2	28.85	1	34.9	1	41.54	1
23.37	1	28.85	1	34.9	1	41.54	1
23.37	1	28.85	1	34.9	1	41.54	1
23.37	1	28.85	1	34.9	1	41.54	1
23.37	1	28.85	1	34.9	1	41.54	1
23.37	1	28.85	1	34.9	1	41.54	1
23.37	1	28.85	1	34.9	1	41.54	1
23.37	1	28.85	1	34.9	1	41.54	1
23.37	1	28.85	1	34.9	1	41.54	1
23.37	1	28.85	1	34.9	1	41.54	1
23.37	1	28.85	1	34.9	1	41.54	1
23.37	1	28.85	1	34.9	1	41.54	1
23.37	1	28.85	1	34.9	2	41.54	1
23.37	1	28.85	1	34.9	2	41.54	1
23.37	1	28.85	1	34.9	2	41.54	2
23.37	1	28.85	1	34.9	2	41.54	2
23.37	1	28.85	2	34.9	2	41.54	2
23.37	1	28.85	2	34.9	2	41.54	2
23.37	1	28.85	2	34.9	2	41.54	2
23.37	1	28.85	2	34.9	2	41.54	2
23.37	1	28.85	2	34.9	2	44.17	1
23.37	1	28.85	2	34.9	2	44.17	1
23.37	1	28.85	2	34.9	2	44.17	1
23.37	1	28.85	2	34.9	2	47.15	1
23.37	1	28.85	2	34.9	2	47.15	1
23.37	1	28.85	2	34.9	2	48.75	1
23.37	2	30.66	1	34.9	2	48.75	2
23.37	2	30.66	1	34.9	2	48.75	2
23.37	2	30.66	1	34.9	2	48.75	2
23.37	2	33.17	1	34.9	2	48.75	2
23.37	2	34.9	1	34.9	3	50.26	1
23.37	2	34.9	1	34.9	3	53.44	1
23.37	2	34.9	1	34.9	3	53.44	1
23.37	2	34.9	1	35.78	1	56.54	1
25.98	1	34.9	1	35.78	1	56.54	2

REFERENCES

Albrecht-Buehler, G. (1977). Daughter 3T3 cells. Are they mirror images of each other? *J. Cell Biol.*: **72**, 595-603.

Aunis, D. & Bader, M.-F. (1988). The cytoskeleton as a barrier to exocytosis in secretory cells. *J. exp. Biol.*: **139**, 253-266.

Aunis, D., Perrin, D. & Langley, O. K. (1987). Cytoskeletal proteins and chromaffin cell activity. In *Stimulus-secretion coupling in chromaffin cells*, 1 (ed. K. Rosenheck & P. I. Lelkes). CRC Press, Inc., Boca Raton, Florida, *pp.* 155-175.

Beisson, J. & Sonneborn, T. M. (1965). Cytoplasmic inheritance of the organization of the cell cortex in *Paramecium aurelia*. *P.N.A.S. USA*: **53**, 275-282.

Brodsky, W. Y. & Uryvaeva, I. V. (1977). Cell ploidy: its relation to tissue growth and function. *Int. Rev. Cytol.*: **50**, 275-332.

Burgess, T. L. & Kelly, R. B. (1987). Constitutive and regulated secretion of proteins. *Ann. Rev. Cell Biol.*: **3**, 243-293.

Burgoyne, R. D. & Cheek, T. R. (1987). Reorganisation of peripheral actin filaments as a prelude to exocytosis. *Biosci. Rep.*: **7**, 281-288.

Campbell, R. D. (1980). Role of muscle processes in *Hydra* morphogenesis. In *Developmental and cellular biology of Coelenterates*, (ed. P. Tardent & R. Tardent). Elsevier/North-Holland Biomedical Press, *pp.* 421-428.

Carlier, M.-F. (1988). Role of nucleotide hydrolysis in the polymerization of actin and tubulin. *Cell Biophys.*: **12**, 105-117.

Cheek, T. R. & Burgoyne, R. D. (1987). Cyclic AMP inhibits both nicotine-induced actin disassembly and catecholamine secretion from bovine adrenal chromaffin cells. *J. Biol. Chem.*: **262**, 11663-11666.

Chen, W.-T., Olden, K., Bernard, B. A. & Chu, F.-F. (1984). Expression of transformation-associated protease(s) that degrade fibronectin at cell contact sites. *J. Cell Biol.*: **98**, 1546-1555.

Condoulis, W. V. & Locke, M. (1966). The deposition of endocuticle in an insect, *Calpodes ethlius* Stoll (Lepidoptera, Hesperiidae). *J.Insect Physiol.*: **12**, 311-323.

Couble, P., Blaes, N. & Prudhomme, J. C. (1984). Actin microfilaments and fibroin secretion in the silk gland cells of *Bombyx mori* : effects of cytochalasin B. *Exp. Cell Res.*: **151**, 322-331.

Cuppoletti, J. & Malinowska, D. H. (1988). Cytoskeletal determinants of control of gastric acid secretion. In *Membrane Biophysics III: Biological Transport*, (ed. Alan R. Liss, Inc., *pp.* 23-35.

Dallai, R., Marchini, D. & Callaini, G. (1988). Microtubule and microfilament distribution during the secretory activity of an insect gland. *J. Cell Sci.*: **91**, 563-570.

Davey, K. G. (1981). Regulation of cell volume in follicle cells of Rhodnius by JH. In *Juvenile hormone biochemistry*, (ed. G. E. Pratt & G. T. Brooks). Elsevier/North-Holland Biomedical Press, *pp.* 233-240.

Dean, R. L., Bollenbacher, W. E., Locke, M., Smith, S. L. & Gilbert, L. I. (1980). Haemolymph ecdysteroid levels and cellular events in the intermoult/moult sequence of *Calpodes ethlius*. *J. Insect Physiol.*: **26**, 267-280.

Delhanty, P. & Locke, M. (1990a). The conservation of a cytoskeletal pattern in epidermal cell doublets. *Devl. Biol.*: submitted.

Delhanty, P. & Locke, M. (1990b). The redistribution of F-actin in the dermal glands of an insect in relation to secretion. *J. Cell Sci.*: submitted.

Diehl, P. A., Germond, J. E. & Morici, M. (1982). Correlations between ecdysteroid titers and integument structure in nymphs of the tick, *Amblyomma hebraeum* Koch (Acharina: Ixodidae). *Rev. suisse Zool.*: **89**, 859-868.

Fain, J. N. & Berridge, M. J. (1979). Relationship between hormonal activation of phosphatidylinositol hydrolysis, fluid secretion and calcium flux in the blowfly salivary gland. *Biochem. J.*: **178**, 45-58.

Foucrier, J., Pechinot, D., Rigaut, J. P. & Feldmann, G. (1988). Transferrin secretion and hepatocyte ploidy: analysis at the single cell level using a semi-automatic image analysis method. *Biol. Cell*: **62**, 125-131.

Franzl, S., Locke, M. & Huie, P. (1984). Lenticles: innervated secretory structures that are expressed at every other larval moult. *Tissue & Cell*: **16**, 251-268.

Fristrom, D. (1976). The mechanism of evagination of imaginal discs of *Drosophila melanogaster*. III. Evidence for cell rearrangement. *Devl. Biol.*, **54**, 163-171.

Fristrom, D. K. (1982). Septate junctions in imaginal disks of *Drosophila*: a model for the redistribution of septa during cell rearrangement. *J. Cell Biol.*: **94**, 77-87.

Fristrom, D. (1988). The cellular basis of epithelial morphogenesis. A review. *Tissue & Cell*: **20**, 645-690.

Fukui, Y. & Katsumara, H. (1979). Nuclear actin bundles in *Amoeba*, *Dictyostelium*, and human HeLa cells induced by dimethylsulfoxide. *Exp. Cell Res.*: **120**, 451-455.

Giloh, H. & Sedat, J. W. (1982). Fluorescence microscopy: reduced photobleaching of rhodamine and fluorescein protein conjugates by *n*-propyl gallate. *Science*: **217**, 1252-1255.

Goodman, C. S., Bastiani, M. J., Doe, C. Q., du Lac, S., Helfand, S. L., Kuwada, J. Y. & Thomas, J. B. (1984). Cell recognition during neuronal development. *Science*: **225**, 1271-1279.

Gotlieb, A. I., May, L. M., Subrahmanyan, L. & Kalnins, V. I. (1981). Distribution of microtubule organizing centers in migrating sheets of endothelial cells. *J. Cell Biol.*: **91**, 589-594.

Gupta, A. P. (1979). Hemocyte types: their structures, synonymies, interrelationships, and taxonomic significance. In *Insect hemocytes. Development, forms, functions, and techniques*, (ed. A. P. Gupta). Cambridge University Press, Cambridge, *pp.* 85-128.

Harris, A. K., Wild, P. & Stopak, D. (1980). Silicone rubber substrata: a new wrinkle in the study of cell locomotion. *Science*: **208**, 177-179.

Herrmann, H. (1989). *Cell biology: an inquiry into the nature of the living state.* Harper & Row, New York, *pp.* 916

Heslop-Harrison, J., Heslop-Harrison, Y., Cresti, M., Tiezzi, A. & Ciampolini, F. (1986). Actin bundles during pollen germination. *J. Cell Sci.*: **86**, 1-8.

Hirano, H., Nakanishi, A., Sakamoto, Y., Gotoh, S. & Higashi, K. (1981). Comparisons of DNA and RNA biosynthetic activities and nucleolar organization in rat liver nuclei with different ploidy. *Biomed. Res.*: **2**, 307-315.

Hirokawa, N. & Heuser, J. E. (1981). Quick-freeze, deep-etch visualization of the cytoskeleton beneath the surface differentiations of intestinal epithelial cells. *J. Cell Biol.*: **91**, 399-409.

Hoffstein, S. T. (1981). The role of microtubules and microfilaments in lysosomal enzyme release from polymorphonuclear leukocytes. *Methods Cell Biol.*: **23**, 259-282.

Horwath, K. L. & Riddiford, L. M. (1988). Stage and segment specificity of the secretory cell of the dermal glands of the tobacco hornworm, *Manduca sexta. Dev. Biol.*: **130**, 365-373.

Huebner, E. & Injeyan, H. S. (1980). Patency of the follicular epithelium in *Rhodnius prolixus*: a re-examination of the hormone response and technique refinement. *Can. J. Zool.*: **58**, 1617-1625.

Izzard, C. S. (1974). Contractile filopodia and in vivo cell movement in the tunic of the ascidian, *Botryllus schlosseri*. *J. Cell Sci.*: **15**, 513-535.

Jackson, A. & Locke, M. (1989). The formation of the plasma membrane reticular systems in the oenocytes of an insect. *Tissue & Cell*: **21**, 463-473.

Jones, J. C. R., Yokoo, K. M. & Goldman, R. D. (1986). Is the hemidesmosome a half desmosome? An immunological comparison of mammalian desmosomes and hemidesmosomes. *Cell Motil. Cytoskeleton*: **6**, 560-569.

Kato, Y., Nair, K. K., Dyer, K. A. & Riddiford, L. M. (1987). Changes in ploidy of epidermal cells during last larval instar of the tobacco hornworm, *Manduca sexta*. *Development*: **99**, 137-143.

Keller, R. & Tibbetts, P. (1989). Mediolateral cell intercalation in the dorsal, axial mesoderm of *Xenopus laevis*. *Devl. Biol.*: **131**, 539-549.

Keller, R. E. & Trinkaus, J. P. (1987). Rearrangement of enveloping layer cells without disruption of the epithelial permeability barrier as a factor in *Fundulus* epiboly. *Dev. Biol.*: **120**, 12-24.

Kirschner, M. & Mitchison, T. (1986). Beyond self assembly: from microtubules to morphogenesis. *Cell*: **45**, 329-342.

Lai-Fook, J. (1972) Comparison between the dermal glands in two insects *Rhodnius prolixus* (Hemiptera) and *Calpodes ethlius* (Lepidoptera). *J. Morphol.*: **136**, 495-504.

Lai-Fook, J. (1973). The fine structure of Verson's glands in molting larvae of *Calpodes ethlius* (Hesperiidae, Lepidoptera). *Can. J. Zool.*: **51**, 1201-1210.

Lane, N. J. (1982). Insect intercellular junctions: their structure and development. In *Insect Ultrastructure*, 1 (ed. R. C. King & H. Akai). Plenum Press, New York and London, *pp.* 402-430.

Lane, S., Riddiford, L. M., Truman, J. W. & Conitz, J. (1986). Development of the prepupal Verson's gland of the tobacco hornworm, *Manduca sexta*, and its hormonal control. *J. Exp. Zool.*: **240**, 83-94.

Le Rumeur, E., Beaumont, C., Guillouzo, C., Rissel, M., Bourel, M. & Guillouzo, A. (1981). All normal hepatocytes produce albumin at a rate related to their degree of ploidy. *Biochem. Biophys, Res, Commun.*: **101**, 1038-1046.

Lelkes, P. I., Friedman, J. E., Rosenheck, K. & Oplatka, A. (1986). Destabilization of actin filaments as a requirement for the secretion of catecholamines from permeabilized chromaffin cells. *FEBS Lett.*: **208**, 357-363.

Locke, M. (1961). Pore canals and related structures in insect cuticle. *J. Biophys. Biochem. Cytol.*: **10**, 589-618.

Locke, M. (1970). The moult/intermoult cycle in the epidermis and other tissues of an insect *Calpodes ethlius* (Lepidoptera, Hesperiidae). *Tissue & Cell*: **2**, 197-223.

Locke, M. (1985). The structure of epidermal feet during their development. *Tissue & Cell*: **17**, 901-921.

Locke, M. (1986). The development of the plasma membrane reticular system in the fat body of an insect. *Tissue & Cell*: **18**, 853-867.

Locke, M. (1987). The very rapid induction of filopodia in insect cells. *Tissue & Cell*: **19**, 301-318.

Locke, M. (1988). Insect cells for the study of general problems in biology-somatic inheritance. *Int. J. Insect Morphol. & Embryol.*: **17**, 419-436.

Locke, M. (1989). Insect epidermis and its differentiation. In *Biology of arthropod cuticle*, (ed. A. Retnakaran & K. Binnington). Inkata Press Pty. Ltd, Victoria, Australia, *pp. In press.*

Locke, M. & Huie, P. (1979). Apolysis and the turnover of plasma membrane plaques during cuticle formation in an insect. *Tissue & Cell*: **11**, 277-291.

Locke, M. & Huie, P. (1981a). Epidermal feet in insect segment morphogenesis. *Nature*: **293**, 733-735.

Locke, M. & Huie, P. (1981b). Epidermal feet in pupal segment morphogenesis. *Tissue & Cell*: **13**, 786-803.

Locke, M. & Huie, P. (1983). A function for plasma membrane reticular systems. *Tissue & Cell*: **15**, 885-902.

Locke, M. & Leung, H. (1985a). Nucleolar necklace formation in response to hemolymph ecdysteroid peaks. *Tissue & Cell*: **17**, 589-603.

Locke, M. & Leung, H. (1985b). The pairing of nucleolar patterns in an epithelium as evidence for a conserved nuclear skeleton. *Tissue & Cell*: **17**, 573-588.

Maupin-Szamier, P. & Pollard, T. D. (1978). Actin filament destruction by osmium tetroxide. *J. Cell Biol.*: **77**, 837-852.

Mitchison, T. & Kirschner, M. (1984). Dynamic instability of microtubule growth. *Nature*: **312**, 237-242.

Mittenthal, J. E. & Mazo, R. M. (1983). A model for shape generation by strain and cell-cell adhesion in the epithelium of an arthropod leg segment. *J. theor. Biol.*: **100**, 443-483.

Mueller, H. & Franke, W. W. (1983). Biochemical and immunological characterization of desmoplakins I and II, the major polypeptides of the desmosomal plaque. *J. Mol. Biol.*: **163**, 647-671.

Nagai, R., Yoshimoto, Y. & Kamiya, N. (1978). Cyclic production of tension force in the plasmodial strand of Physarum polycephalum and its relation to microfilament morphology. *J. Cell Sci.*: **33,** 205-225.

Nagl, W. (1978). *Endoploidy and polyteny in differentiation and evolution.* North-Holland Publishing Company, Amsterdam, New York, Oxford, *pp.* 283

Nardi, J. B. & Kafatos, F. c. (1976a). Polarity and gradients in lepidopteran wing epidermis I. Changes in graft polarity, form, and cell density accompanying transpositions and reorientations. *J. Embryol. exp. Morph.*: **36,** 469-487.

Nardi, J. B. & Kafatos, F. C. (1976b). Polarity and gradients in lepidopteran wing epidermis II. The differential adhesiveness model: gradient of a non-diffusible cell surface parameter. *J. Embryol. exp. Morph.*: **36,** 489-512.

Nardi, J. B. & Magee-Adams, S. M. (1986). Formation of scale spacing patterns in a moth wing. I. Epithelial feet may mediate cell rearrangement. *Dev. Biol.*: **116,** 278-290.

Neville, A. C. (1975). *Biology of arthropod cuticle.* Springer-Verlag, New York, Heidelberg, Berlin, *pp.* 448

Nishikawa, S. & Kitamura, H. (1987). Microtubules, intermediate filaments, and actin filaments in the odontoblast of rat incisor. *Anat. Rec.*: **219,** 144-151.

Noirot, C. & Quennedey, A. (1974). Fine structure of insect epidermal glands. *Ann. Rev. Entomol.*: **19,** 61-80.

Otto, J. J. (1977). Orientation and behaviour of epithelial cell muscle processes during *Hydra* budding. *J. Exp. Zool.*: **202,** 307 322.

Rafferty, N. S. & Scholz, D. L. (1985). Actin in polygonal arrays of microfilaments and sequestered actin bundles (SABs) in lens epithelial cells of rabbits and mice. *Curr. Eye Res.*: **4,** 713-718.

Richards, A. G. (1951). *The integument of arthropods*. University of Minnesota Press, Minneapolis, *pp.* 411

Sanger, J. W., Sanger, J. M., Kreis, T. E. & Jockusch, B. M. (1980). Reversible translocation of cytoplasmic actin into the nucleus caused by dimethyl sulfoxide. *Proc. Natl. Acad. Sci. USA*: **77,** 5268-5272.

Sasaki, S., Nakajima, E., Fujii-Kuriyama, Y. & Tashiro, Y. (1981). Intracellular transport and secretion of fibroin in the posterior silk gland of the silkworm *Bombyx mori*. *J. Cell Sci*: **50,** 19-44.

Schoenwolf, G. C. & Alvarez, I. S. (1989). Roles of neuroepithelial cell rearrangement and division in shaping of the avian neural plate. *Development*: **106,** 427-439.

Schulze, E. S. & Blose, S. H. (1984). Passage of molecules across the intercellular bridge between post-mitotic daughter cells. *Exp. Cell Res.*: **151,** 367-373.

Shienvold, F. L. & Kelly, D. E. (1976). The hemidesmosome: new fine structural features revealed by freeze-fracture techniques. *Cell Tiss. Res.*: **172,** 289-307.

Shivers, R. R. & Brightman, M. W. (1977). Formation of hemi-desmosomes during regeneration of crayfish nerve root sheath as studied with freeze-fracture. *J. Comp. Neur.*: **173,** 1-22.

Simmonds, D., Setterfield, G. & Brown, D. L. (1983). Organization of microtubules in dividing and elongating cells of Vicia hajastana Grossh. in suspension culture. *Eur. J. Cell Biol.*: **32,** 59-66.

Small, J. V. (1984). Factors affecting the integrity of actin meshworks in cultured cells. In *Cell motility: mechanism and regulation*, (ed. H. Ishikawa, S. Hatano & H. Sato). Alan R. Liss, New York, *pp.* 493-506.

Solomon, F. (1979). Detailed neurite morphologies of sister neuroblastoma cells are related. *Cell*: **16,** 165-169.

Solomon, F. (1980). Neuroblastoma cells recapitulate their detailed neurite morphologies after reversible microtubule disassembly. *Cell*: **21**, 333-338.

Solomon, F. (1981). Specification of cell morphology by endogenous determinants. *J. Cell Biol.*: **90**, 547-553.

Stecher, P. G. (1968). *The Merck Index: an encyclopedia of chemicals and drugs*. Merck & Co., Inc., Rahway, N. J., U.S.A, *pp.* 1714

Steinberg, M. S. & Poole, T. J. (1982). Cellular adhesive differentials as determinants of morphogenetic movements and organ segregation. In *Developmental Order: its origin and regulation*, (ed. Alan R. Liss, New York, *pp.* 351-378.

Takahashi, Y., Mutasim, D. F., Patel, H. P., Anhalt, G. C., Labib, R. S. & Diaz, L. A. (1985). The use of human pemphigoid autoantibodies to study the fate of epidermal basal cell hemidesmosomes after trypsin dissociation. *J. Invest. Dermatol.*: **85**, 309-313.

Tamm, S. & Tamm, S. L. (1988). Development of macrociliary cells in *Beroë*. 1. Actin bundles and centriole migration. *J. Cell Sci.*: **89**, 67-80.

Tashiro, Y., Matsuura, S. & Sasaki, S. (1982). Roles of the cytoskeletal systems in the biosynthesis, intracellular transport and secretion of fibroin in the posterior silk gland cells of *Bombyx mori*. In *The Ultrastructure and Functioning of Insect Cells*, (ed. H. Akai, R. C. King & S. Morohoshi). Society for Insect Cells Japan, Sapporo, *pp.* 149-152.

Tilney, L. G. (1983). Interactions between actin filaments and membranes give spatial organization to cells. In *Spatial Organization of Eukaryotic Cells*, 2 (ed. J. R. McIntosh). Alan R. Liss, Inc., New York, *pp.* 163-199.

Truman, J. W. (1985). Hormonal control of ecdysis. In *Comprehensive insect physiology, biochemistry and pharmacology*, 8 (ed. G. A. Kerkut & L. I. Gilbert). Pergamon Press, Oxford, *pp.* 413-440.

Tsui, H.-C. T., Lankford, K. L. & Klein, W. L. (1985). Differentiation of neuronal growth cones: Specialization of filopodial tips for adhesive interactions. *Proc. Natl. Acad. Sci. USA*: **82**, 8256-8260.

Tsui, H.-C. T., Schubert, D. & Klein, W. L. (1988). Molecular basis of growth cone adhesion: anchoring of adheron-containing filaments at adhesive loci. *J. Cell Biol.*: **106**, 2095-2108.

Tuck, A. & Locke, M. (1985). Nucleolar cycles during the fifth stadium in *Manduca* epidermis. *Tissue & Cell*: **17**, 349-357.

Vincent, J. F. V. (1981). Morphology and design of the extensible intersegmental membrane of the female migratory locust. *Tissue & Cell*: **13**, 831-853.

Walter, M. F. & Biessmann, H. (1984). Intermediate-sized filaments in Drosophila tissue culture cells. *J. Cell Biol.*: **99**, 1468-1477.

Warn, R. M. & Magrath, R. (1983). F-actin distribution during the cellularization of the *Drosophila* embryo visualized with Fl-phalloidin. *Exp. Cell Res.*: **143**, 103-114.

Weeds, A. (1982). Actin-binding proteins - regulators of cell architecture and motility. *Nature*: **296**, 811-816.

Wieland, T. & Govindan, V. M. (1974). Phallotoxins bind to actins. *FEBS Lett.*: **46**, 351-353.

Wielgus, J. J. & Gilbert, L. I. (1978). Epidermal cell development and control of cuticle deposition during the last larval instar of *Manduca sexta*. *J. Insect Physiol.*: **24**, 629-637.

Wigglesworth, V. B. (1933). The physiology of the cuticle and of ecdysis in Rhodnius Prolixus (Triatomidae, Hemiptera); with special reference to the function of the oenocytes and of the dermal glands. *Quart. J. Micr. Sci.*: **76**, 269-318.

Wigglesworth, V. B. (1947). The epicuticle in an insect, *Rhodnius prolixus* (Hemiptera). *Proc. Roy. Soc. B.*: **134,** 163-181.

Wigglesworth, V. B. (1959). ***The control of growth and form: a study of the epidermal cell in an insect.*** Cornell University Press, Ithaca, *pp.* 140

Wolfgang, W. J. & Riddiford, L. J. (1981). Cuticular morphogenesis during the continuous growth of the final instar larva of a moth. *Tissue & Cell*: **13,** 757-772.

Wollweber, L., Stracke, R. & Gothe, U. (1981). The use of a simple method to avoid shrinkage during SEM preparation. *J. Microscopy*: **121,** 185-189.

Woods, A. & Couchman, J. R. (1988). Focal adhesions and cell-matrix interactions. *Collagen Rel. Res.*: **8,** 155-182.